GDF3: a new player in cancer stem cell biology

vorgelegt von

Dipl. Ing. Karolina Tykwinska

aus Polen

von der Fakultät III – Prozesswissenschaften

Fachgebiet Medizinische Biotechnologie

Technische Universität Berlin

zur Erlangung des akademischen Grades

Doktorin der Naturwissenschaften

- Dr. rer. nat. -

genehmigte Dissertation

Promotionsausschuss:
Vorsitzender: Prof. Dr. Jens Kurreck
Berichter 1: Prof. Dr. Petra Seemann
Berichter 2: Prof. Dr. Leif-Alexander Garbe

Tag der wissenschaftlichen Aussprache: 17.05.2013

Berlin 2013

D 83

"When a man does not know what harbour he is making for,

no wind is the right wind"

Lucius Annaeus Seneca

ACKNOWLEDGMENT

In the first place I would like to thank Prof. Roland Lauster for giving me the opportunity to join his group and work on my doctoral thesis. The unrestricted freedom in the project development taught me a great deal.

I would like to thank Prof. Petra Knaus for the scientific input and the opportunity to learn a new method in her lab.

I would like to express my gratitude to Dr. Mark Rosowski for the support in the experimental design and reviewing my work.

Special thanks goes to Devasena Kanthi, with whom I shared not only the office, the lab space and the flat, but also personal and professional highs and lows. The life has become bright and shiny, as you promised!

Furthermore, I would like to acknowledge Jessica Kopf and Julian Braun, my truthful companions inside the 'PhD bubble'. Thank you for valuable scientific discussions, proofreading and motivating me to go on.

I owe sincere and earnest thankfulness to Luzia Schramm and Agnes Schumacher for technical assistance and brilliant lab management, which made the lab work as easy and pleasant as possible.

I am obliged to all of my colleagues who created a nice working atmosphere, especially Shirin Fatehi and Jennifer Binder.

I thank my climbing friends Sandra & Tom, Bjoern & Maria, Hermine & Lars for keeping my mind off things, when it was necessary, and

Last but not least, I thank my family for the faith.

ABSTRACT

Misexpression of growth factors, particularly those related to a stem cell-like phenotype, is often observed in several cancer types. It has been found to influence parameters of disease progression like cell proliferation, differentiation, maintenance of undifferentiated phenotype and modulation of the immune system. Growth and Differentiation Factor 3 (GDF3) is a TGFβ family member associated with pluripotency and differentiation during embryonic development, which has been previously reported to be re-expressed in a number of cancer types. However, its role in tumor development and progression has not been clarified yet.

In this study a thorough analysis of GDF3 signalling was performed to decipher the role of GDF3 in an *in vitro* model of cancer stem cells, the NCCIT cells. The overexpression of chimeric precursors to track the translation, processing and secretion of the ligand, revealed that the bioavailability of GDF3 is tightly regulated by its prodomain. The prodomain mediates a rapid degradation of GDF3, limiting its spacial range and time of action.

Using classical approaches to study protein function combined with high-throughput technique for transcriptome analysis and differentiation assays I evaluated GDF3 as a potential therapeutic target.

I observed that GDF3 robustly induces a panel of genes related to differentiation, among which are several potent tumor suppressors, such as HoxA9, HoxA10 and HoxB13, without impacting the proliferative capacity. Additionally, the expression of several BMP ligands, BMP receptor and extracellular inhibitor Gremlin was affected. The expression of these molecules is sustained by the presence of GDF3 and drops upon GDF3 knockdown. The overrepresentation analysis of genes regulated by GDF3 as well as qPCR uncovered the previously unknown role of GDF3 in angiogenesis regulation. Tie2 is particularly strongly upregulated in the absence of GDF3, indicating involvement of this ligand in negative angiogenesis regulation.

On the basis that GDF3 is involved in development and differentiation the capacity of NCCIT cells to *in vitro* differentiate upon stimulation with retinoic acid was exploited. It was observed that the level of BCL2, a pro-survival factor, was significantly upregulated in the control cells, which escaped the apoptosis as a consequence, while NCCIT cells with GDF3 knockdown failed to do so. I report for the first time the protective effect of GDF3 against retinoic acid-induced apoptosis in cells with stem cell-like properties. Furthermore, this study provides strong evidence that blocking of GDF3 combined with retinoic acid-treatment of solid cancers is a compelling direction for further investigations, which may lead to re-design of cancer differentiation therapies.

ZUSAMMENFASSUNG

In vielen Krebszelltypen wird ein verändertes Expressionsmuster verschiedener Wachstumsfaktoren beobachtet. Dabei handelt es sich häufig um Proteine, die den Stammzellphänotyp der Zelle definieren. Dadurch werden verschiedene Parameter moduliert, die sich auf den Krankheitsfortschritt auswirken, wie Zellproliferation, Differenzierung, das Aufrechterhalten des undifferenzierten Phänotyps sowie Modulation des Immunsystems. Growth and Differentiation Factor 3 (GDF3) ist ein Zytokin aus der TGFβ Familie, das vor allem für die Pluripotenz embryonaler Stammzellen und während der frühen Embryonalentwicklung eine Rolle spielt. Obwohl seine Re-expression in Krebszellen nachgewiesen werden konnte, ist seine Funktion in der Tumorinitiation und -progression ungeklärt.

Im Rahmen dieses Projektes, wurde die Rolle des GDF3 und seiner Signalkaskade in einem *in vitro* Krebsstammzell-Modell, NCCIT Zelllinie, untersucht. Mittels einer Überexpression chimärer Prekursormoleküle zur Untersuchung der Translation, Prozessierung und Sekretion konnte der entscheidende Einfluss der GDF3-Prodomäne auf die Bioverfügbarkeit des Zytokins demonstriert werden. Die GDF3-Prodomäne vermittelt einen rapiden Abbau des Liganden, was mit einer deutlichen Einschränkung des räumlichen und zeitlichen Wirkungsspektrums von GDF3 einhergeht.

Außerdem wurden ein klassischer Ansatz zur Proteinfunktionsuntersuchung, ein modernes Hochdurchsatzverfahren zur Transkriptomanalyse und Differenzierungsassays eingesetzt, um das Potenzial von GDF3 als therapeutisches Target zu evaluieren.

Es konnte gezeigt werden, dass GDF3 eine Reihe von differenzierungsassoziierten Geneinduziert, darunter auch potente Tumorsuppresorgene, wie HoxA9, HoxA10 and HoxB13, ohne die Proliferationskapazität der Zellen zu beeinflussen. Zusätzlich moduliert GDF3 die Expression einiger BMP-Liganden, -Rezeptoren und des extrazellulären Inhibitors Gremlin. Die Expression dieser Moleküle wird durch das Vorhandensein von GDF3 aufrecht erhalten und verringert sich, wenn GDF3 mittels shRNA runterreguliert wurde. Mittels Gene Ontology-Analyse und qPCR konnte auch ein Zusammenhang zwischen GDF3 und Angiogenese festgestellt werden. Die starke Tie2 Induktion, des Angiopoietin 1 und 2 Rezeptors, nach GDF3 knockdown weist auf eine Rolle von GDF3 als negativer Angiogenese-Regulator hin.

Aufgrund der Feststellung, dass GDF3 die Expression von differenzierungs- und entwicklungsassoziierten Genen moduliert, wurde im nächsten Schritt die Differenzierungskapazität der NCCIT Zellen untersucht. Nach Stimulation mit Retinsäure wurde beobachtet, dass die Kontrollzellen erwartungsgemäß einer neuronalen Differenzierung, begleitet durch eine

Verringerung der Proliferationsrate, durchlaufen. Die GDF3-knockdown Zellen hingegen leiteten verstärkt die Apoptose ein. Dies kann auf die differenzielle Induktion des anti-apoptotischen Faktors BCL2 zurückgeführt werden. BCL2 wird vermehrt exprimiert in den Kontrollzellen exprimiert, jedoch nicht in GDF3 knockdown-Zellen induziert.

Dies ist die erste Studie, die über einen Schutzeffekt von GDF3 vor der Retinsäure-induzierten Apoptose berichtet. Eine Kombination aus Retinsäure und gleichzeitiger Blockade der GDF3 Signalkaskade könnte zur Entwicklung neuartiger Anti-Krebstherapien bzw. zum Re-design von Differenzierungstherapien eingesetzt werden.

TABLE OF CONTENT

Acknowledgment II

Abstract III

Zusammenfassung IV

Table of content VI

Abbreviations VIII

1 Introduction 1

1.1 Heterogeneity of cancer 1

1.2 Cancer stem cells 2

1.3 'Stemness'-signature of cancer 3

1.4 Modeling of CSC *in vitro* 4

1.5 Differentiation therapy 5

1.6 RA signalling and its anti-cancer effects 7

1.6.1 RA signalling cascade 7

1.6.2 TRAIL-mediated apoptosis 8

1.7 TGFβ family 9

1.7.1 Structure of TGFβ ligands 10

1.7.2 Signalling pathways triggered by TGFβ ligands 10

1.8 GDF3 - a TGFβ family member associated with stemness 11

1.8.1 Signalling mode 11

1.8.2 Function of GDF3 12

1.8.3 GDF3 in cancer 13

2 Aims of the study 14

3 Material & methods 15

3.1 Cell culture 15

3.1.1 Neuronal differentiation 15

3.1.2 Stimulation with ligands from TGFbeta family 15

3.2 Apoptosis assay 15

3.3 Proliferation assay 15

3.4 Lentivirus production and transduction 16

3.5 Gene expression analysis 16

3.5.1 RNA isolation and cDNA preparation 16

3.5.2 qPCR analysis 17

3.5.3 Microarray analysis 19

3.6 Cloning 19

3.6.1 General procedures 19

3.6.2 Cloning strategies 21

3.7 Luciferase assay 24

3.8 Immunoprecipitation 24

3.9 SDS-PAGE, protein transfer and immunobloting 25

3.10 Immunofluorescence staining **26**
3.11 *In silico* promoter analysis **27**
3.12 Statistical analysis **27**

4 Results **28**
4.1 NCCIT cells as a model of CSCs. **28**
4.2 GDF3 signalling in NCCIT cells: inhibition of Smad1/5/8 pathway vs. activation of Smad2/3 pathway **29**
4.3 Monitoring of GDF3-synthesis, processing and secretion **31**
4.3.1 GDF3-overexpression constructs 31
4.3.2 Proregion-mediated effects on the stability of GDF3 33
4.4 GDF3 and Nodal stimulation of NCCIT cells - concentration kinetic **35**
4.5 GDF3 knockdown in NCCIT cells **35**
4.6 Influence of GDF3 on proliferation of NCCIT cells **37**
4.7 Transcriptome analysis of NCCIT cells upon GDF3 stimulation and knockdown **38**
4.7.1 Design of microarray analysis 39
4.7.2 Gene ontology (GO) term overrepresentation analysis 40
4.7.3 Validation of microarray data – new GDF3 target genes 41
4.7.4 Blocking of GDF3-receptors 43
4.8 HoxA9 as a new target gene of GDF3 – promoter analysis **44**
4.9 Effect of GDF3 on differentiation of NCCIT cells **46**
4.9.1 Microscopic analysis of the phenotype 46
4.9.2 Molecular analysis of the differentiation process 47
4.9.3 Growth kinetic, proliferation and apoptosis during RA-differentiation 48
4.9.4 Expression analysis of pro-apoptotic and pro-survival markers 49

5 Discussion **51**
5.1 NCCIT cells as a suitable CSC model to investigate the role of GDF3 ..... **51**
5.2 Genetic manipulation of GDF3 expression in NCCIT cells **52**
5.2.1 Prodomain-mediated instability of exogenous GDF3 ..... **52**
5.2.2 GDF3 knockdown in NCCIT cells **54**
5.3 Impact of GDF3 on proliferation **54**
5.4 Transcriptome analysis of GDF3 effects in NCCIT cells **54**
5.5 HoxA9 promoter analysis **58**
5.6 RA-induced apoptosis upon GDF3-knockdown in NCCIT cells **59**

6 Conclusions **62**

7 Perspectives **64**

8 List of references **66**

9 Appendix **82**

List of publications and presentations **86**

Eidesstattliche erklärung **87**

ABBREVIATIONS

ACVR2	Activin type 2 receptor
ALK	Activin-like reptor
ALP	alkaline phosphatase
AML	acute myeloid leukemia
Ang	Angiopoietin
APL	acute promyelocytic leukaemia
BAK	BCL2 homologous antagonist killer
BAMBI	BMP and activin membrane-bound inhibitor
BAX	BCL2 associated protein X
BCL2	B cell lymphoma 2
BMP	bone Morphogenetic Protein
BMPR2	BMP receptor 2
BRCA1	breast cancer 1
BRE	BMP responsive element
BSA	bovine serum albumin
CDK4	cyclin dependent kinase 4
cDNA	complementary DNA
CLL	chronic lymphocytic leukemia
CSC	cancer stem cell
CXCL12	Chemokine (C-X-C motif) ligand 12
DAVID	Database for Annotation, Visualization and Integrated Discovery
DIABLO	diablo, IAP-binding mitochondrial protein
DISC	death-inducing signalling complex
DMEM	Dulbeco´s modified Eagle medium
dNTP	deoxyribonucleotide triphosphate
DR	death receptor
EC	embryonal carcinoma
ECM	extracellular matrix
EOC	epithelial ovarian cancer
EpCAM	epithelial cell adhesion molecule
ESC	embryonic stem cells
FACS	fluorescence activated cell sorting
FBS	fetal bovine serum
Fig.	figure
GAPDH	Glyceraldehyde 3-phosphate dehydrogenase
GDF	Growth and Differentiation Factor
GFP	green fluorescent protein
GO	gene ontology
Grem2	Gremlin 2
Hox	homeobox
IL-6	Interleukin 6
MAPK	mitogen-activated protein kinase
MIS	Müllerian inhibiting substance
mRNA	messenger RNA
MSK1	mitogen- and stress-activated kinase
Oct4	octamer-binding transcription factor 4
Pax6	Paired Box 6
PB	phenylbutyrate
PBS	phosphate buffered saline
PC	proprotein convertase
PML	promyelotic leukemia
qPCR	quantitative PCR
RA	retinoic acid
RAR	retinoic acid receptor
RARE	RA response elements
rh	Recombinant human
RXR	with retinoid X receptors
SBE	Smad binding element
scr	scrambled
shRNA	short hairpin RNA
Sox2	SRY (sex determining region Y)-box 2
Tab.	Table
TBX3	T Box 3
TGFbeta	Transforming Growth Factor beta
TRAIL	tumor necrosis factor-related apoptosis-inducing ligand
TUJ1	Neuron-specific class III beta-tubulin
VEGF-A	vascular endothelial growth factor A

1 INTRODUCTION

1.1 Heterogeneity of cancer

The first written record about cancer was made in approx. 3000 BC in the Egyptian Edwin Smith Papyrus and describes a case of breast cancer [1]. More than 5000 years later, cancer is the leading cause of dead in the developed world and the second one in the developing world [2] and account for 13% of all deaths each year [3].

The understanding of cancer pathology evolved dramatically in the recent decades. Instead of a bulk mass of vastly proliferating cells, solid tumors are now considered to resemble an organ-like structure comprising of neoplastically changed cells, as well as non-transformed host stromal cells embedded in an extracellular matrix. Among the cancer cells a high grade of functional and morphological heterogeneity can be observed. Varying grades of heterogeneity have been detected between different types of tumor, patients and even the primary tumor and the metastasis in one individual [4][5].

The intratumoral heterogeneity arises in multiple ways. The most common and well-established theory is clonal evolution (Fig. 1.1). It postulates that stochastic genetic [6] and epigenetic [7] changes occur in cancer cells, which generates several subpopulations characterized by different genotype, gene expression profile and differential response to therapeutic agents. New high-throughput sequencing technologies deliver growing body of evidence supporting the assumption that due to high mutation rate in cancer, each tumor displays multiple clonal phenotypes. Therefore, each tumor is to be considered and treated as multiple diseases [8].

Such differences can also be driven by extrinsic factors, such as microenvironmental cues. The surrounding tissue is responsible for providing specific signals, which shape the morphology of the tumor and modulate its gene expression [9][10]. An impressive example was given by the injection of teratocarcinoma cells into a mouse blastocyst. The embryonic environment completely reversed malignant character of the tumor cells, so that healthy animals of mixed genetic background were born [11].

Conversely, a second model explaining the origin of tumor heterogeity - the 'cancer stem cell' (CSC) model postulates that only a small population of cancer cells with stem cell-like properties accounts for self-renewal, metastasis and therapy resistance. The differentiation of CSCs generates a variety of phenotypically and functionally different non-tumorigenic cells with limited proliferative capacity and a hierarchical organization of cells in the tumor (Fig. 1.1). This process provides a mechanism to

generate a phenotypical variety beyond the heterogeneity that can be attributed to clonal selection or environmental differences [12].

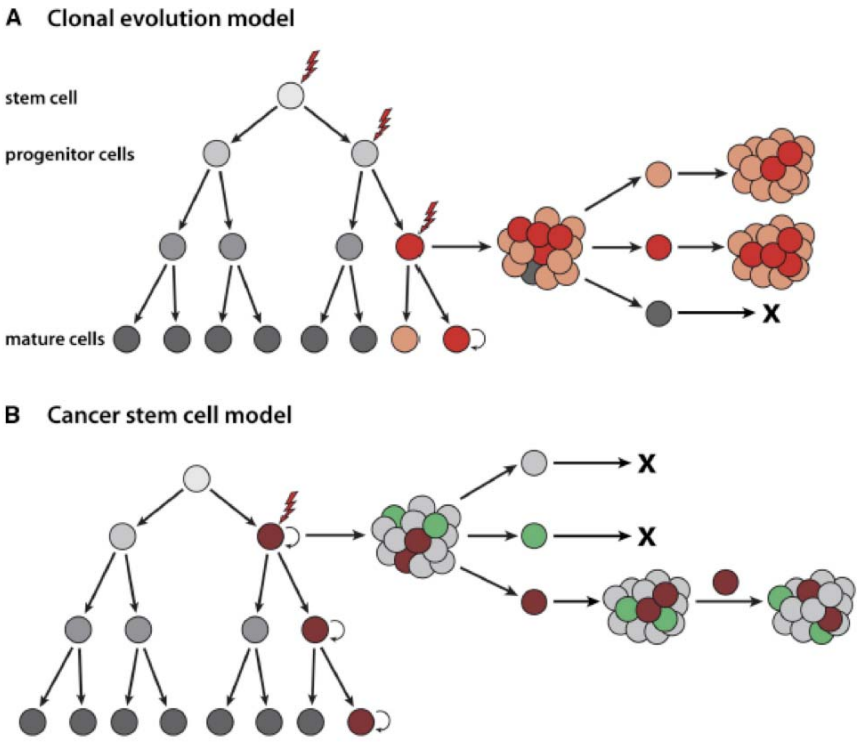

Fig. 1.1 Clonal evolution vs. CSC models (from [13]).
A. Clonal evolution model: the red cell acquires a series of mutations and represents a dominant clone. The red and orange cells have similar tumorigenic potential. Grey cells have lost their proliferative capacity due to stochastic events. The heterogeneity results from the diversity of the cells in the tumor.
B. CSC model with hierarchical organization: the brown cell represents a progenitor cell, which has acquired CSC phenotype due to mutation. It can divide asymmetrically giving rise to progenies of the same phenotype (self-renewal) or to a range of tumor cells with limited proliferative potential.

1.2 Cancer stem cells

The concept of the CSC model arose more than 50 years ago from observations that in some cancers, such as germ lineage cancer, neuroblastomas and some myeloid leukemias, cellular progenies having limited proliferative potential exist, despite retaining the oncogenic mutations of their malignant progenitors [13]. The advent of flow cytometry facilitated the characterization of different cancer cell populations and enabled the isolation of rare CSCs, so that their existence could be proven also in other cancer types, such as breast cancer [14], colon cancer [15][16], pancreatic cancer [17], ovarian cancer [18–20] and many more. However, no universal CSC marker panel has been defined so far. A number of markers have proven useful to enrich the CSC subsets, such as CD133, CD44, EpCAM and CD34 and CD38, but none of these are expressed exclusively by CSC. More reliable information regarding CSC identity can be obtained from *in vivo* transplantation experiments. Such assays can also be employed to roughly estimate the frequency of CSC, although great technical limitations,

including species-specific differences in growth factors and receptors and the level of immune recognition should be taken into consideration.

It has been observed, that the frequency of CSC in specific tumors can vary substantially [21]. These differences have important clinical consequences. Since the differentiation grade and the stage of maturation arrest in the tumor lineage correlates with its malignancy and clinical outcome for the patient (Fig. 1.2), Boiko et al. proposed that at early stages of cancer, the self-renewing, rare, tumorigenic population can differentiate into non-malignant progeny, and at later stages the self-renewing cancer cell population may become the dominant population in a tumor [22]. Examples of poorly differentiated, fast progressing cancer with little or no differentiation are acute myeloid leukemia (AML) or some of the neuroblastomas. The opposite is represented by chronic lymphocytic leukemia (CLL). In the latter, most of the cancer cells comprise of resting lymphocytes, which do not die, but accumulate instead.

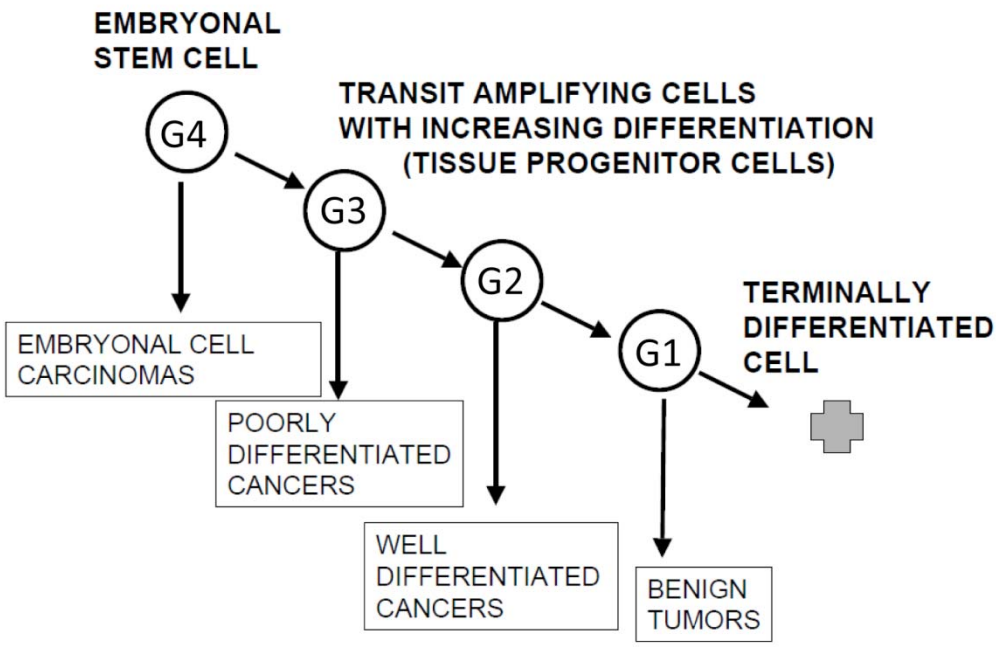

Fig. 1.2 Relation between the differentiation stage of cell lineage and cancer type (adapted from [23]).
G1-G4 refers to tumor grades according to American Joint Committee on Cancer.

1.3 'Stemness'-signature of cancer

In order to characterize CSC as a cell population, there have been attempts to define their gene expression profile [24–26]. The bioinformatic analysis of two cohorts of individuals with AML, revealed that despite the putative genomic heterogeneity among the CSC pool a core transcriptional program is shared by tissue stem cells and corresponding CSC. Confirming the existence of CSC as a clinically relevant aspect of cancer biology, Eppert *et al.* [24] and also others [27–29] showed that the level of stemness influences the clinical outcome of the disease: cells with stem cell-like activity are

the main drivers of cancer progression and therefore the key determinants of therapeutic response [30].

Since Yamanaka established reprogramming of somatic cells to pluripotent cells by defined factors [31], the expression of the 'master' stemness genes, such as Nanog and Oct4, in cancerous tissue drew growing attention from the scientific community. An ES cell-like gene expression signature has been detected in poorly differentiated, aggressive, human solid tumors arising in various tissues, including the breast, the bladder and the brain [32][33] and was associated with a poor prognosis. This signature is also important for the diagnostic of germ cell tumors with metastatic potential [34][35]. Oct4 was recently described as the definitive marker of CSC in a mouse model with p53 deletion, in which tumors are formed spontaneously [36]. These Oct4-expressing cells displayed increased self-renewal capacity and higher tumorigenic and metastatic potential than other cell subsets, although Oct4 was expressed only at low level, when compared with ESC. These results are in agreement with other reports about enhancement of cell line malignancy *in vivo* and *in vitro* upon Oct4 overexpression [37–40]. Similar to Oct4, Nanog has also been reported to be expressed in putative CSC and to account for increased self-renewal capacity and drug resistance in several cancer types [33], [41–43]. A couple of other markers, associated with pluripotency, such as Nodal or GDF3, are also considered as definitive features of CSC.

In cancers which follow the CSC model, the differences between cells with stem cell-like properties and their non-tumorigenic progenies may have a significant impact on the clinical outcome of the therapy: eradication of the CSC would, in theory, cure the cancer. However, CSC have repeatedly been reported not to respond to treatment and are therefore considered responsible for disease recurrence. Many mechanisms accounting for the chemo- and radio-resistance have been identified, including ABC transporter expression, aldehyde dehydrogenase activity and activation of key (stemness-associated) signalling pathways [44]. Therefore, the qualitative and quantitative characterization of the stemness-signature is proposed to serve not only as diagnostic and prognostic marker, but also as an indicator for the choice of therapy.

1.4 Modeling of CSC *in vitro*

The existence of CSC has been proven in practically all tumors where these cells have been searched for. The CSC can be propagated by transplantation assays, but their cultivation *in vitro* remains a challenge. In the quest for a suitable model of CSC *in vitro*, a variety of cell lines have been tested for the presence of CSC. As in primary cancer, the frequency of CSC in the established cell lines varies dramatically and strongly depends on the microenvironment. It has been shown that a 3D culture in spheres, but not in monolayer [45][46], as well as medium conditioned with particular cytokines (e.g.

VEGF, HGF) enrich the CSC population [47][48]. To date isolation of CSC from existing cell lines and their subsequent cultivation as a pure population has not been successful. This fact is not surprising, since almost all types of stem cells - except for embryonic stem cells (ESC) and mesenchymal stem cells (MSC) - need partner cells to maintain their phenotype.

Embryonal carcinoma (EC) cells represent the stem cells of teratocarcinoma [49] and have also been termed the malignant equivalent of embryonic stem cells [50]. Just like ESC, EC can be cultured indefinitely without phenotypic changes, display ES-like signature, including the expression of main pluripotency-network associated transcription factors, and are not only able to differentiate *in vitro*, but are also highly tumorigenic *in vivo*. As many of the molecular pathways that underlie tumorigenesis are also involved in normal embryogenesis, the study of EC cells provides an excellent model to elucidate the mechanisms involved in tumour growth and self-renewal. In the scope of this framework, EC are expected to be a suitable model of CSC *in vitro* [51–53].

1.5 Differentiation therapy

The CSC theory implies that the stem-like cells in tumors undergo a (series of) mutation(s), which results in delayed or aberrant differentiation, or even a maturation arrest [54–56]. Therefore, the idea of fighting cancer by overriding the differentiation block, to specifically target CSC by exploiting their capacity to differentiate, is an obvious choice. The strategy for getting the malignant potential under control is to force the tumor cells into finally differentiated status with only limited proliferative capacity.

Several differentiation agents of distinct molecular structure and displaying variable modes of action have been described in literature, such as sodium phenylbutyrate (PB), bone morphogenetic protein 4 (BMP4) or retinoic acid (RA), among others.

PB is an aromatic fatty acid, which is converted by the cell into phenyl acetate and acts as an inhibitor of histone deacetylase. It accounts for its use as an anti-cancer agent by induction of differentiation through epigenetic modifications. PB was reported to affect glioblastoma [57][58] and also displays positive effects in patients with AML and myelodyspalstic syndrome [59].

BMP4 is a potent cytokine from the TGFβ family, which induces differentiation as early as in the embryo during gastrulation [60][61]. Its ability to shape the cell fate, however, does not cease after early stages of development. BMP4 can display distinct, even opposite effects on stem cells and cancer cells of different origin. On one hand, it has been reported that it promotes terminal differentiation and apoptosis in colorectal cancer CSC [62], inhibits cell proliferation and induces cell death in glioma stem cells [63] or induces neuronal differentiation in synovial sarcoma [64]. On the

contrary, pro-proliferative and pro-invasive properties of BMP4 have been demonstrated in prostate and breast cancer [65][66].

The only established and clinically approved cyto-differentiating agents are retinoic acid and its derivatives. Retinoic acid can be produced from retinol (Vitamin A) by simple oxidation. Epidemiological studies show that lower vitamin A intake results in a higher risk of developing cancer, which aligns with observations of vitamin A-deficient animals [67]. The most successful application of retinoic acid is the treatment of acute promyelocytic leukaemia (APL), which is a subtype of AML. The disease arises from a chromosomal translocation resulting in the formation of a fusion oncoprotein PML-RARα, whose signalling differs from that of PML and of RARα [68][69]. Application of retinoic acid promotes the degradation of the mutant PML-RARα protein and dissociation of its co-receptor, causes cell cycle arrest at G1 phase and inhibits cell proliferation [70], leads to differentiation and eventual apoptosis of APL cells through the induction of the tumor-selective death ligand tumor necrosis factor-related apoptosis-inducing ligand (TRAIL) [71].

Although a great deal of success of the anti-APL therapy is due to specific interaction of RA with the PML-RARα protein, not only APL patients can profit from RA as a anti-cancer agent. Retinoids suppress carcinogenesis in animal models for skin, oral, lung, breast, bladder, ovarian, and prostate tumorigenesis [72–76]. In humans, retinoids reverse premalignant human epithelial lesions, induce the differentiation of myeloid cells, and prevent lung, liver, and breast cancer [77–79]. Furthermore, clinical trials employing all retinoid derivatives individually or in combination with other agents to treat breast cancer [80], squamous cell carcinoma [81], neuroblastoma [82] and hepatocellular carcinoma [83] are ongoing .

However, there are several obstacles to overcome in order to enhance the efficiency of the RA-treatment. A common problem is the resistance due to downregulation of RA-receptors. This phenomenon accounts for the non-responsiveness to RA-treatment when the breast tumor becomes more aggressive [84][85], although in early stages of breast cancer the RA-therapy proves efficient.

Retinoic acid syndrome represents another problem connected to RA-therapy to circumvent. This syndrome consists of fever, weight gain, respiratory distress, interstitial pulmonary infiltrates, pleural and pericardial effusion, episodic hypotension, and acute renal failure. Therefore, the dosing schedule is critical to avoid these severe side effects. However, if recognized early, this syndrome is well treatable [86].

Ironically, although the growth-inhibitory, pro-differentiation and -apoptotic effects of RA were discovered by treatment of teratocarcinomas *in vitro*, this has not proven to be effective treatment

in vivo. Clinical studies have shown, that upon RA-treatment some cells might differentiate, but the malignant core remains [30]. However, the investigations were performed a long time ago, when no synthetic retinoids or specialised delivery methods (e.g. by liposomal enrichment) were available and combination of retinoids with other small molecules exhibiting cumulative effect on the outcome of the therapy had not been routinely tested. A likely reason explaining the varying success of the RA-treatment in solid cancer is the broad range of pleiotropic effects caused by the retinoids [87]. While in some cell types RA affects only cell growth, in others apoptosis can be efficiently induced. Therefore, the molecular basis of RA signalling and its interaction with other signalling pathways have to be investigated in more detail.

1.6 RA signalling and its anti-cancer effects

1.6.1 RA signalling cascade

RA is a lipophilic molecule, which can easily cross the cell membrane and bind to specific nuclear receptors - retinoic acid receptors (RARs) of 3 subtypes: α, β and γ. For each subtype there are at least 2 isoforms, which differ only in the N-terminal region. RARs remain in the heterodimeric complex with retinoid X receptors (RXRs), which also consists of 3 types - α, β and γ. This complex can enter the nucleus and bind to specific DNA sequences named RA response elements (RAREs). In the absence of a ligand, RARs are associated with large protein complexes endowed with enzymatic activities to maintain chromatin in a condensed and repressed state. Upon ligand binding the RARs become phosphorylated, the co-repressor proteins are released from the complex and an ordered and coordinated recruitment of co-regulators with different enzymatic activities takes place. This results in changes in the chromatin structure surrounding the promoter region, enabling the docking of transcription machinery including RNA Polymerase II and general transcription factors and the transcription initiation (reviewed in [85][87][88]).

There is additionally a range of non-genomic effects triggered by RARs. Some of the receptors are anchored at the cytoplasmic side of the plasma membrane. Upon ligand binding and phosphorylation, RARs can activate several kinase cascades, such as p38-MAPK and mitogen- and stress-activated kinase MSK1, in order to fine-tune the transcription [89].

In several tissues and organs, the loss of a RAR subtype has been associated with tumorigenesis. Consequently, RARs have been considered as tumor suppressors. In lung, breast and cervix loss of RARβ is often correlated with tumorigenesis. In such cancers RARβ is often either deleted or its promoter has been silenced. These findings were complemented by experiments, where expression level of RARβ was restored and the tumorigenicity of the cancer cells decreased [90][91].

Furthermore, non-responsiveness to RA-therapy was shown to be possible to overcome by exogenous introduction of RARβ.

RARγ was found to be absent in oral keratinocytes from head and neck cancers [92]. In the mouse model, RARγ knockout predisposes the animals to skin cancer.

However, still very little is known about the specific gene set activated by particular receptors and the molecular mode of action of RARs remains unclear.

1.6.2 TRAIL-mediated apoptosis

Most recently it has been observed that RA exerts its pro-apoptotic effects selectively on tumor cells by activating the TRAIL pathway [93]. RA was reported to either induce production of TRAIL ligand or upregulation of TRAIL receptors. TRAIL is a ligand formed by homotrimerization (secreted or anchored in the plasma membrane), which can bind to so called 'death receptors' (DR4/DR5). Those are characterised by an intracellular 'death domain' transmitting apoptotic signal. Three other receptors capable of binding TRAIL act as 'decoys' [94][93] .

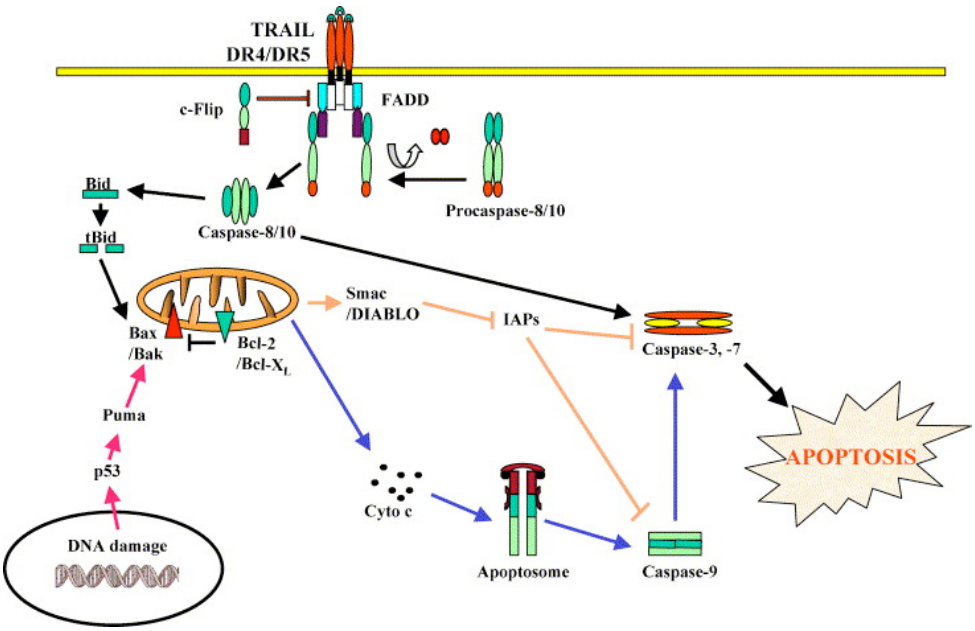

Fig. 1.3 TRAIL signalling pathway in cancer (from [95]).

After binding of TRAIL to the 'death receptors', the trimerized receptors recruit a variety of proteins building up a death-inducing signalling complex (DISC), with associated Caspase-8. This molecule can induce two pathways. The 'extrinsic' one involves direct activation of effector caspases (caspase-3, -6, -7) leading to disassembly of the cell. The 'intrinsic' pathway starts with cleavage of Bid. Truncated Bid translocates to the mitochondria, where it interacts with members of BCL2 family, Bax and Bak to from pores in the outer mitochondrial membrane. This results in release of pro-apoptogenic factors,

such as cytochrome c and Smac/DIABLO, which in turn initiate assembly of a functional apoptosome [96].

Employment of TRAIL in anti-cancer therapy is a tempting opportunity, but its short half-life in plasma, inherent instability and potential hepatotoxicity hampers the systemic application in patients [97][98]. Additionally some cancer types display TRAIL resistance due to e.g. overexpression of BCL2 [99].

1.7 TGFβ family

The cytokines from the TGFβ family are encoded by 42 open reading frames in human, 9 in flys and 6 in worms [100] (Fig. 1.4). It contains two subfamilies: (1) the TGFβ/Nodal/Activin and (2) BMP (bone morhogenetic protein)/GDF (growth and differentiation factor)/MIS (Müllerian inhibiting substance) subfamily, as defined by sequence similarities and specific signalling pathways they activate [101].

Although the ligands are expressed in different temporal and tissue specific patterns and elicit a plethora of cellular responses, they all share a set of common structural features and signalling pathways.

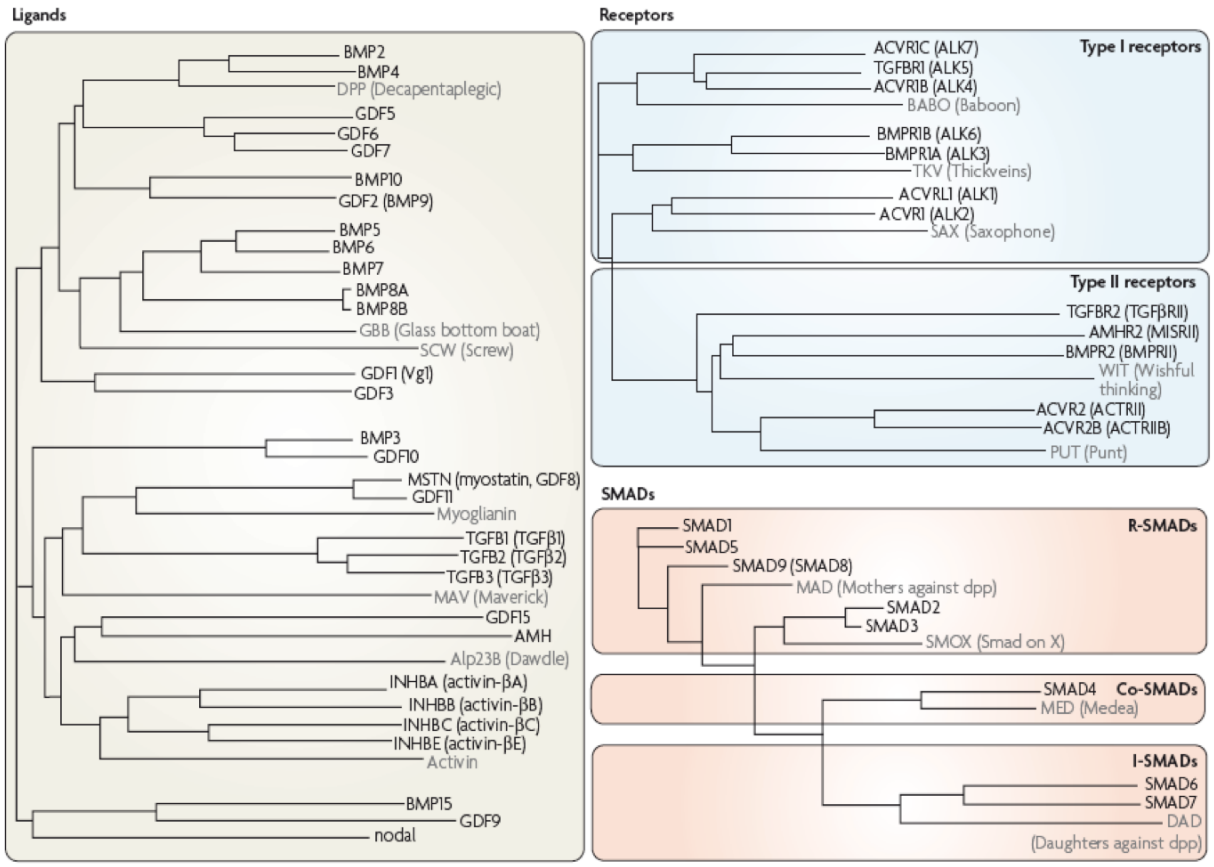

Fig. 1.4 Ligands of TGFβ family, receptors and intracellular signalling mediators Smads (from [101]).

1.7.1 Structure of TGFβ ligands

All TGFβ ligands are synthesized as large precursor molecules, consisting of a signal peptide, an N-terminal prodomain and a C-terminal mature domain. During synthesis, prodomains interact non-covalently with mature domains, maintaining the molecules in a conformation competent for dimerization. Dimeric precursors have to undergo proteolytic processing by proprotein convertases to release the mature peptide - the active form of the ligand [102]. The active ligand is a dimer stabilized by hydrophobic interactions, which are further strengthened by an inter-subunit disulfide bridge in most cases [103]. The maturation process takes place either intracellularly, before protein secretion, or extracellularly, in the vicinity of the producer cell or at distant sites, adjacent to the acceptor cell [104][105]. The distinct spacial processing as well as the prodomain identity regulates the half-life and bioavailability of the ligands [106].

1.7.2 Signalling pathways triggered by TGFβ ligands

The dimeric ligand binds to and joins the dimers of receptors of type I, type II and sometimes additional co-receptor to a signalling complex (Fig. 1.5). A series of phosphorylation events takes place, leading to phosphorylation of the receptor complex as well as intracellular signalling mediators R-Smads in the C-terminal region: Smad1/5/8 or Smad2/3. Once phosphorylated, R-Smads associate with co-Smad, Smad4, and translocate into the nucleus. The Smad-complex then acts as a transcription factor and incorporates different DNA-binding cofactors that confer target gene selectivity and influence the recruitment of either transcriptional coactivators or corepressors [107].

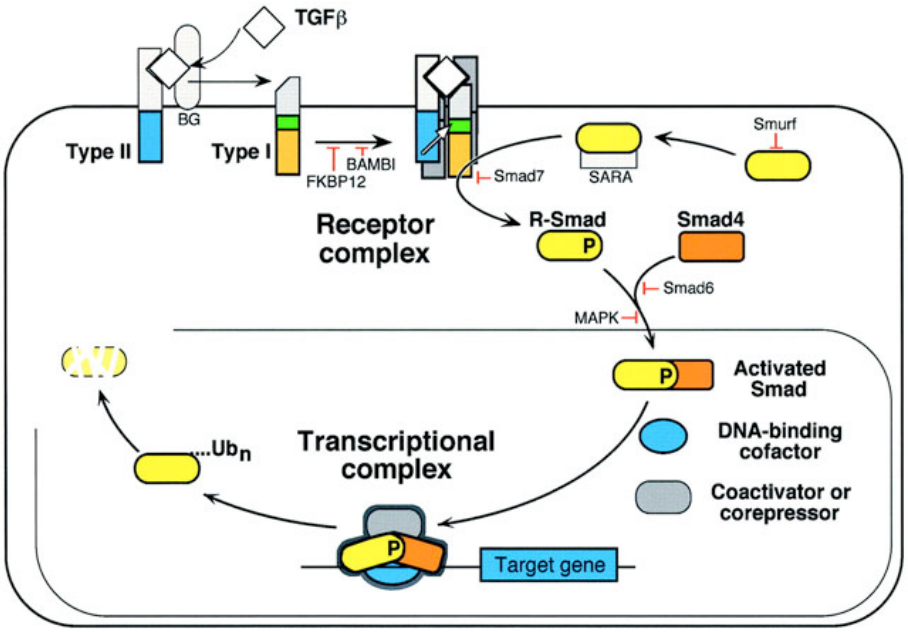

Fig. 1.5 Signalling pathways of ligands from TGFβ family (from [108]).
The ligand TGFβ assembles a receptor complex that activates Smads, and the Smads assemble multisubunit complexes that regulate transcription. The central components of this signalling system are indicated along with the sites of action of various positive and negative regulators.

The phosphorytaled receptor complex can also activate various mitogen-activated protein kinase (MAPKs) and phosphoinositide 3-kinase (PI3K) pathways - a process that is collectively referred to as non-canonical or alternative TGFβ signalling. Mitogens, acting through MAPKs and cell cycle events acting through cyclin dependent kinase 4 (CDK4) can in turn phosphorylate R-Smad in the linker region restricting their availability for the canonical TGFβ signalling [109].

Several variables determine the extent of stimulation by ligands from TGFβ family, depending on the cytokine itself, cell type and the microenvironment. To give an impression about the complexity of the process, few mechanisms will be briefly described. The first level of signalling control is the availability of the ligand in the extracellular space. Various ligand-trapping proteins control the formation of ligand-receptor complex [110]. The interplay of Nodal and its extracellular inhibitors Leftys highlights the importance of this mechanism, constituting the left-right patterning during early embryonic development [111]. At the receptor-level, the signalling strength can be modulated by the presence of decoy receptors, such as BAMBI (BMP and activin membrane-bound inhibitor), which prevent the Smad phosphorylation. Other possibility to restrict the signalling is the interaction with intracellular, inhibitory Smads (I-Smads), Smad 6 and 7. Binding of I-Smads limits the availability of R-Smad by acting as 'decoy' and preventing the shuttling of Smad-complexes into the nucleus. Finally, in the nucleus SKIL and Sno can repress the transcriptional activity of Smads (reviewed in [101], [112][113]).

1.8 GDF3 - a TGFβ family member associated with stemness

1.8.1 Signalling mode

GDF3 has been discovered only 20 years ago using degenerate oligonucleotides corresponding to conserved regions among known members of TGFβ family [114]. It shares the common structure and biosynthesis pathway with other TGFβ family members, consisting of large prodomain and 14-16kDa mature peptide. The characteristic feature of this ligand that has only six of the classical seven cysteins present in other TGFβ superfamily members [115], is that it ismissing the fourth cysteine – the one involved in inter-molecular interactions between TGF-β family members and with their secreted inhibitors [116].

GDF3 was postulated to be processed very poorly, which significantly influences its signalling capacity. Using the approach of domain swap, Andersson [117] and Chen [118] showed that this effect is mediated by the GDF3-prodomain. On the contrary to the natural GDF3, once a hybrid protein with BMP2- or Activin-prodomain was expressed, a robust induction of Smad2/3 signalling pathway could be observed. The activation of Smad2/3 signalling cascade by GDF3 depends on the presence of ALK4 or ALK7 (type I receptors), ACVR2A or ACVR2B (type II receptors) and co-receptor

Cripto. However, different mode of signalling has also been proposed for GDF3. Levine [119] found that GDF3 is an inhibitor of its own subfamily and blocks classic BMP signalling by direct interaction with BMP proteins in frog embryos and mouse embryonic stem cells.

1.8.2 Function of GDF3

GDF3 is one of only three members of TGFβ family, along with Nodal and Leftys [120], that are highly expressed in the pluripotent cells of the blastocyst during the early mouse embryonic development and in ESC *in vitro*. In fact, GDF-3 has become one of the most reliable markers of stemness [121]. The exact, temporal expression pattern during embryonic development remains to be defined, since collected data is contradictory. On one hand, GDF3 expression throughout until day E10.5 with a peak at day E8.5 was reported [119], on the other - no GDF3 could be detected at day E6.5 [118].

To assess the protein function of GDF3 during the embryonic development, Andersson [122] and Chen [118] generated GDF3 knockout mice. Both groups observed increased embryonic lethality with slightly different survival rates (50% vs. 70% respectively). The most severely affected embryos were either resorbed, or corresponded to empty visceral yolk sacs at E8.5. Less severely affected embryos exhibited characteristic morphological phenotypes, including prominent constriction at the embryonic/extra-embryonic junction, poorly differentiated anterior structures and abnormal mesoderm derivatives. In summary, GDF3 functions through a Nodal-like pathway to provide a crucial signal for anterior visceral endoderm formation and movement in pre-gastrulation development [118].

In vitro experiments with overexpression and knockdown of GDF3 in ESC have revealed that GDF3 has a species-dependent role: higher levels of GDF3 support stemness in human ESC, while lower levels of GDF3 support stemness in mouse ESC [119].

The majority of GDF3 mutants survive until adulthood without any overt abnormality and are fertile. They do not display any phenotype under normal conditions. However, GDF3 knockout mice gain less weight and accumulate less adipose tissue during diet-induced obesity despite normal food intake [117]. The involvement of GDF3 in the metabolism of adipose tissue was also profoundly demonstrated in mice transduced with GDF-3, which gain weight significantly more than wildtype individuals, when fed with high fat diet. The phenotype included greatly expanded adipose tissue mass, increased body adiposity, highly hypertrophic adipocytes, hepatic steatosis, and elevated plasma leptin [123].

Apart from adipose tissue, GDF3 has also been reported to be expressed also in adult bone marrow, spleen, thymus and brain. There is little information not only about the identity of GDF3-producing cells, but also about GDF3 function in these tissues.

1.8.3 GDF3 in cancer

With growing body of evidence for reactivation of embryonal signalling pathways in cancer, role of GDF3 in tumorigenesis and tumor progression has drawn more attention. Along with other embryonic stem cell markers, GDF3 was shown to be expressed in several cancer types such as breast carcinoma [124][125], melanoma [126], seminoma [125] and testicular germ cell tumors [127]. While Nanog, Oct4 and Sox2 were identified as stemness-promoting transcription factors, the role of GDF3 is poorly understood. Results published by others to date, regarding the putative role of this molecule in cancer biology are contradictory. It was demonstrated, that GDF3 inhibits the proliferation of breast carcinoma cell line MCF7 [124], but augments proliferation of B16 myeloma and can promote neuronal differentiation of PC12 cells [128].

To date, no extensive analysis of GDF3 role in cancer has been undertaken.

2 AIMS OF THE STUDY

CSCs, characterized by their extensive self-renewal capacity and multidifferentiation potential, are believed to be the chief cause of chemotherapy resistance and disease relapse in various forms of cancer. Recent reports have shown that the most aggressive cancer phenotype correlates with ES-like signature of CSCs. However, little is known about the role of the pluripotency marker GDF3, a cytokine from the potent TGFβ family, in cancer. The aim of this work was to shed more light on GDF3-mediated signalling, downstream targets and its impact on differentiation events in CSCs. In order to establish a CSC model, an embryonic carcinoma cell line, NCCIT, was extensively characterized. The following questions were to addressed by this study:

1. What is the signalling pathway of GDF3 in NCCIT cells?

2. What is the influence of GDF3 on proliferation of NCCIT cells?

3. What are the target genes of GDF3 and which processes are regulated by this cytokine?

4. How does GDF3 influence the differentiation of NCCIT cells *in vitro*?

For this purpose, NCCIT cells were stimulated with GDF3 and the signalling cascade thus triggered was characterized by luciferase assays, immunofluorescence staining and western blot. Additionally, the secretion, processing and stability of the GDF3 precursor molecule and mature GDF3 were assessed. Further, a comprehensive transcription profiling by cDNA microarray of NCCIT cells stimulated with different concentrations of GDF3 and Nodal - a GDF3 agonist, or with endogenous GDF3 signalling disrupted by shRNA-mediated knockdown, was undertaken. The microarrays results, confirmed by qPCR, revealed which biological processes GDF3 is involved in. Finally, to investigate the role of GDF3 in differentiation, RA-mediated neurogenesis was induced *in vitro* in GDF3-knockdown and control NCCIT cells. The results of transcriptome analysis and differentiation assays were the extrapolated to draw conclusions about the role of GDF3 in the biology of CSCs.

3 MATERIAL & METHODS

3.1 Cell culture

293T cells and NCCIT cells were obtained from ATCC (American Type Cell Collection). The cells were maintained and expanded in DMEM with 10%FCS and 1% penicillin/streptomycin. When the confluence reached 95% the cells were splitted using 1x Trypsin/EDTA in ratio 1:5-1:8.

3.1.1 Neuronal differentiation

The NCCIT cells were seeded at the density $1.5x10^5$ cells/well in CollagenR (Sigma)-coated 24-well plate in RPMI medium with 5%FCS and 1% Penicillin/Streptomycin. On the next day the medium was changed to RPMI medium with 5%FCS and 1% Penicillin/Streptomycin with 10µM all-trans retinoic acid (Sigma) diluted in DMSO (Roth). The medium was changed every 2 day and the cells were splitted when the confluency reached 95%.

3.1.2 Stimulation with ligands from TGFbeta family

The NCCIT cells were seeded in 24-well plate ($2x10^5$ cells/well) one day before stimulation. Prior to stimulation the medium was changed and the indicated concentrations of rhGDF3, rhNodal or BMP2 were added. The SB431542 inhibitor was applied to the cell culture medium with final concentration of 10µM. Cells were harvested after 3h by aspirating the medium and adding 300µl of RA1 buffer.
The ligands and the inhibitor were purchased from R&D Systems.

3.2 Apoptosis assay

The NCCIT cells were harvested by 1x Trypsin/EDTA and washed once in 1x Annexin V staining buffer. Then the cells were stained with Annexin V-Pacific Blue (1:25) purchased from Cell signalling for 15min at RT. Afterwards one washing step with 1mL of 1x Annexin V staining buffer was performed and the sample was immediately analyzed by flow cytometry.
Flow cytometry analysis was carried out using a MACSQuant® Analyzer (Miltenyi, Germany) flow cytometer and the data was analyzed using FlowJo software, version 7.6.5 (Tree Star Inc., USA).

Tab. 3.1 Recipes for buffers used for apoptosis assay

10x Annexin V Binding buffer	Running buffer for FACS analysis
0.1M Hepes pH7.4	PBS
1.4M NaCl	0,5 % BSA
25mM CaCl2	0,01% NaN3

3.3 Proliferation assay

$1x10^6$ cells were stained with 10µM CellTrace® Violet (Invitrogen) diluted in DMEM with 10%FCS and

1% Penicillin/Streptomycin for 1h at 37°C in water bath. The remaining dye was washed out, the cells were resuspended in the culture medium and seeded in 24 well plate. The efficiency of the staining was tested by flow cytometry after harvesting the cells 24h later.

3.4 Lentivirus production and transduction

To produce lentivirus containing shRNA cassette a three-plasmid system was used, on which the viral genes are subdivided for the biosafety reasons. Plasmid pAX2 carries the *gag-pol* region and pVSV-G encodes envelope proteins from the viral env region. The third plasmid pLL3.7 contains the insertion cassette including the shRNA constructs and GFP reporter.

The virus was produced by tranfection of 293T cells by calcium phosphate transfection method. 5,6 x 10^6 HEK 293 T cells were seeded the day before transfection in a 10 cm culture dish (Corning, Germany). On the day of transfection, the transfection mixture was prepared as followed:

15 µg pLL3.7 (containing shRNA cassette)

10 µg pAX2

5 µg pVSV-G

in 790 µl H_20.

+ 200 µl $CaCl_2$ (1,25 M).

1 ml BES puffer (50 mM (*N,N*-bis[2-hydroxyethyl]-2-aminoethanesulfonic acid), 280mM sodium salt, 1,5 mM Na2HPO4, pH6,95) was added drop-wise to the mixture with simultaneous agitating by bubbling air into the mixture. The solution was directly added drop-wise onto the cells and medium was changed after 5-6 hours at 37°C to DMEM with 2%FCS. Virus was collected after 24 and 48 hours and stored at 4°C.

Virus containing supernatant of HEK 293T cells was filtered through a 0,45 µm syringe filter (Filtropur S, Sarstedt, Germany) , concentrated in Spin® FX® UF Concentrator (Corning, Germany) and mixed with NCCIT cells with addition of 10µg/mL polybrene (Sigma, Germany). The medium was changed to regular medium the next day. 5 days after transduction, the transduction efficiency was monitored by GFP expression by fluorescence microscopy or flow cytometry.

3.5 Gene expression analysis

Basic gene expression as well as changes in expression upon stimulation with ligands or GDF3-knockdown were quantified on mRNA level by quantitave PCR (qPCR) and cDNA microarray.

3.5.1 RNA isolation and cDNA preparation

Isolation of RNA was performed using the NucleoSpin® RNA II kit (Macherey-Nagel, Germany) following the manufacturer's instructions. For monolayer cultures 350 µl RA1 buffer containing 1:1000 beta-mercaptoethanol (Sigma) were directly added onto the PBS-washed cell layer and

detached using a cell scraper (Sarstedt, USA). For the elution step, 20 or 30 µl RNAse-free H20 were used. Isolated RNA was stored at -80 °C.

Reverse transcription of purified RNA was carried out using the TaqMan® Reverse Transcription Reagents cDNA kit (Applied Biosystems, USA) as follows:

200-400 ng RNA

2 µl TaqMan 10x buffer

0,5 µl oligodTs

0,5 µl Random Hexamer

4,4 µl $MgCl_2$ (25 mM)

0,3 µl Reverse Transcriptase

0,4 µl RNase Inhibitor

4 µl dNTPs (25mM each)

in 20 µl H_20 (DMSO free)

Transcription was carried out in a thermo cycler (Peqlab, Germany) with an annealing step for 10 minutes at 25°C, an elongation step for 40 min at 48°C and an inactivation step for 5 min at 95°C to inactivate the reverse transcriptase. Samples were stored at -20°C until further use.

3.5.2 qPCR analysis

qPCR was performed using 1 µl cDNA with 1µl primer mix and SensiFAST™ Sybr No-ROX kit (Bioline, Germany) in a volume of 20 µl. 96-well PCR plates (Biozym Scientific, Germany) were read with Stratagene MX 3005P™ Multiplex Quantitative PCR System (Agilent Technologies, USA).

First, samples were heated to 95°C for four minutes to achieve complete dissociation of the RNA-DNA double strain. Next, 45 cycles of DNA melting (95°C, 12 seconds), primer annealing (64°C, 15 seconds) and elongation (72°C, 12 seconds) of cDNA templates were performed. A dissociation curve was recorded by cooling the samples to 62°C and stepwise heating up to 95°C. The fluorescence intensity of SybrGreen was measured with every 0.5°C increment.

Melting curve analysis was performed to verify the amplification of the specific product without contamination by unspecific side products or primer dimers. The expression was normalized to housekeeping gene expression (GAPDH) and presented as housekeeping gene ratios in logarithmic charts. This data representation allows the possibility of comparing the expression strength of several genes. Expression rations were calculated according to the following formula:

Ratio:E^{cp}_{HK} / E^{cp}_{gene}

[cp: crossing point; E: amplification efficiency; gene, gene of interest; HK, house keeping gene]

As the deviation of the determined amplification efficiencies for particular target genes appeared to be smaller than 4%, the value was set to 1,95 for all calculations.

To detect expression of genes important for GDF3 pathways as well as pluripotency factors, the samples were prepared and run like described above for 30 cycles. After the run, the samples were mixed with 4µl of 6x loading buffer (Fermentas) and applied to 2% agarose gel with 5µl of etidium bromide (Roth). The gel electrophoresis was performed by 130V for 1h. The pictures of gels were taken by Fusion FX (PeqLab).

Tab. 3.2 List of qPCR primers

Gene	primer upstream	primer downstream
GDF3	GACTGACCGCAACACAAACATT	TTCGCTTTCTCCCAGACCAA
Cripto	GCTAACGCCTCTTTTCCCCCTA	CCCGAGATGGACGAGCAAAT
HoxA9	GAGAGCGGCGGAGACAAG	CGGTGAGGTTGAGCAGTCG
HoxA10	CGCAGAACATCAAAGAAGAGAGC	CTGAGAAAGGCGGAAGTAGCC
HoxB13	GTCTTGGGCTCTCGCTGGT	CGCCTCTTGTCCTTGGTGAT
TBX3	AGTCCTCCAGTGAACAAGCAG	TCAGCAGCGAAAAGGTGAG
Lefty2	GCACACCCTGGACCTCAG	TGCCCACACACTCGTAAGC
Nanog	GCGGACTGTGTGTTCTCTCAGGC	TTCCAGATCCGTTCACCAGATAG
Oct4	GACAACAATGAGAACCTTCAGGAGA	CTGGCGCCGGTTACAGAACCA
BMPR2	CATAATAGGCGTGTGCCAAAAA	GCTTGTGCTTGCTGTCGTTC
Wnt5A	ACGCCAAGGGCTCCTACG	CTTCTCCTTCAGGGCATCACC
ACVR2A	GGGAACTGGCTTCTCGCTGT	TAACCTGGCTTCTGCGTCGT
ACVR2B	ATGCTGCCCTTTGAGGAAGA	AGTCCGAGGTAGTGCCGTTG
ALK4	AGGGTCGGTTTGGGGAAGTA	AGCTGTGTCCAGGTGCCATT
ALK7	TATGATGTGACCGCCTCTGG	TCTGCCTCACGAAACCAAGA
Nodal	GAGGAGTTTCATCCGACCAACC	GAGGCACCCACATTCTTCCAC
Smad2	GCCGCCAGTTGTGAAGAGAC	TGGAGACGACCATCAAGAGACC
Smad3	GCTGACACGGAGACACATCG	AGCCTCAAAGCCCTGGTTG
Smad4	CTTTGAGGGACAGCCATCGT	GCCACAGGAATGTTGGGAAA
Smad7	GCTGAAACAGGGGGAACGA	AGTATGCCACCACGCACCA
Grem2	TTCCCTGTCCTTGTTCCTGGT	CCTCCTCGCTCACCGTCT
GAPDH	TGTTGCCATCAATGACCCCTT	CTCCACGACGTACTCAGCG
Pax9	CCTACCACAGCCCCAAGGT	AGCAACATAACCAGAAGGAGCAG
Nestin	GGCAGCGTTGGAACAGAGGTTGGA	CTCTAAACTGGAGTGGTCAGGGCT
LC Bmp2	CCTCATCCCAGCCCTCTGAC	GGTTGTTTTCCCACTCGTTTCTG
BMP4 LC	CGGGATCTTTACCGGCTTC	TCTGCTGGGGGCTTCATAAC
LC BMP7	ACTGTGAGGGGGAGTGTGC	CGAAGTAGAGGACGGAGATGG
Tie2	TGTTCCTGTGCCACAGGCTG	CACTGTCCCATCCGGCTTCA
BCL2	ACTTCTCCCGCCGCTACC	ATGACCCCACCGAACTCAAA
BAK	CCGTCCTCCACTGAGACCTG	GCCTCCTGTTCCTGCTGATG
BAX	TGGAAGACGGAGAGGAAACC	CCCAGACCACAACACAGTCC
TRAIL	CCTGGGAATCATCAAGGAG	GGACCATTTGTTTGTCGTTC
RARbeta2	GTTTGATGGAGTTGGGTGGAC	GATTGAGCAGTGTGCCGATG
Sox2	GCCCCCAGCAGACTTCAC	TCCCATTTCCCTCGTTTTTC
KLF4	GTCCCGCCGCTCCATTAC	GTTCGCAGGTGTGCCTTGA

3.5.3 Microarray analysis

cDNA microarray analysis was conducted in order to determine genome wide differential expressed genes upon differentiation or cell stimulation. For this application the human genome CGH Microarray 44K (Agilent) was utilized according to manufactures protocol. The microarray experiment was based on two-color ratio hybridization and a Low RNA Input Fluorescent Linear Amplification kit (Agilent) for RNA labeling. In brief, 500ng of total RNA was reverse transcribed with an oligo(dT)-T7 promoter primer and Moloney murine leukaemia virus-reverse transcriptase (MMLV-RT) to synthesize first and second-strand of cDNA. Fluorescence anti-sense cRNA was synthesized with T7 RNA polymerase that simultaneoulsy incorporates either cyanine 3-cytidine 5'-triphosphate (3-CTP) or cyanine 5-CTP. Labeling efficiency was verified with a Nanodrop photometer (Kisker). Before hybridization 2µg of each labeled cRNA product were fragmented and mixed with control targets and hybridization buffer according to the suppliers protocol (Agilent). Hybridizations were done overnight for approx. 19h at 60°C. The slides were then washed according to the manufacturer's protocol. Scanning of microarrays was performed with 5µm resolution using DNA microarray laser scanner (Agilent). Features were extracted with the image analysis tool A 6.1.1. (Agilent Technologies, USA) using default settings. Data analysis was performed with Rosetta Informatics Platform Resolver Built 4.0.

The overrepresentation analysis was undertaken by uploading the gene sets with p-value<0.05 and fold change>1.5 to Database for Annotation, Visualization and Integrated Discovery (DAVID) v6.7 and performing teh Gene Onthology analysis using Panther_BP_ALL entry.

Microarray data (accession number GSE44670) has been published in the NCBI GEO database.

3.6 Cloning

3.6.1 General procedures

All enzymes were purchased from Thermo Scientific.

<u>Oligonucleotides dimerization</u>

Oligos were resuspended in water at 60 pmol/µl. For DNA annealing 60 pmol of each oligo were mixed in 60 µl H_2O and placed at 95 °C for 5 min. Optimized hybridization conditions were provided by a slow continuous incubation temperature decrease (0,5 °C/min) to 65 °C followed by accelerated cooling rate of 2°C/min to 40°C.

<u>PCR</u>

To amplify a DNA fragment of choice, a PCR was performed, using cDNA (for cloning of expression vectors) or genomic DNA (for cloning of promoter constructs). The primers were designed using Primer3-freeware and ordered by TibMolBiol.

Vector restriction

2µg of plasmids or purified PCR products were digested with the restriction enzymes of choice according to the manufacturer's protocol. For the plasmids SAP treatment to dephosphorylate the 5´ends of the linearized fragment followed. The plasmid DNA was separated by agarose gel electophoresis and purified from agarose slices by Nucleospin extraction kit according to manufacturers protocol. The PCR Products were directly subjected to the purification by the same kit.

Ligation

Concentration of purified DNA was determined via absorption at 260nm using the Nanodrop (Kiesker) quantification system in order to adjust the DNA amount for optimal ligation. Linearized plasmids and annealed oligos or PCR Products were ligated with a 5-fold equimolar excess of DNA oligomers or PCR products. In total, 100ng DNA in 10 µl reaction volume was ligated at 14 °C over night.

Transformation

After ligation the vector constructs were transformed into E.coli (Top10 strain) by heat shock method. For this purpose 4µl of each ligation assay was incubated with 50µl chemical competent cells on ice for 5 min. Heat shock was performed for 40 seconds at 42°C and subsequently 300 µl SOC medium was added. The eppendorf tubes with bacteria suspension were shaken at 37°C for 20 min the cells were plated on ampicillin agar plates (100ng/ml) and incubated at 37 °C over night.

Screening for positive clones

Colonies were picked from agar plates by a pipet tip and cultured in 3mL liquid LB medium in 15mL tubes (Sarstedt, Germany) over night. Plasmid DNA was extracted by plasmid isolation kit NucleoSpin® Plasmid (Macherey-Nagel, Germany) according to suppliers instructions. To test for insert incorporation, purified DNA was digested with enzymes of choice and the resulting fragments were separated and evaluated by 1-2% agarose gel electrophoresis.

Sequencing

For DNA sequencing 200ng plasmid DNA was applied in the following reaction:

2µl sequencing buffer (5x)

0,75µl sequencing primer

1µl Big dye (containing dNTP and ddNTP and DNA polymerase)

200ng plasmid DNA

add dH_20 to 10µl final volume

Sequencing reaction was carried out for 30 cycles in a thermocycler (96 °C 10sec, 45 °C 5 sec, 60 °C 4 min). Unincorporated nucleotides were removed by Ethanol precipitation.

For this purpose, 250 µl Ethanol (95%) and 10µl Na-acetate (3M) were mixed to the sequencing reaction and centrifuged for 20 min at 4°C (13000rpm). The supernatant was discarded and the resulted pellet was washed with 350 µl Ethanol (70%) and centrifuged again. The washing solution was removed and the DNA pellet was dried at 50°C and resuspended in 20 µl water. The purified DNA fragments were analyzed (Abi prism 310 genetic Analyzer, Applied Biosystems) and the sequence was evaluated by Chromas sequence analysis software.

Plasmid prep

In order to obtain plasmid DNA in sufficient amount and quality for virus production plasmid maxi preparations were performed of a 400 ml E.coli Top 10 culture by the Nucleobon Xtra maxi plus kit (Macherey-Nagel, Germany) according to manufactures protocol.

3.6.2 Cloning strategies

Cloning of shRNA-cassette into pLL3.7 vector

The shRNA-cassettes targeting GDF3 were cloned into the LentiLox-vector [129]. Briefly, the oligonucleotides coding shRNA were designed by freewere offered by Sigma, purchased from TibMolBiol and are listed in the Tab. 3.3. They were annealed and ligated into HpaI/XhoI digested and purified pLL3.7 plasmid. Positive clones were identified by a band shift of ~60bp in the XbaI/NotI fragment compared to parental vector and sequenced.

Tab. 3.3 List of shRNA oligonucleotides

The resulting siRNA sense and anti-sense strain are marked in green and red. The integrated loop sequence is depicted in black.

Name	Sequence
scrambled up	TTTGCTATCGAGAAGATCAGCC TTCAAGAGA GGCTGATCTTCTTTAGC TTTTTTCTCGA
scrambled do	TCGAGAAAAAA GCTAAAGAAGATCAGCC TCTCTTGAA GGCTGATCTTCTCGATAGC AAA
sh1GDF3 up	T GCAGAAGCTCCTCTACTTTAA TTCAAGAGA TTAAAGTAGAGGAGCTTCTGC TTTTTTC
sh1GDF3 do	TCGAGAAAAA AGCAGAAGCTCCTCTACTTTAA TCTCTTGAA TTAAAGTAGAGGAGCTTCTGC A
sh2GDF3 up	T GCTTTCAGCTTCCTGTTAATT TTCAAGAGA AATTAACAGGAAGCTGAAAGC TTTTTTC
sh2GDF3 do	TCGA GAA AAA A GCTTTCAGCTTCCTGTTAATT TCTCTTGAA AATTAACAGGAAGCTGAAAGC A

Cloning of FLAG-tagged vectors

For the cloning of GDF3 expression constructs BMP2-GDF3, GDF3-GDF3 and GDF3compl pLL-GFPIRES vector was used as a backbone. The cloning of BMP2-GDF3 and GDF3-GDF3 was conducted in 2 major steps: (1) cloning of prodomain and C-terminal FLAG-peptide and (2) cloning of mature GDF3 with N-teminal recognition site for PC (RKRR). For this purpose, the BMP2- and GDF3-prodomains were amplified by PCR using NCCIT cDNA as a template, with primers BMP2pro up/BMP2pro and

GDF3eukup/GDF3pro_BamHI, respectively. The products and the plasmid pLL-GFPIRES were digested with NheI/BamHI, purified and ligated. The newly cloned vectors BMP2pro and GDF3pro were used in the next cloning step as target vectors. Mature GDF3 was amplified from the same cDNA with GDF3mat_BamHI up/GDF3mat_BstBI do primers. The PCR Product and target vectors BMP2pro and GDF3pro were digested with BamHI and BstBI, purified and ligated. The positive clones were sequenced.

Cloning of GDF3compl

The GDF3compl vector comprised of pLL-GFPIRES backbone and complete GDF3 ORF. GDF3 was amplified using NCCIT cDNA as a template with primers GDF3eukup/GDF3euk_BamHI do and cloned into the vector via NheI and BamHI restriction sites.

Cloning of BMP2-2HIS-GDF3, GDF3-2HIS-GDF3 and GDF3-2HIS-BMP2

First, 2 starting vectors, HIS-RKRR and ScaI-HIS were cloned by inserting hybridized oligonucleotides coding HIS-tag with PC recognition site and HIS-tag with N-terminal ScaI restriction site via MluI/XbaI restriction sites in pIRES. Next, the BMP2- and GDF3-podomains without PC recognition site were amplified by PCR using BMP2-GDF3 or GDF3-GDF3 vectors as template with BMP2pro up/BMPpro-RKRR_MluI do and GDF3eukup/GDF3-RKRR_MluI do, respectively cloned into HIS-RKRR plasmid via NheI/MluI. The mature peptide sequences of GDF3 and BMP2 were amplified in the same manner using hGDF3mat_XbaI up/ hGDF3mat_NotI do and BMP2mat_XbaI up/BMP2mat_NotI do primers, respectively. The PCR products were cloned into ScaI-HIS plasmid via XbaI/NotI restriction sites. Finally, the tagged mature peptides were excised from the ScaI-HIS plasmids via ScaI/NotI and were cloned into HIS-RKRR plasmids containing the prodomain of interest.

Tab. 3.4 Primer used in cloning of tagged GDF3 expression constructs

Primer name	Primer sequence
BMP2pro_NheI up	ATTAGCTAGCGTCCCCGCGTGCTTCTTAG
BMP2pro_BamHI do	ATTAGGATCCCTTATCGTCGTCATCCTTGTAATCACGTTTTTCTCTTTTGTGGAGAG
GDF3mat_BamHI up	ATTAGGATCCGCAGCCATCCCTGTCCC
GDF3mat_BstBI do	ATTATTCGAACCTACCCACACCCACATTCAT
GDF3eukup	GTACGCTAGCAGCCACTCCAGAGGCCAT
GDF3pro_BamHI do	ATTAGGATCCCTTATCGTCGTCATCCTTGTAATCTCTCCTTTTCCGAGAAG
ScaI-HIS up	CGCGTAGTACTCATCATCATCATCATCATT
ScaI-HIS do	CTAGAATGATGATGATGATGATGAGTACTA
HIS-RKRR up	CGCGTCATCATCATCATCATCATCGGAAAAGGAGAAGTACTT
HIS-RKRR do	CTAGAAGTACTTCTCCTTTTCCGATGATGATGATGATGATGA
BMPpro-RKRR_MluI do	ATTAACGCGTTTTGTGGAGAGGATGCCC
GDF3-RKRR_MluI do	ATTAACGCGTAGAAGGGTGGCACTGATC
hGDF3mat_XbaI up	ATTATCTAGAGCAGCCATCCCTGTCCC
hGDF3mat_NotI do	ATTAGCGGCCGCCGTACGCCTACCCACACCCACATTC
BMP2mat_XbaI up	ATTATCTAGACAAGCCAAACACAAACAG
BMP2mat_NotI do	ATTAGCGGCCGCCGTACGCTAGCGACACCCACAACC

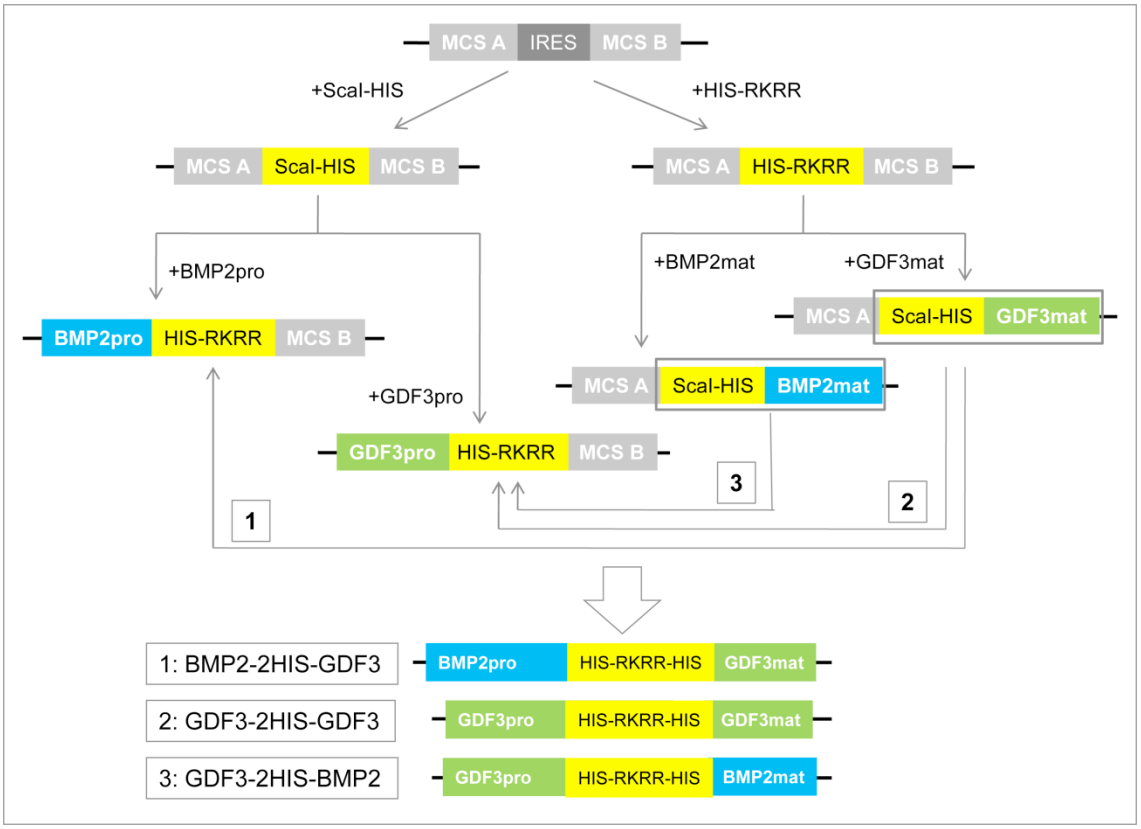

Fig. 3.1 Cloning strategy of double tagged precursors BMP2-2HIS-GDF3, GDF3-2HIS-GDF3, GDF3-2HIS-GDF3

Cloning of Cripto expression vector

Cripto expression plasmid was created by amplification of complete Cripto ORF using NCCIT cDNA as a template with primers Cripto1_NheI up/Cripto1_BamHI do. The PCR Product was inserted into pIRES2-EGFP (BD Biosciences, Germany) via NheI/BamHI restriction sites.

Tab. 3.5 Primers used for cloning of Cripto-expression construct

Cripto_NheI up	ATTAGCTAGCTGGAAACTGATCTTCAATGCAC
Cripto_BamHI do	ATTAGGATCCTTCACCCAGTGCTTCAGCTT

Cloning of HoxA9 promoter constructs A-C

The promoter fragments A and B were amplified with primers Prom123_KpnI up/Prom123_HindIII do for construct A and mirna_prom up/mirna_prom do for construct B. Both PCR products were cloned into pGL3-basic plasmid (Promega, Germany) via KnpI/HindIII restriction site. Contruct C was generated in 2 steps. Product of the first PCR with primers Prom123_NheI up/Prom123_HindIII do was cloned into pGL3-basic via NheI/HindIII. Second PCR Product generated with primers mirna_NheI up and Prom123_HindIII do was digested with NheI/NdeI and a 4865 fragment was cloned into plasmid created in step one. The DNA extracted from NCCIT cells was used as the template in all PCRs.

Tab. 3.6 Primer used in the cloning of HoxA9 promoter constructs

Primer name	Primer sequence
Prom123_KpnI up	ATTAGGTACCTATTTTGGGGCTAAGGCTGT
Prom123_HindIII do	ATTAAAGCTTGCTGCTGGGTTATCTGCG
mirna_prom up	ATTAGGTACCCTTCCACTTTATCCCGTTCA
mirna_prom do	ATTACTCGAGAAGGCAGGGAGAGAGGAATA
Prom123_NheI up	TATTAGCTAGCCCGTGGGGTCCTCGTAG
mirna_NheI up	TATTAGCTAGCCTTCCACTTTATCCCGTTCA

3.7 Luciferase assay

For the luciferase assay the NCCIT or 293T cells were seeded in 48 well plate, so that they reached 70% confluency on the next day. 24h later the cells were transfected with TurboFect according to the manufacturers protocol (Fermentas). For the transfection different luciferase vectors (such as BRE-Luc, SBE-Luc, CAGA-Luc or Promoter contructs A-C) and the same renilla vector (Promega) were applied, in ratio 1:5. The amount of DNA in the transfection was 0,5µg for 293T cells and 1µg for NCCIT cells. 24h after transfection the medium was changed to serum-free DMEM for 3h with subsequent stimulation with indicated ligands in serum-free medium for 20-24h. Then the cells were washed once with PBS and lysed by addition of 100µl of 1x passive lysis buffer of the Dual-luciferase reporter assay system from Promega. The plate was stored at -80°C until the measurement was performed.

For luminescence measurement 10µl of the lysate was pipetted into a white 96-well plate and the plate was inserted into microplate reader Omega (BMC Labtech). The first enzymatic reaction was induced by adding 100µl of luciferase substrate solution. The plate was shaken and after 2sec the values were acquired every sec, for 20 sec. After this, renilla substrate solution was added to the plate and the luminescence values were acquired in the same way.

For the evaluation, a mean value of measurement points between 5 and 10 sec was calculated and a ration of firefly to renilla mean values was built.

Tab. 3.7 Recipes for luciferase and renilla substrate solutions

Luciferase subtrate solution (pH=7,8):	Renilla subtrate solution (pH=5,0):
470µM D-Luciferin	1,1M NaCl
270µM Coenzym A	2,22M Na2EDTA
33,3mM DTT	0,22M KxPO4
530µM ATP	0,44mg/mL BSA
2,67mM MgSO4	1,3mM NaN3
20mM Tricine	1,43µM Coelenterazin (diluted in EtOH)
0,1mM EDTA	

3.8 Immunoprecipitation

The cells were rinsed once with cold PBS and scraped off in 5mL cold PBS by cell scraper and spun down for 10min. at 300g. The pellet was resuspended in 1mL ice-cold hypotonic buffer, transferred to eppendorf tubes and incubated on ice for 10min. Then, a 2M NaCl was added, to reach the NaCl

concentration of 150mM (approx. 70µl/1mL cell suspension) and the cell suspension was incubated on ice for another 5min to extract the cellular proteins and spun down at max. speed for 15min to pellet cell debris. In the meantime 40µl of anti-FLAG-M2 agarose slurry/per sample was transferred to eppendorf tubes and washed twice with 1mL NET-2 buffer. The supernatant containing the cellular proteins was combined with the anti-FLAG-M2 agarose slurry and rotated on MACSmix rotator for 2-4h at 4°C. The agarose slurry was then pelleted, the supernatant removed. 3 subsequent washing steps with 1ML of NET-2 buffer followed. Finally, the FLAG-proteins bound to the agarose slurry were eluted with 40µl Laemmli buffer. The protein extracts were frozen down until the analysis by western blot was undertaken.

Tab. 3.8 Recipes for buffer used for immunoprecipitation

Hypotonic buffer	NET-2 buffer
10mM Tris-HCl, pH 7.5	50mM Tris-HCl, pH 7,5
10mM NaCl	150mM NaCl
2mM EDTA	0,05% Triton X-100
0,5% Triton X-100	
1mM PMSF	
1µg/mL aprotonin	
1µg/mL leupeptin	

3.9 SDS-PAGE, protein transfer and immunobloting

Samples were run using the Biorad Mini-PROTEAN gel electrophoresis system.

Samples were loaded onto a 10% SDS polyacrylamide gel and electrophoresed at 15mA/gel in 1x Running buffer. A protein standard ladder was run on each gel to confirm the sizes of proteins being investigated. Following electrophoresis, proteins were transferred to a PVDF membrane using a semi-dry transfer system in 1x transfer buffer for 1 h at 25 V.

Following protein transfer, nitrocellulose membranes were blocked with 5% (w/v) skim milk powder in 1x TTBS for 1 h with gentle shaking. Membranes were washed 3 x 5 min in TTBS and incubated with specific primary antibody (Table 3.10) in 5% BSA/TTBS solution overnight at 4°C with gentle shaking. Membranes were washed 3 x 5 min in TTBS followed by incubation with either rabbit or mouse HRP-conjugated antibody for 1 h at room temperature with rotating. Membranes were washed 3 x 5 min and placed in ECL substrate reagent for 1 min. Alternatively the membranes were incubated in BCIP/NBT substrate according to manufacturer's protocol. Photographs were taken by Fusion XS.

Tab. 3.9 Recipes for buffers used in SDS PAGE, protein transfer and immunobloting

5x Laemmli sample buffer	1x TTBS	1x transfer buffer	1x Running buffer
50% glycerol (v/v) 10% SDS (w/v) 250 mM Tris-HCl pH 6.8 1 mg/mL bromophenol blue 0,5 M DTT	0.5 M Tris-base 1.5 M NaCl + 0,05% Tween-20 pH 7.4	20% methanol (v/v) 2.5 mM Tris-base 19.2 mM glycine	25 mM Tris-base 192 mM glycine 0.1% SDS (w/v)

Tab. 3.10 List antibodies and reagents used for immunoblotting

Antibody	Manufacturer
anti-GAPDH rabbit	Cell signaing
Mouse anti-Smad2	BD Biosciences
anti-pSmad2 rabbit	Invitrogen
anti-pSMAD-L (S245/250/255) rabbit	Cell signalling
Mouse Anti-FLAG M2 AP-conjugated	Sigma
Mouse Anti-HIS AP-conjugated	Sigma
Anti-rabbit HPR goat	Acris
Anti-mouse-HPR goat	Cell signaing
ECL substrate reagent	PeqLab
BCIP/NBT	Sigma

3.10 Immunofluorescence staining

The NCCIT cells were seeded in CollagenR-coated chamber slides. On the next day the medium was removed, the cells were washed once with PBS and fixed in 4%PFA for 15min. Then, the cells were permeabilized with 0,25% Triton X-100 in PBS. The detergent was washed away by PBS and the unspecific binding sites were blocked by incubation in 3% BSA in PBS at 37°C for 30min. After this, cells were stained with indicated primary antibodies overnight at 4°C. On the next day the primary antibody was removed and washed out in 3 steps with PBS. To visualize the binding of the primary antibody, the cells were stained with appropriate secondary antibody (1:200) together with Hoechst (0,4µg/mL) to label the nuclei. After 3 washing steps with PBS the chamber was removed. A thin layer of mounting solution was spread over the surface of cell growth, which was subsequently covered with a cover glas. The analysis was performed at fluorescence microscope (BZ 9000, Keyence, Germany).

Tab. 3.11 List of reagents used for immunofluoresce staining

Reagent	Manufacturer
Paraformaldehyd (PFA)	Sigma, Germany
Bovine Serum Albumine (BSA)	Serva, Germany
mouse anti-Smad2	Invitrogen
rabbit anti-beta-tubulin-III (Tuj1)	Sigma
Hoechst 33342	Sigma
anti-Maus IgG (Fab`)2 - Alexa 594	Molecular Probes

3.11 *In silico* promoter analysis

The analysis was performed by MatInspector (www.genomatix.com).

The proximal HoxA9 promoter sequence, comprising the 5kbregion between HoxA9 and HoxA10 genes and the HoxA9 intron sequence was inserted into the input form of the analysis tool and the transcription factor binding sites (weight matrices) option was selected as library. After selection of the library (vertebrates – Matrix Library 7.1) the query was submitted. The resulting table listed the potential transcription factor binding sites, which were then transferred into a sortable excel data sheet for further evaluation.

Only binding sites of Smad3 with matrix similarity scores higher than 0,8 were considered for further design of promoter constructs.

3.12 Statistical analysis

All statistical analyses were performed using Prism5 (GraphPad Software, La Jolla, CA, USA). Mean values ± standard deviation (SD) are displayed. Significance was tested using Student T-test and results with p-value below 0,05 (*), 0,01 (**) and 0,001 (***) were regarded as statistically significant.

4 RESULTS

4.1 NCCIT cells as a model of CSCs.

GDF3 and its obligatory co-receptor Cripto have a narrow expression pattern and are associated with pluripotent phenotype in embryonic stem cells and cancer. To establish the embryonal carcinoma cell line NCCIT as a suitable CSC model to study the role of GDF3, we evaluated the expression of important components of GDF3 signalling pathway by RT-PCR. We detected expression of GDF3 and other secreted ligands potentially involved in GDF3 signalling, such as Nodal and Lefty2 (Fig. 4.1A). Nodal utilizes the same type I and type II receptors [130] and can therefore compete with GDF3 for the receptor binding sites. Lefty2 is a natural, extracellular inhibitor of Nodal and GDF3 [131]. Also, transcripts of both, type I (ALK4 and ALK7) and type II (ACVR2A and B) receptors are present in NCCIT cells, along with the obligatory co-receptor Cripto (Fig. 4.1B) and the intracellular signalling mediators activating Smads (Smad2 and Smad3), co-Smad (Smad4) and the inhibitory Smad7 (Fig. 4.1C), involved in the negative feedback loop of Smad2/3 signalling cascade in embryonic stem cells.

CSCs are characterised by ES-like signature, therefore we confirmed the expression of main pluripotency markers, as shown in Fig. 4.1D.

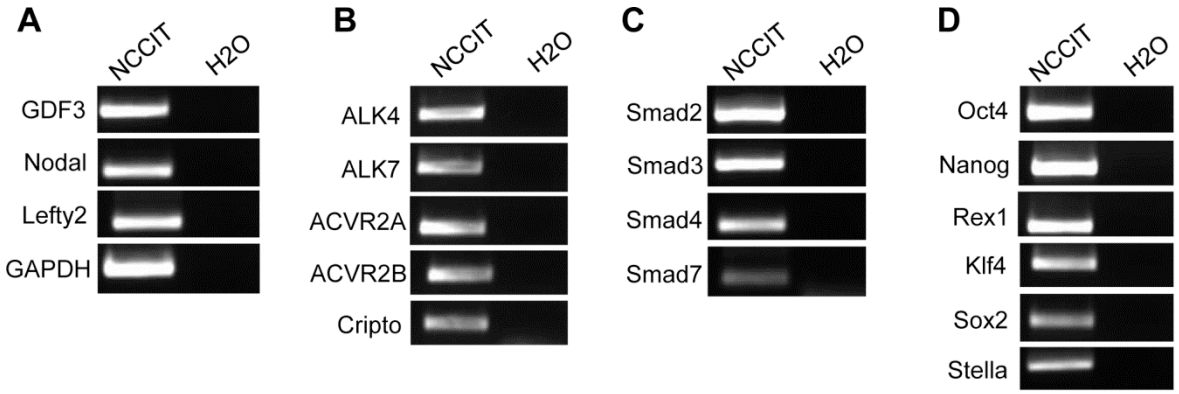

Fig. 4.1 Expression of components of Smad2/3 signalling pathway essential for GDF3 signalling and of pluripotency markers in NCCIT cells

The expression of several genes related to Smad2/3 signalling and associated with pluripotency was determined by RT-PCR in cDNA of NCCIT cells.

A. Expression of GDF3, agonistic ligand Nodal and extracellular inhibitor Lefty2 and GAPDH.
B. Expression of GDF3 receptors.
C. Expression of intracellular signal transducers.
D. Expression of pluripotency markers.

4.2 GDF3 signalling in NCCIT cells: inhibition of Smad1/5/8 pathway vs. activation of Smad2/3 pathway

GDF3 was reported to (1) be able to block Smad1/5/8-signalling by binding to BMPs, e.g. BMP4 in the extracellular space and (2) induce Smad2/3 signalling cascade. In the latter case GDF3 acts by binding to and joining cell surface receptors Cripto and dimers of type I and type II receptors that leads to phosphorylation of Smad2 or Smad3 as intracellular effectors that are subsequently translocated into the cell nucleus to act as co-transcription factors. To test which pathway GDF3 has impact on in NCCIT cells, I employed several assays, such as luciferase assays, western blot and immunoflueorescence staining.

First, a luciferase assay was performed. The NCCIT cells were transfected with vectors containing BMP-responsive elements (BRE-Luc) and subsequently stimulated with a mixture of BMP2 and GDF3 in 1-, 3-, or 10-fold molar excess. To allow the binding of BMP2 and GDF3 in the solution, the ligands were preincubated together before application to the cells. As shown in Fig. 4.2A, the luciferase expression was robustly activated by BMP2, despite GDF3 presence in the medium.

To assess the activation of Smad2/3 pathway, we transfected the cells with a vector containing Smad Binding Element (SBE-Luc) and stimulated the cells with increasing concentrations of GDF3. The maximal activation of promoter construct was achieved with 300ng/mL and did not increase any further with rising concentration of the ligand (Fig. 4.2B).

The identity of the phosphorylated Smad was confirmed by protein extraction from GDF3-stimulated NCCIT cells and detection of phosphorylated Smad2 by western blot. Stimulation with recombinant Nodal was performed as a positive control for activation of Smad2/3 signalling cascade (Fig. 4.2C). We were also able to track the translocation of Smad2 into the nucleus upon GDF3-stimulation by immunofluorescence staining, shown in Fig. 4.2D. In the left panel (untreated cells) only diffuse staining of Smad2 in the cytoplasm can be seen, while 1h after GDF3 stimulation (right panel), Smad2 staining co-localizes with the Hoechst-stained nuclei.

The last step in a signalling cascade is the activation of target genes. In case of ESC, phosphorylated Smad2/3 is known to induce expression of Smad7 and Nodal [132]. To confirm the functionality of the Smad2/3 signalling triggered by GDF3 stimulation, the GDF3-dependent induction of these target genes was tested in NCCIT cells. A significant induction of Nodal and Smad7 could be already observed after 3h stimulation with 100ng/mL of GDF3. 300-500ng/mL of GDF3 accounted for maximal induction of Nodal, while expression of Smad7 could be further increased with rising GDF3 concentration.

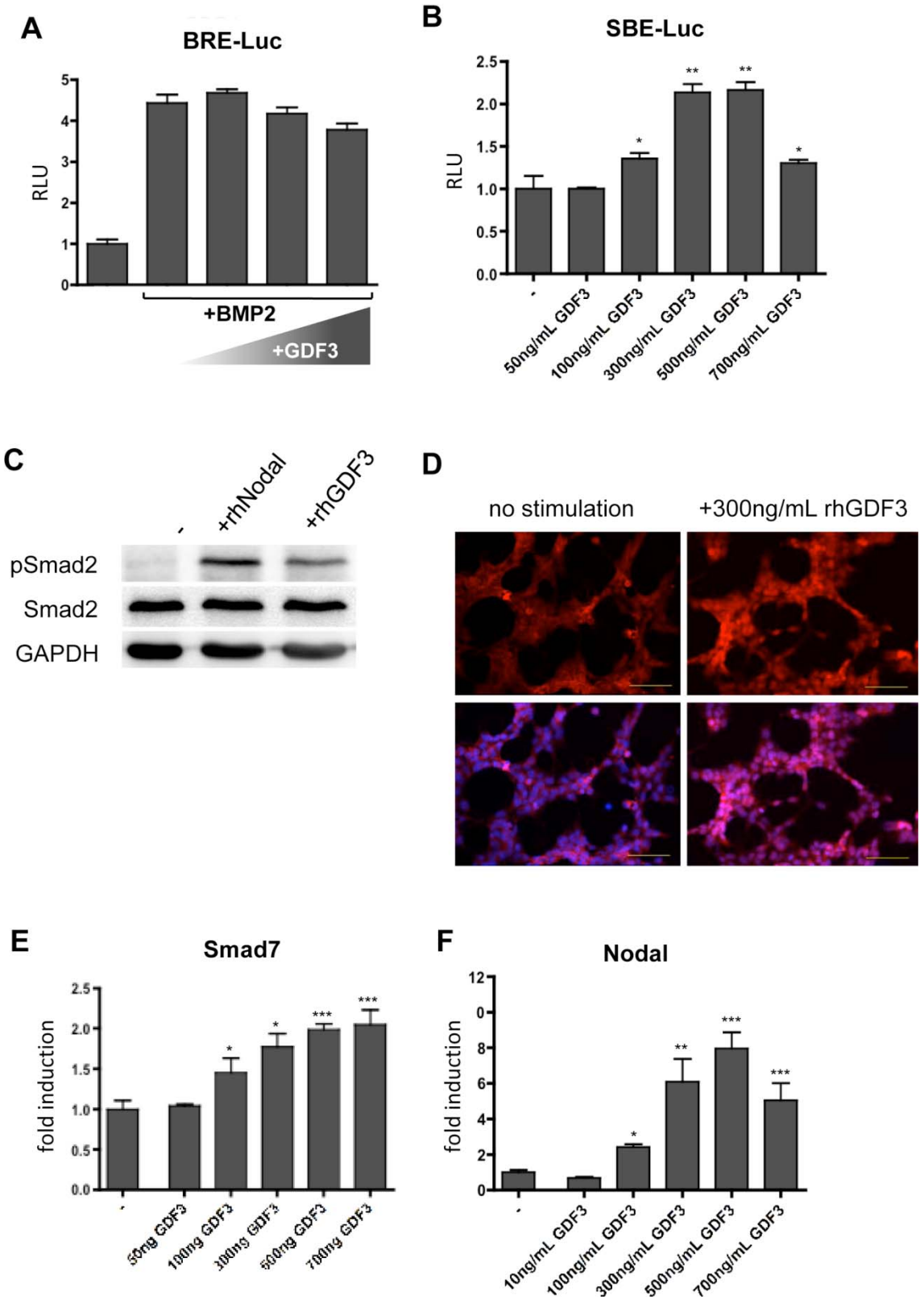

Fig. 4.2 GDF3 signalling in NCCIT cells

A. BRE-dependent luciferase activity in NCCIT cells treated with BMP2 alone as a positive control or with pre-icubated mixtures of BMP and 3x, 5x, 10x molar excess of GDF3. The results in D-E are showed as a firefly to renilla ratio and normalized to non-stimulated sample. n=3

B. SBE-dependent luciferase activity in NCCIT stimulated with GDF3 in various concentrations.

C. Phosphorylation of Smad2 in NCCIT cells after starvation and treatment with 100ng/mL GDF3, 300ng/mL Nodal for 1h. GAPDH was used as a loading control.
D. Translocation of Smad2 in NCCIT upon stimulation with 300ng/mL GDF3. The cells were stained with anti-Smad2 and anti-mouse-Alexa594 (upper panel) antibody and counterstained with Hoechst (lower panel). The yellow bar indicates 100µm.
E-F. GDF3-dependent activation of known Smad2/3 target genes Smad7 (E) and Nodal (F) in NCCIT cells. The gene expression was determined by qPCR, the results are presented as GAPDH ratio and normalized to untreated cells. Student t-test was applied to compare values to unstimulated control. n=3

Members of TGFβ family were reported to induce not only the canonical Smad-pathway, but also alternative signalling cascades, such as Ras/MAPK [109]. An indicator of activation of non-Smad pathway is phosphorylation of the Smad-linker. Therefore, I performed a time kinetic of GDF3 stimulation and monitored phosphorylation of Smad2 in the linker region (at serine 245/250/255) between MH1 and MH2 domain additionally to phosphorylation at carboxyl terminus (at serine 465/467). Western blot analysis (Fig. 4.3) revealed rapid and sustaining phophorylation in the linker region of Smad2.

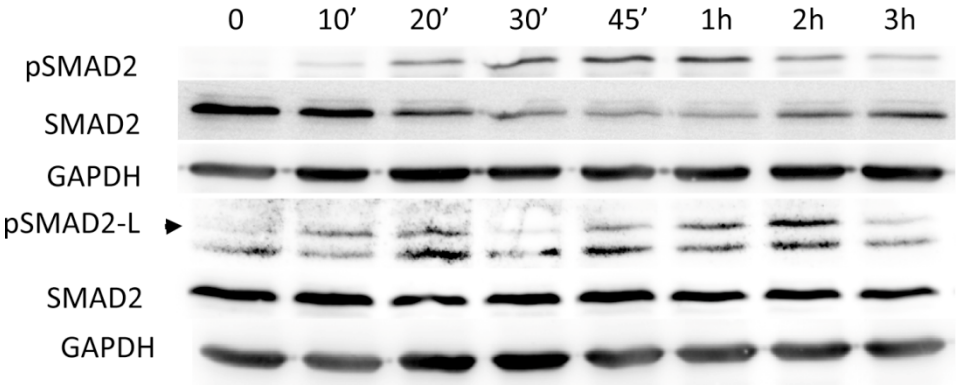

Fig. 4.3 Kinetic of Smad2 phosphorylation in NCCIT cells upon GDF3 stimulation
Kinetic of Smad2 phosphorylation in NCCIT cells at Ser465/467 (labeled as pSmad2) and Ser245/250/255 (labeled as pSMAD2-L). The cells were starved and stimulated with 300ng/mL rhGDF3 and collected at given time points. Only the upper band of pSMAD2-L (labeled with an arrowhead) corresponds to pSMAD2-L.

In summary, I was able to show that GDF3 induces Smad2/3 pathway in NCCIT cells, and does not extracellularly inhibit BMP-signalling.

4.3 Monitoring of GDF3-synthesis, processing and secretion

4.3.1 GDF3-overexpression constructs

The activity of TGFβ ligands has been reported to be regulated by the processing of the precursor molecule, among others. Chen *et al.* [118] and Andersson [117] demonstrated only little activity of exogenously overexpressed GDF3 as a result of low processing efficiency. To investigate GDF3 processing and secretion, I designed three overexpression constructs consisting of: (1) GDF3 complete open reading frame – GDF3compl, (2) GDF3 with its endogenous prodomain and tagged mature peptide – GDF3-GDF3, (3) a chimeric precursor molecule with heterologous BMP2-

prodomain and tagged GDF3 mature peptide – BMP2-GDF3 (Fig 4.4A). BMP2-prodomain was previously reported to mediate an efficient processing by furin [106]. The insertion of the tag at the N-terminus of the mature peptide and C-terminal from the recognition site of the processing enzyme allows the tracking of mature peptide after the processing.

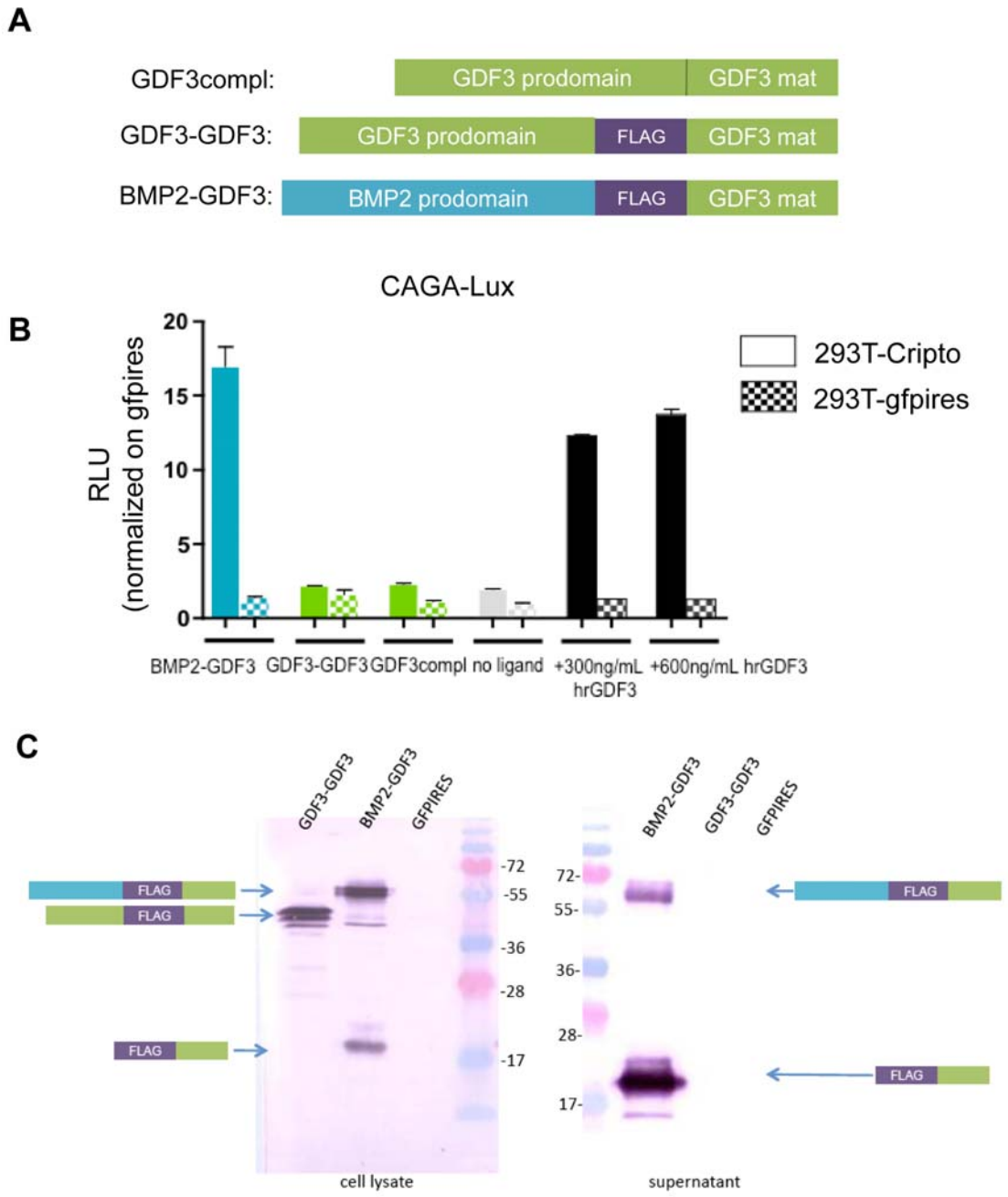

Fig. 4.4 The effect of distinct proregions on biological activity of GDF3 in 293T cells

A. Scheme of GDF3 overexpression constructs.

B. CAGA-dependent luciferase activity in Cripto- or gfpires-expressing 293T cells transfected with GDF3 constructs, depicted in 4A. The results are presented as a firefly to renilla ratio and are normalized to the ratio in gfpires-expressing 293T cells. The bars without pattern correspond to Cripto-expressing 293T cells, while those with pattern – to 293T-gfpires. n=3

C. Western blot analysis of FLAG-tagged proteins in the cell lysate and the supernatant of 293T cells transfected with BMP2-GDF3, GDF3-GDF3 and gfpires. Staining with anti-Flag antibody. Molecular masses of the standard proteins are indicated in kDa.

The biological activity of the aforementioned constructs was determined by a luciferase assay in Cripto-expressing 293T cells. I detected luciferase activity in cells stimulated with rhGDF3, as well as in cells transfected with the chimeric construct BMP2-GDF3. No luciferase activity could be measured in cells transfected with both GDF3-constructs containing endogenous GDF3-prodomain (Fig. 4.4B).

To investigate whether lack of biological activity in GDF3-prodomain containing constructs is mediated by insufficient processing of the precursor, I transfected 293T cells with BMP2-GDF3 and GDF3-GDF3 constructs and immunoprecipitated FLAG-tagged proteins from both the cell lysate and the supernatant. The analysis of precipitated proteins by SDS-PAGE and western blot revealed that GDF3 from both expression constructs is efficiently translated in the cell, however, only BMP2-GDF3 construct could be detected in the supernatant in both, processed and unprocessed, forms. On the contrary, no FLAG-tagged proteins could be detected in the supernatant of GDF3-GDF3 transfected 293T cells (Fig. 4.4C). Multiple bands detected by antibody targeting FLAG-tagged proteins indicate that GDF3 was posttranslationally modificated.

To exclude the possibility that the GDF3-proregion-mediated effects are 293T cell-specific, I transfected NCCIT cells with the tagged GDF3-expression constructs and performed immunoprecipitation of FLAG-tagged proteins from the cell supernatant. I detected high amount of mature peptide GDF3 in the supernatant of NCCIT cells transfected with the BMP2-GDF3 construct and neither precursor molecule nor processed, mature GDF3, when the cells were transfected with GDF3-GDF3 construct (Fig. 4.5).

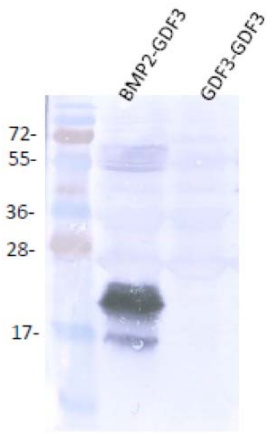

Fig. 4.5 The effect of distinct proregions on biological activity of GDF3 in NCCIT cells
Western blot analysis of FLAG-tagged proteins in the supernatant of NCCIT cells transfected with BMP2-GDF3 and GDF3-GDF3 expression constructs. Staining with anti-Flag antibody. Molecular masses of the standard proteins are indicated to the right in kDa.

4.3.2 Proregion-mediated effects on the stability of GDF3

To clarify the fate of mature GDF3 when expressed along with its endogenous prodomain, I designed and cloned double tagged (His-tag) constructs with heterologous prodomains (Fig. 4.6A). His-tags were placed N- and C-terminal of protein convertase recognition site. This strategy enabled

simultaneous tracking of prodomain and mature peptide. I added to the vector portfolio a hybrid construct of BMP2-mature peptide with GDF3-prodomain (GDF3-2HIS-BMP2) for the purpose of distinction between prodomain- and mature peptide-mediated effects.

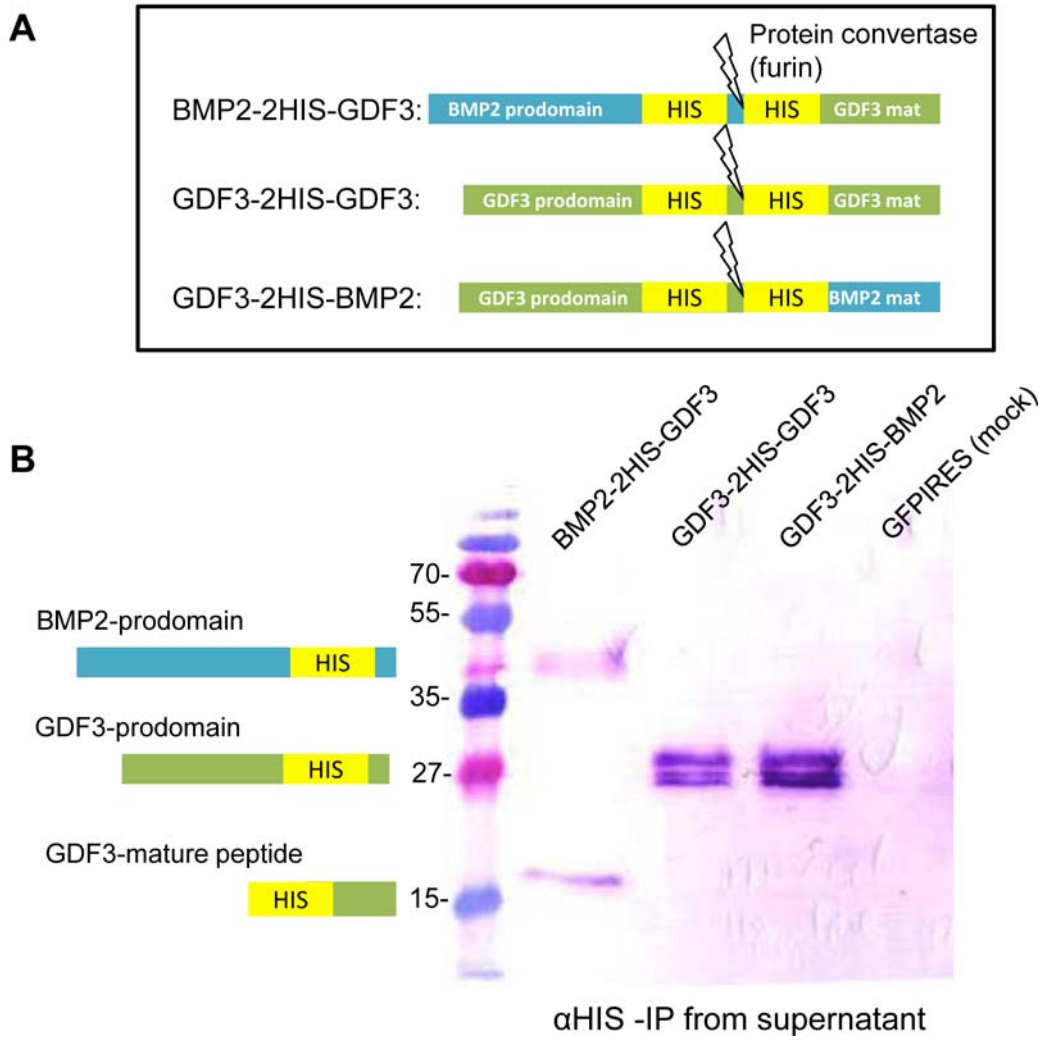

Fig. 4.6 The effects of GDF3 proregion on the mature peptide.

A. Scheme of double-His-tagged overexpression constructs. The lightening indicates the site of action of protein convertase.

B. Presence of tagged GDF3 and BMP2 species in the supernatant of transfected 293T cells was analysed by western blot. Staining with anti-his antibody.

The 293T cells were transfected with double-tagged constructs and His-tagged molecules were subsequently immunoprecipitated from the cell supernatant and subjected to the SDS-PAGE and western blot. I was able to detect mature GDF3 yielded by BMP2-2HIS-GDF3 constructs, as well as the corresponding BMP2-prodomain. Due to prodomain tagging, I detected GDF3 prodomain in the supernatant of cells transfected with both GDF3-2HIS-GDF3 and GDF3-2HIS-BMP2, but neither of the corresponding mature peptides (Fig. 4.6B).

4.4 GDF3 and Nodal stimulation of NCCIT cells - concentration kinetic

For the subsequent investigation of GDF3 effects, NCCIT cells were stimulated with raising concentration of rhGDF3, rhNodal and a mixture of both (Fig. 4.7). Several goals were to achieve by this experiment: (1) to estimate minimal GDF3 concentration triggering maximal signalling strength, (2) to compare the signalling strength of GDF3 and Nodal and (3) to examine the effects of both ligands together on Smad2/3 signalling in target cells.

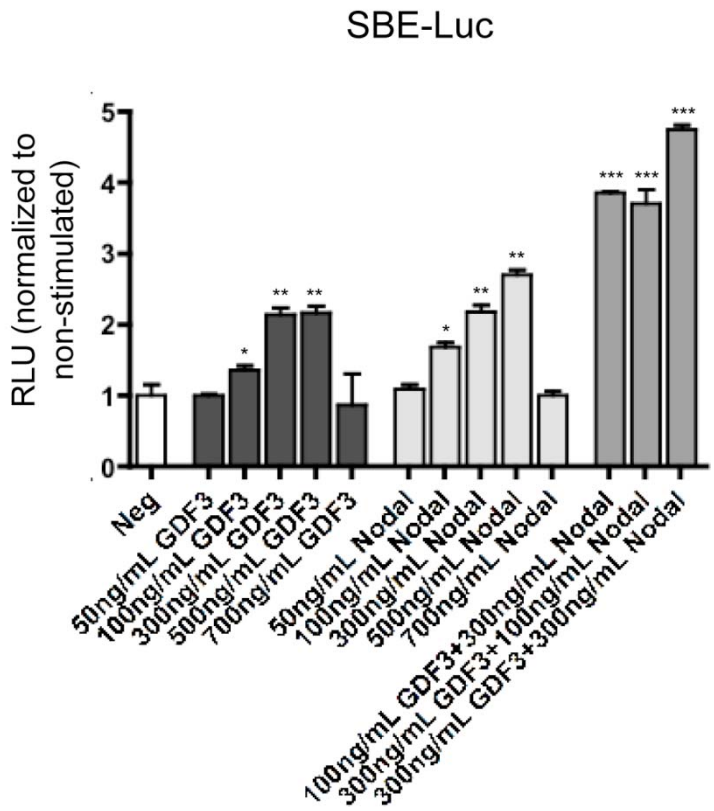

Fig. 4.7 The strength of Smad-signalling triggered by GDF3, Nodal and the mixture of both
SBE-dependent luciferase activity in NCCIT stimulated with rhGDF3, rhNodal and mixture of both in various concentrations. The results are presented as a firefly to renilla ratio and normalized to untreated cells. n=3

According to the SBE-Luc luciferase assay performed in NCCIT cells, the signalling strength of Nodal and GDF3 was comparable. The concentration of 300ng/mL of rhGDF3 and rhNodal was chosen for subsequent stimulation experiments. While GDF3 concentration higher than 300ng/mL was not able to increase the luciferase activity in the SBE-Luc transfected cells any further, the addition of Nodal to the stimulation cocktail potentiated the signalling further.

4.5 GDF3 knockdown in NCCIT cells

To test the effect of decreased concentration of endogenous GDF3 in NCCIT cells, I created a stable GDF3 knockdown cell line, by transduction of NCCIT cells with lentivirus containing a shRNA-cassette targeting GDF3. Additionally, a control cell line with lentivitus containing a scrambeld shRNA was generated. The efficiency of the transduction was monitored by GFP expression. Approx. 95% of

transduced cells were GFP positive and the efficiency was comparable for all applied lentiviruses (Fig. 8A). Of the two shRNA constructs tested, GDF3 knockdown in the cell line generated with sh1GDF3 was more efficient and reached 96%, and sh1GDF3 was therefore employed for all following experiments (Fig. 4.8B).

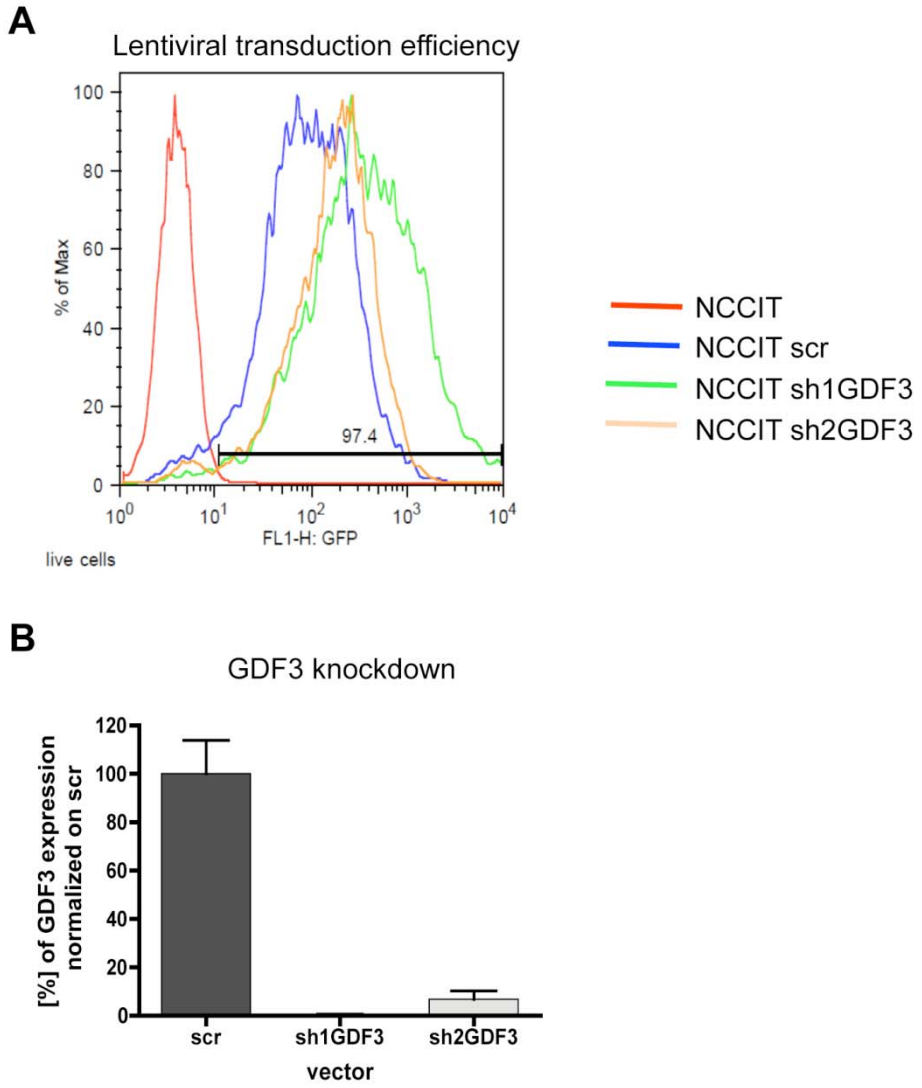

Fig. 4.8 Knockdown of GDF3 by shRNA

A. Efficiency of lentiviral transduction detected by GPF expression.
B. Reduction of GDF3 expression upon GDF3 knockdown with two different constructs sh1GDF3 and sh2GDF3. The expression was determined by qPCR, the results are presented as GAPDH ratio and normalized to scramled. n=6

Having observed instability of GDF3 expressed with its endogenous prodomain previously (Chapter 4.2.2), we investigated whether GDF3 knockdown decreased the amount of biologically active GDF3 produced by NCCIT cells. For this purpose 293T cells transfected with CAGA-Luc and Cripto- or gfpires-vectors (GDF3-recipient cells) were co-cultured with NCCIT sh1GDF3 or NCCIT scr cells (GDF3-donor cells). The luciferase activity in cells co-cultured with NCCIT cells with GDF3-knockdown was

significantly lower, indicating that the secretion profile of NCCIT cells was changed due to the knockdown (Fig. 4.9). The remaining activation of luciferase activity in 293T-Cripto cells co-cultured with NCCIT sh1GDF3 can be caused by other Cripto-dependent ligands produced by NCCIT cells, like Nodal.

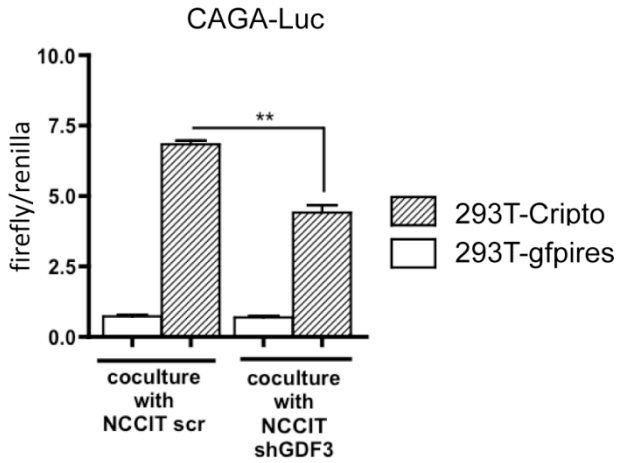

Fig. 4.9 GDF3-knockdown changes the secretion profile of NCCIT cells regarding molecules triggering Smad2/3 molecules.

CAGA-dependent luciferase activity in cripto- or GFPIRES-expressing 293T cells co-cultured with NCCIT scr or NCCIT sh1GDF3. The results are shown as a firefly to renilla ratio normalized to ration in 293T cells tranfected with GFPIRES, respectively. n=3

4.6 Influence of GDF3 on proliferation of NCCIT cells

Since GDF3 was reported to influence proliferation of cancer cells previously [124][126], I determined whether GDF3 has an impact on proliferation of NCCIT cells. The NCCIT cells were stained with a CellTrace® Violet, seeded and stimulated with GDF3 every 24h. The cells were harvested every day and the amount of incorporated dye in GDF3-treated cells was assessed by FACS and compared. No differences were found, as shown in Fig. 4.10A and Tab. 4.1.

Similarly, NCCIT sh1GDF3 and NCCIT scr cells were stained with CellTrace® Violet, seeded, collecetd and analyzed by FACS every 24h. GDF3-knockdown did not influence the proliferative capacity of NCCIT cells, when compared to the control cells, transduced with scrambled vector (Fig. 4.10B-C and Tab. 4.1).

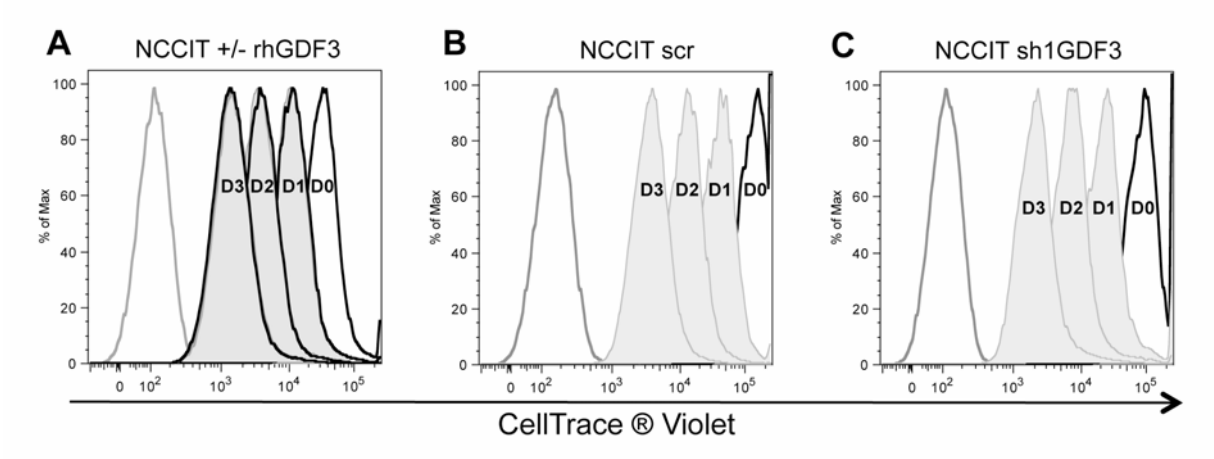

Fig. 4.10 The effect of GDF3 on proliferation of NCCIT cells

A. FACS analysis of the amount of CellTrace® Violet incorporated into NCCIT cells repetitively stimulated with 300ng/mL rhGDF3 (tinted curve) and untreated (black line).

B-C. FACS analysis of the amount of CellTrace® Violet incorporated into NCCIT scr (B) and NCCIT sh1GDF3 (C) cells.

The cells were stained, seeded and harvested each day (indicated as D0-D3). Grey line indicates unstained cells.

Tab. 4.1 List of the normalized differences of mean fluorescence intensity peaks.

The values were normalized to the mean fluorescence value of the peak representing the previous day. Upper panel represents quantification of Fig. 4.10A, the lower one of Fig. 4.10B. No significant differences between either GDF3-stimulated and untreated NCCIT cells, or NCCIT scr and NCCIT sh1GDF3 could be detected.

normalized difference of mean fluorescence intensity	NCCIT			NCCIT + rhGDF3		
T0-T1	0.641	+/-	0.015	0.642	+/-	0.005
T1-T2	0.641	+/-	0.018	0.657	+/-	0.006
T2-T3	0.623	+/-	0.003	0.583	+/-	0.021
normalized difference of mean fluorescence intensity	**NCCIT scr**			**NCCIT sh1GDF3**		
T0-T1	0.677	+/-	0.003	0.693	+/-	0.006
T1-T2	0.671	+/-	0.001	0.667	+/-	0.008
T2-T3	0.710	+/-	0.003	0.699	+/-	0.006

4.7 Transcriptome analysis of NCCIT cells upon GDF3 stimulation and knockdown

To get more insight into the putative role of GDF3 in CSC and identify GDF3-downstream targets, global gene expression profiles of NCCIT cells stimulated with GDF3 or with GDF3 knockdown were analyzed by cDNA microarray platform. A short stimulation period of 3h was chosen, to assess primary effects of the ligand stimulation.

4.7.1 Design of microarray analysis

The transcriptional response to stimulation by various TGFβ family members that signal via the same pathway often varies, depending in the first place on the strength of Smad-signalling triggered in target cells and activation of non-Smad pathways [133][134]. Additionally, ligand concentration-dependent Smad2/3 signalling was reported to trigger differential, even opposing effects [112]. Therefore, in our study I aimed to cover a broad range of transcriptional effects caused by decreasing strength of Smad2/3 signalling in NCCIT cells (Table 1, microarrays A to E). In detail, I applied low (100ng/mL) and high (300ng/mL) dose of GDF3 (microarray C & D). GDF3 signalling was shown to be potentiated by Nodal [119], what I could observe in the CSC model as well (Fig. 4.7). Therefore, I investigated the transcriptional response to co-stimulation with Nodal (150ng/mL GDF3 + 300ng/mL Nodal) and high dose of Nodal (300ng/mL) (microarray A & B), as Nodal also induces Smad2/3 phosphorylation, but appears to have different biological role from GDF3, since Nodal and GDF3 cannot compensate for each other in the knockout mice models [118][135] . On the microarray E the effects of GDF3 knockdown in NCCIT cells were investigated.

Tab. 4.2 Impact of GDF3 knockdown and stimulation with GDF3, Nodal and mixture of both on the transcriptome of NCCIT cells

The NCCIT cells were stimulated with indicated ligands for 3h (microarrays A-D) or GDF3 was knocked down by lentivirally delivered shRNA-constuct (microarray E).

		p≤0.05	FC≥1.5	# of genes with official gene annotation	#of up-/downregulated genes		# of genes mapped and annotated by DAVID
Analysis flow		→					
A	100ng/mL GDF3 + 300ng/mL Nodal vs. untreated	3197	2104	1226	↑up	459	1147
					↓do	767	
B	300ng/mL Nodal vs. untreated	1978	1270	604	↑up	292	553
					↓do	312	
C	300ng/mL GDF3 vs. untreated	1287	778	421	↑up	247	385
					↓do	174	
D	100ng/mL GDF3 vs. untreated	1348	891	390	↑up	201	370
					↓do	189	
E	GDF3 KD vs. scrambled	5395	3291	2075	↑up	834	1827
					↓do	1241	

For the evaluation of microarray data, only spots with p-value <0.05, fold change >1.5 and with official gene annotation were included (Tab. 4.2). This narrowed the amount of differentially expressed genes to 390 and 421 due to stimulation with low and high dose of GDF3, 604 and 1226 due to stimulation with Nodal and Nodal in cooperation with GDF3. The number of regulated

transcripts positively correlated with the strength of Smad2/3 signalling induced by the applied ligand(s) (compare with Fig. 4.7) The most prominent transcriptional changes with 2075 differentially regulated genes were observed as a result of GDF3 knockdown. While due to GDF3 treatment more genes were downregulated than upregulated (microarrays C & D, Tab. 4.2), the opposite pattern is displayed as a result of GDF3 knockdown (microarray E, Tab. 4.2).

4.7.2 Gene ontology (GO) term overrepresentation analysis

To address the biological role of GDF3, genes regulated due to GDF3/Nodal stimulation and GDF3 knockdown (Tab. 4.2) were categorized on the basis of their biological function. For this purpose regulated genes with official gene names were extracted from each microarray and an overrepresentation analysis was performed by Database for Annotation, Visualization and Integrated Discovery (DAVID) v6.7 [136]. A selection of biological processes is presented in Table 3. Although the differentially regulated genes were assigned to all selected categories, the calculated enrichment was not always significant (labeled as 'ns.' in Tab. 4.3). Main categories to which genes regulated by GDF3/Nodal were classified are developmental processes, mesoderm and ectoderm development, neurogenesis and signal transduction (Appendix and Table 4.3). Between 14,1% and 19,3% of genes regulated on all microarrays were associated with developmental processes. Among them 4,7% on the microarray A, 6% on the microarray B and 5,3% on the microarray E were associated with mesoderm development. Regulation of genes with function in ectoderm development and neurogenesis was noted on microarrays A (5% and 4,6%), B (7,5% and 7,1%), C (6,5% and 6,5%) and E (6,5% and 5,8%), but not D. Approx. 25% of genes on all microarrays, except of A, were associated with signal transduction. Overrepresentation analysis revealed also that a small, but significant ($p<0.05$) number of genes related to angiogenesis on microarrays B (1,5%) and E (0,9%) is regulated by Smad2/3 signalling.

Taken together, the data indicates that GDF3 and Nodal have different impact on target cells, although both cytokines trigger the same signalling pathway in the NCCIT cells. Nodal, but not GDF3, induces expression of genes associated with mesoderm development. Additionally, more genes related to ectoderm development and neurogenesis are regulated by Nodal than GDF3, Both cytokines regulate expression of molecules involved in signal transduction. Interestingly, even low dose of GDF3 (microarray D) significantly changes the transcriptome of the target cells.

Tab. 4.3 Overrepresentation analysis of genes regulated on microarrays A-E.
A selection of biological processes is depicted. Genes sets with a p-value >0,05 (not significant) are indicated with 'ns.'

	Stimulation / knockdown		Developmental processes	Mesoderm development	Ectoderm development	Neurogenesis	Signal transduction
A	100ng/mL GDF3 + 300ng/mL Nodal	# genes	176	54	57	52	ns.
		%	15,5	4,7	5	4,6	ns.
		p-Value	1,40E-07	1,90E-04	4,30E-03	2,20E-03	ns.
B	300ng/mL Nodal	# genes	109	33	41	39	137
		%	19,3	6	7,5	7,1	25
		p-Value	4,20E-10	7,30E-05	5,60E-06	1,10E-06	5,80E-07
C	300ng/mL GDF3	# genes	59	ns.	25	25	103
		%	15,3	ns.	6,5	6,5	26,8
		p-Value	2,30E-02	ns.	1,10E-02	1,80E-03	4,70E-05
D	100ng/mL GDF3	# genes	52	ns.	ns.	ns.	85
		%	14,1	ns.	ns.	ns.	23,1
		p-Value	5,60E-02	ns.	ns.	ns.	6,40E-03
E	GDF3 KD	# genes	329	95	117	105	415
		%	18,2	5,3	6,5	5,8	23
		p-Value	1,40E-21	2,90E-08	4,10E-10	4,70E-10	4,40E-09

4.7.3 Validation of microarray data – new GDF3 target genes

The GO term analysis revealed that the main categories to which most of the genes regulated on the microarrays A-E are assigned are signal transduction and developmental processed (Tab. 4.3). To validate microarray results, I chose several genes related to abovementioned categories and validated their expression upon GDF3 stimulation by qPCR. I focused on members of TGFβ family and transcription factors reported previously to govern the developmental processes and act as main switches in cell fate decisions.

The expression of Lefty2, a known Smad2/3 target in embryonic stem cells [137], was strongly upregulated by low and high dose of GDF3 (Fig. 4.11A) and served as a positive control for the stimulation.

Gremlin 2 (Grem2) and BMP receptor type 2 (BMPR2), molecules involved in BMP signalling, were induced upon GDF3 stimulation (Fig. 4.11B-C), indicating that GDF3 has an impact on Smad1/5/8-signalling pathway.

Among the genes involved in development, we focused on transcription factors. Stimulation with GDF3 robustly activated expression of transcripts from Hox-family, inducing 16-fold increase in HoxA9, 9-fold increase in HoxA10 and 4-fold increase in HoxB13 expression (Fig. 4.11D-F). I could also validate induction of TBX3, which role in neuroepithelial differentiation in hESC was recently described [138] (Fig. 4.11G).

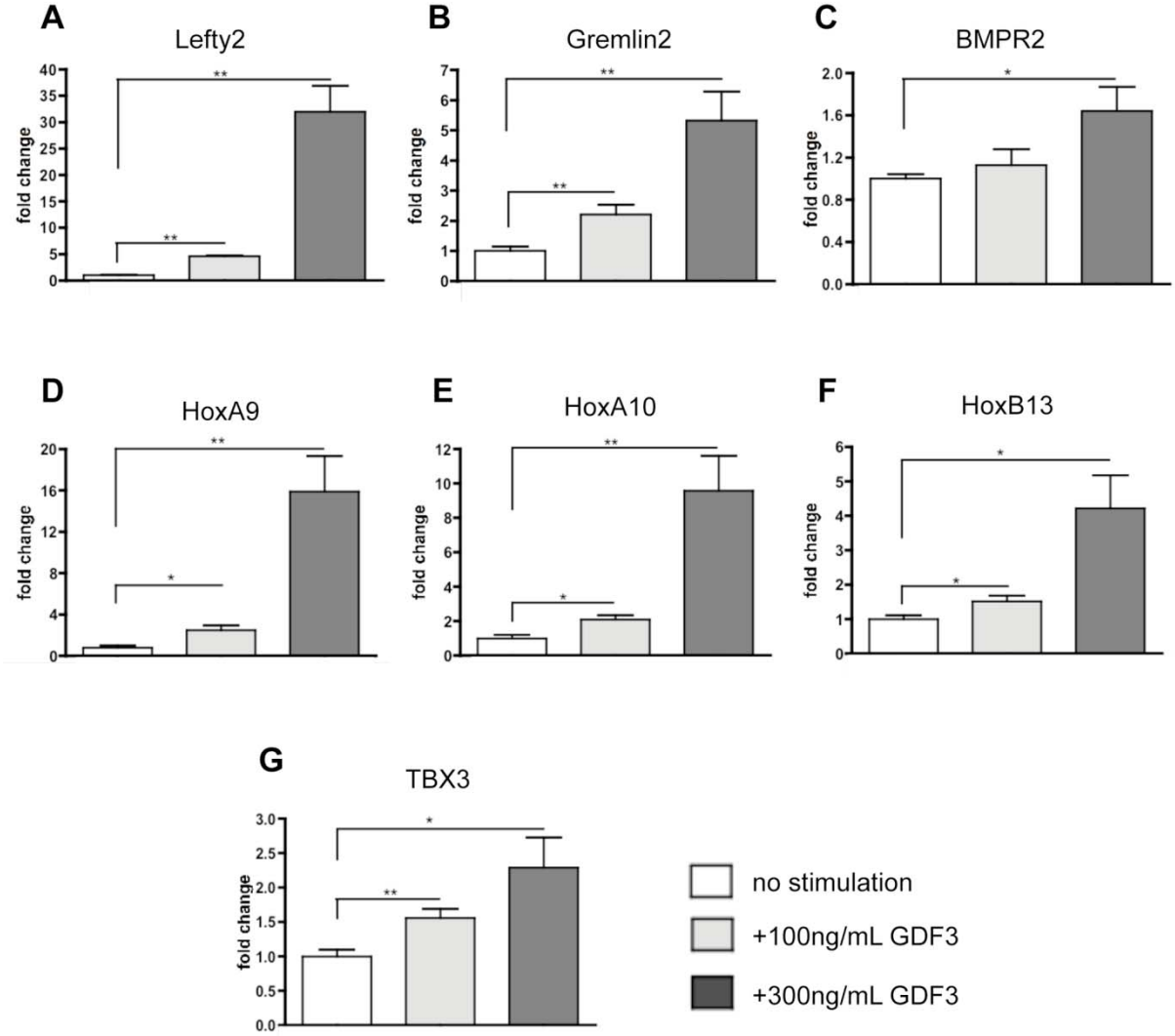

Fig. 4.11 GDF3 induces expression of various genes associated with signal transduction and development
Effect of stimulation with different GDF3 concentrations on transcription of several genes regulated on the microarray. The expression was measured by qPCR, the results are presented as GAPDH ratio and normalized to unstimulated cells (A-G). n=5

Validation of microarray E revealed reciprocal regulation of several genes found to be induced by GDF3 stimulation. Grem2 was 2-fold and HoxB13 4.5-fold downregulated in GDF3-knockdown NCCIT cells (Fig. 4.12). We also found several BMP-ligands, such as BMP-2, -4 and -7 to be downregulated due to decreased GDF3 expression. Moreover, the expression of Tie2, an Angiopoietin 1 and 2 receptor, was 7-fold increased upon GDF3 knockdown.

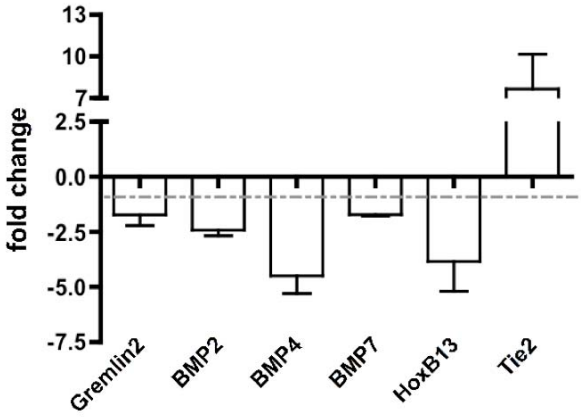

Fig. 4.12 Validation of genes regulated by GDF3 knockdown in NCCIT cells
The expression was measured by qPCR, the results are presented as GAPDH ratio and normalized to NCCITscr cells (A-G). Dotted line indicates fold change of 1. n=5

Briefly, the microarray results have been verified and thereby new potential GDF3 target genes could be defined.

4.7.4 Blocking of GDF3-receptors

As induction of several genes upon GDF3 stimulation was observed, it was important to verify, that the effects are GDF3 specific. For this purpose, we stimulated the cells along with addition of ALK4-inhibitor, SB43152. The inhibitor completely abolished induction of investigated potential GDF3-target genes like HoxA9, HoxA10, HoxB13, TBX3 and Grem2, and prevented the GDF3-induced downregulation of Tie2 (Fig. 4.12). In the case of HoxA10 and TBX3 the addition of SB43152 caused reduction of the endogenous level of the respective molecule.

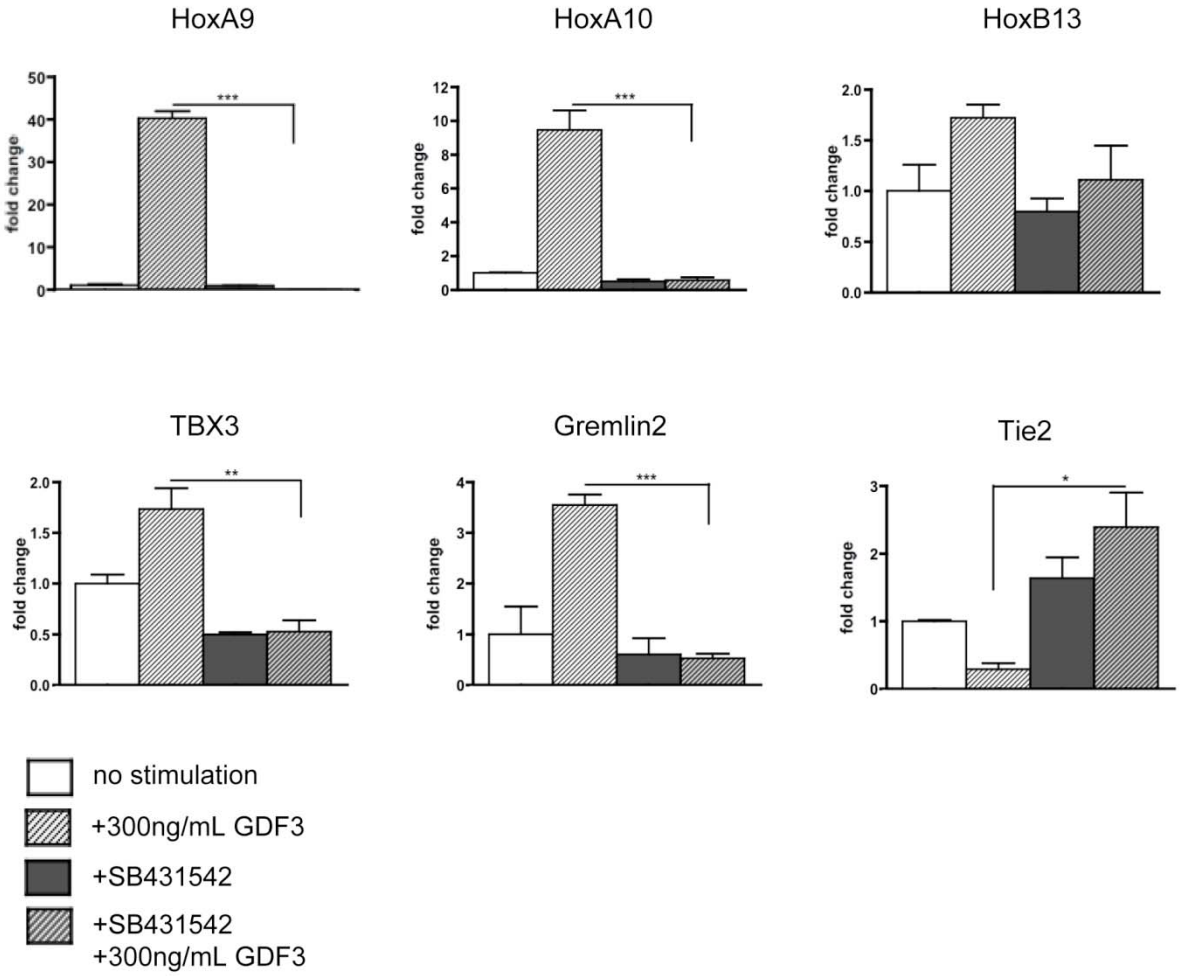

Fig. 4.13 Effect of GDF3 and ALK4-inhibitors SB431542 on the expression of HoxA9, HoxA10, HoxB13, TBX3, Gremlin2 and Tie2.

The expression was measured by qPCR, the results are presented as GAPDH ratio and normalized to untreated cells. n=3

4.8 HoxA9 as a new target gene of GDF3 – promoter analysis

High induction of HoxA9 (Fig. 4.11 & 13) upon short stimulation with GDF3 indicates that HoxA9 is very likely a direct GDF3 target gene. To address this issue, the sequence of HoxA9 gene was analyzed with MatInspector-software. Several Smad3-binding sites in the intron and proximal promoter of HoxA9 could be found, as depicted in the Fig. 4.14A and B. To investigate which of those elements are important for activation of HoxA9 transcription upon GDF3 stimulation, I cloned fragments of the promoter and intron containing Smad3-binding elements (Fig. 4.14A). Promoter constructs A-C along with Cripto-expression vector were then applied in luciferase assay to detect the promoter activity in 293T-cells. Significant induction of luciferase activity could be observed only in the shortest promoter construct B (Fig. 4.14C).

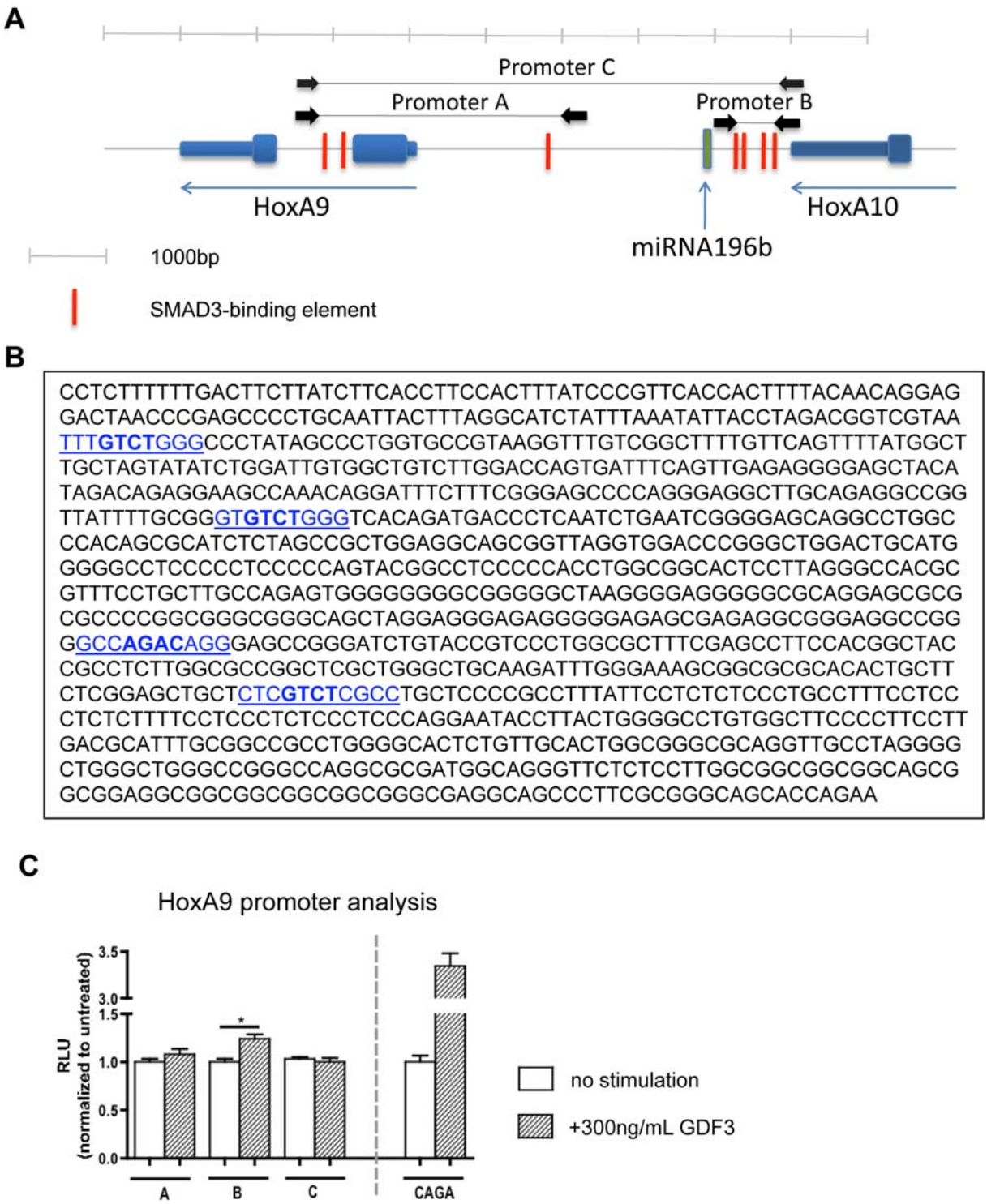

Fig. 4.14 HoxA9 promoter analysis

A. Structure of HoxA9-HoxA10 loci. The location of Smad3-binding elements in the intron and proximal promoter of HoxA9 are highlighted by red ticks. Black arrows indicate location of promoter sections investigated by luciferase assay.

B. Sequence of Promoter B. CAGA-boxes are labeled in blue and underlined.

C. Luciferase activity in 293T cells transfected with HoxA9 promoter constructs, Cripto- and renilla expression vectors. The cells were stimulated with 300ng/mL GDF3 for 24h. The dotted line serves as a distinction between natural (A, B, C) and artificial (CAGA) promoter. The results are showed as a firefly to renilla ratio and normalized to non-stimulated sample. n=3

4.9 Effect of GDF3 on differentiation of NCCIT cells

The microarray data clearly hinted at involvement of GDF3 in the signal transduction and differentiation events. Since NCCIT cells were reported to differentiate *in vitro* into neuronal lineage, the influence of GDF3 on this process was tested. NCCIT cell lines expressing shRNA targeting GDF3 or a scrambled one (sh1GDF3 or scr) were differentiated by treatment with retinoic acid (RA).

4.9.1 Microscopic analysis of the phenotype

NCCIT cell lines expressing shRNA targeting GDF3 or a scrambled one (sh1GDF3 or scr) were differentiated 14d with RA. Both cell lines could be successfully differentiated into neuronal progenitors. As depicted in Fig. 4.15, the cells markedly changed their morphology from small, cobblestone-like cells with big nuclei, forming multilayer colonies to heterogeneous population of large, flat cells with long, branched neurites.

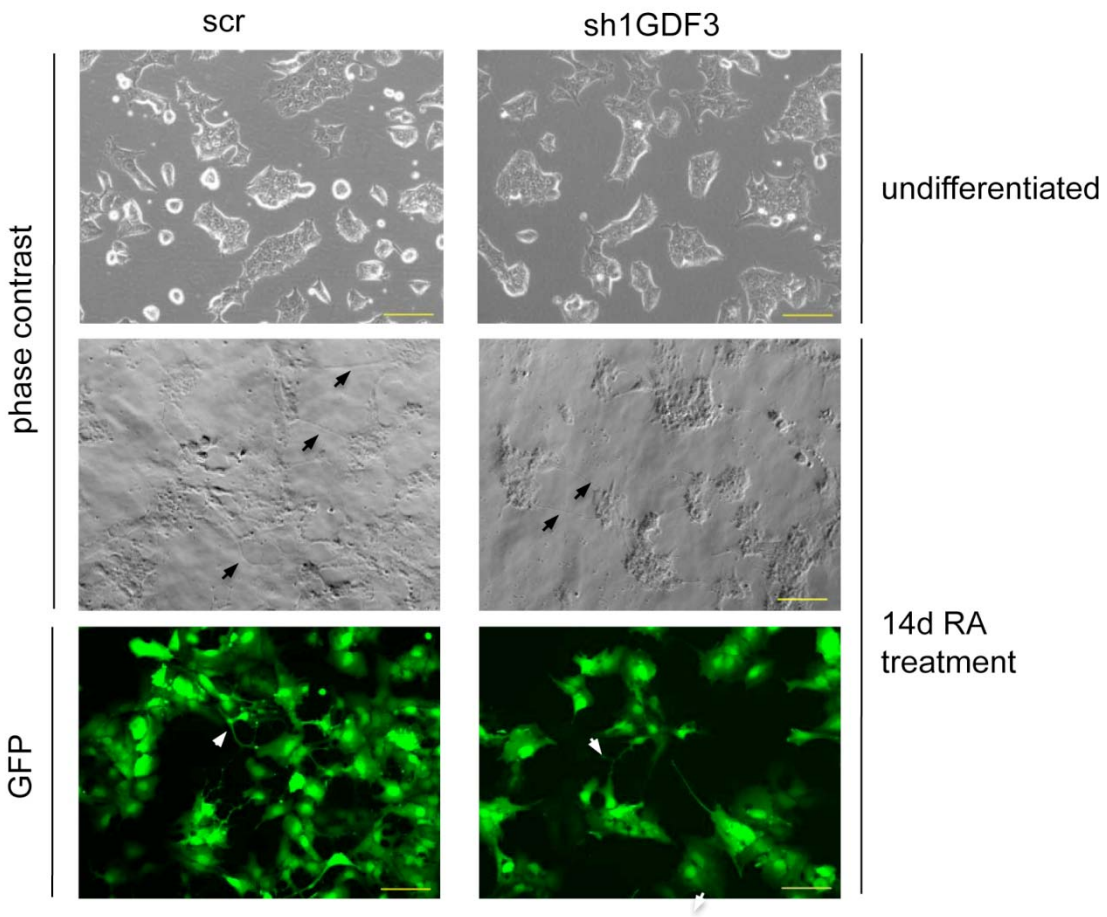

Fig. 4.15 Microscopic analysis of RA-differentiated NCCIT scr and sh1GDF3 cells

Phase contrast and immunofluorescence photographs demonstrating morphological changes of NCCIT scr and NCCIT sh1GDF3 due to RA-differentiation. Upper panel shows morphology of undifferentiated cells. GFP labels cells transduced with lentivirus delivering shRNA-cassette. Black and white arrows indicate the characteristic features of neuron-like structures.

TUJ1 immunofluorescence staining confirmed the neuronal differentiation, whereas the efficiency of the process in both cell lines was very similar (Fig. 4.16).

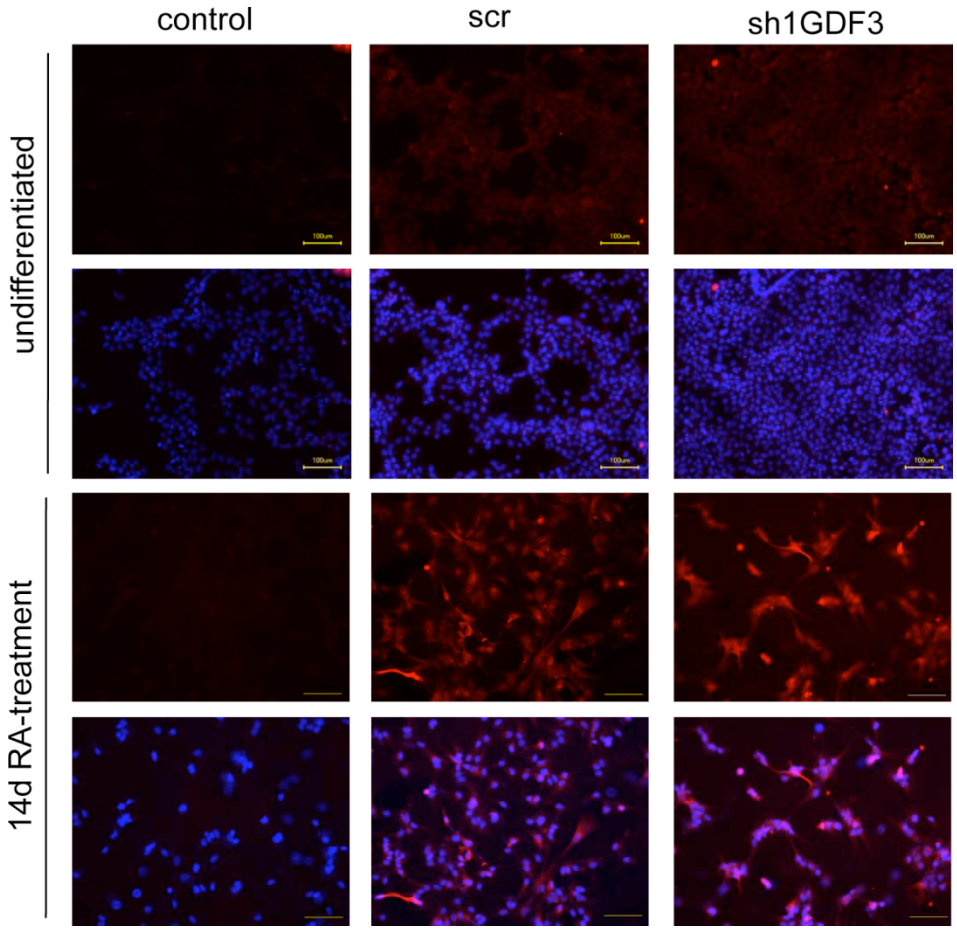

Fig. 4.16 TUJ1-immunofluorescence staining of undifferentiated and 14days RA-differentiated NCCIT scr and NCCIT sh1GDF3 cells.
The cells were stained with anti-Tuj1 and anti-mouse-Alexa594 (upper panel) antibody and counterstained with Hoechst (lower panel). The yellow bar indicates 100µm.

4.9.2 Molecular analysis of the differentiation process

For further characterization of the differentiation process the expression of Pax6, Nestin and TBX3 as markers of neuronal differentiation, and Oct4, GDF3 and Cripto as markers of pluripotency was tracked over the course of RA-treatment by qPCR (Fig. 4.17). The time kinetic revealed that after 14 days the expression of investigated neuronal markers was similar. However, in the early phase of differentiation, especially on the day 4, significant differences could be observed. Nestin and TBX3 were higher expressed in the GDF3 knockdown cell line at the day 4. The expression of Pax6 could be already detected on day 4 in the sh1GDF3 cell line, but not in the control cells. In the course of differentiation the pluripotency markers were downregulated. The Oct4 expression decreased similarly, independently of GDF3 expression status, while Cripto downregulation occurred faster in sh1GDF3 cells. GDF3 was strongly downregulated in the control cells during first 4 days of differentiation.

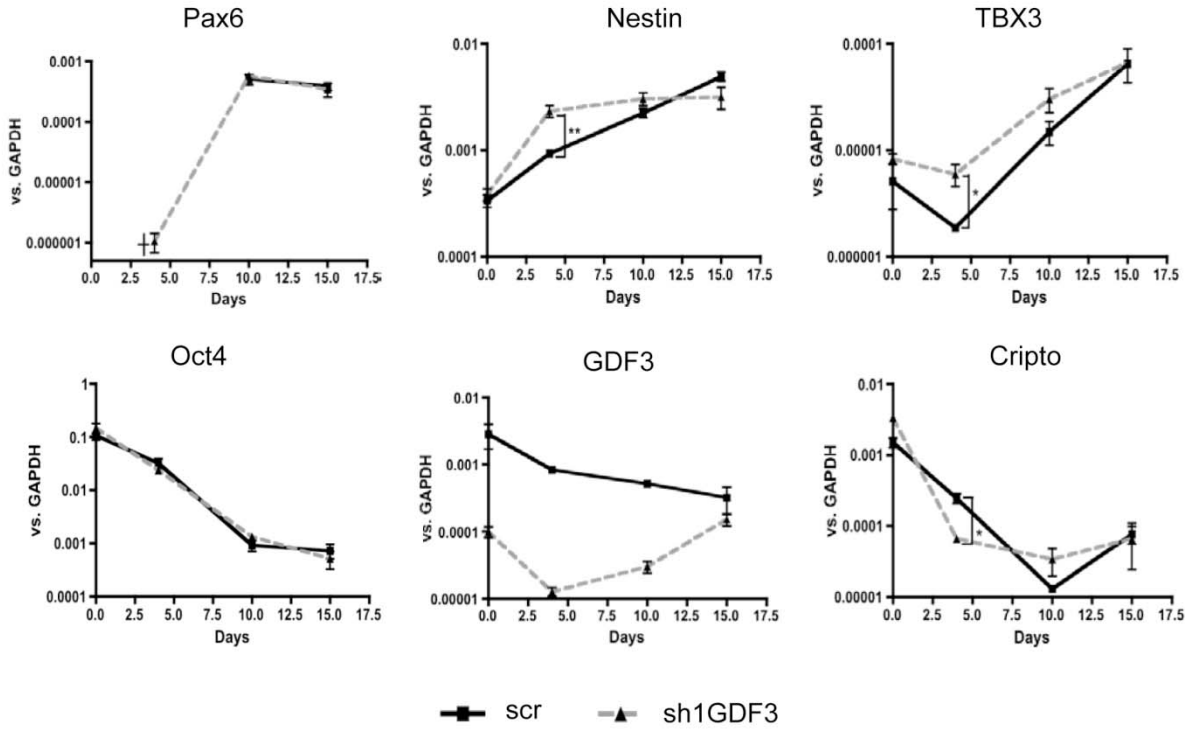

Fig. 4.17 Expression of neuronal markers (upper panel) and pluripotency markers (lower panel) during RA-differentiation of NCCIT cells.
The expression was measured by qPCR, the results are presented as GAPDH ratio and normalized to untreated cells. n=3

Taken together, the expression pattern of differentiation and pluripotency markers suggest, that RA-induced differentiation occurs faster in the absence of GDF3.

4.9.3 Growth kinetic, proliferation and apoptosis during RA-differentiation

RA can trigger not only differentiation, but also apoptosis and growth arrest [71][88]. During the RA-induced differentiation of NCCIT cells we observed significant difference in cell numbers between the GDF3-expressing and –knockdown cells. The growth kinetic in Fig. 4.18A shows that after 14 days of differentiation the growth of control cell line slowed down, while cell number of sh1GDF3 cells did not increase from day 7 on. This effect could be mediated either due to changes in (1) changes in proliferation rate or (2) enhanced apoptosis. I investigated the proliferation after 14 days of RA-differentiation and observed the same rate in both cell lines (Fig. 4.18B-C). As next step, I determined the apoptosis rate by Annexin V-staining. Both cell lines displayed the same rate of apoptosis before the RA-differentiation was initiated, as shown in Fig. 4.18D. However, after 14 days of RA-treatment the number of apoptotic cells among GDF3-knockdown cells increased to 70% (Fig. 4.18F) and was more than 2,3-fold higher than in the control cells. When the differentiation period was extended for additional 14 days I observed that, on the contrary to NCCIT scr cell line, all the sh1GDF3 cells died (data not shown).

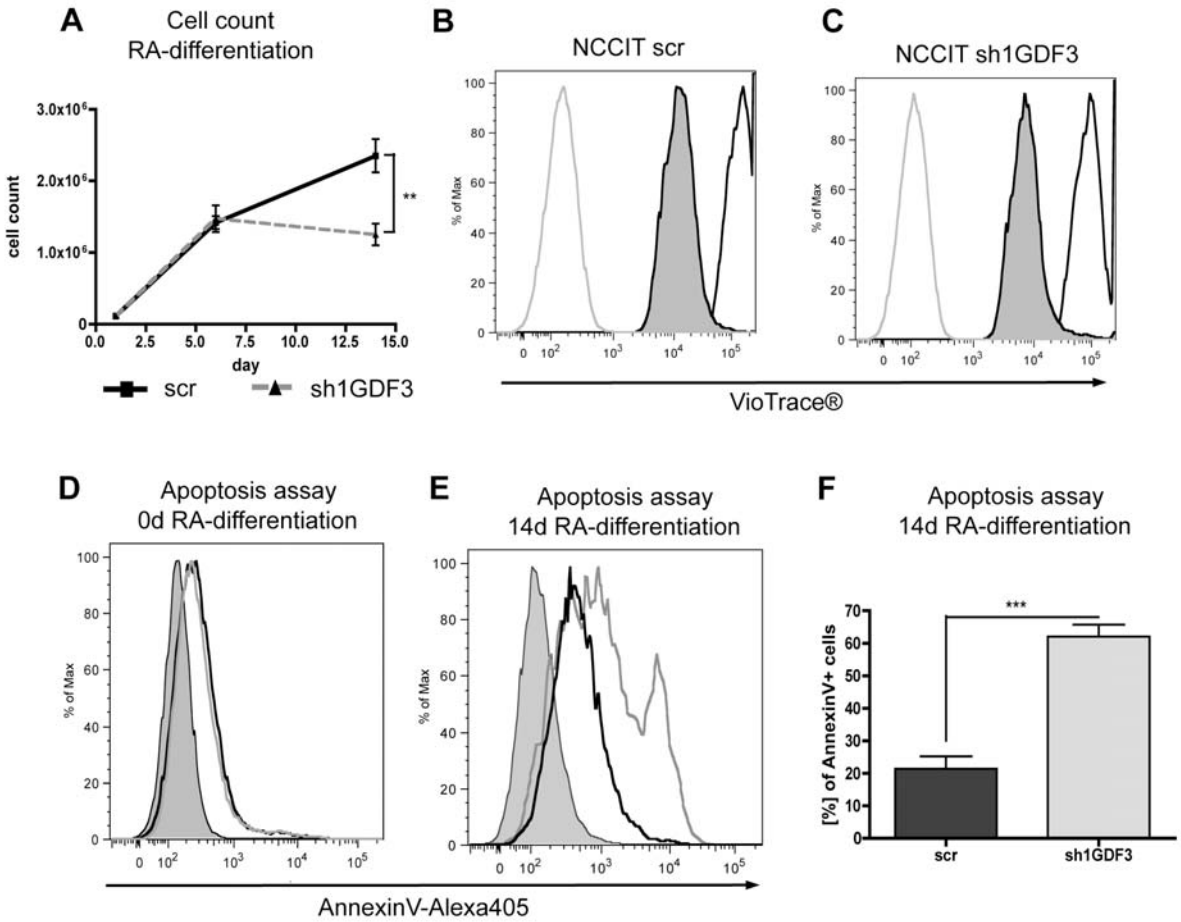

Fig. 4.18 Impact of GDF3-knockdown on growth rate, proliferation and apoptosis during RA-mediated differentiation.

A. Growth curve of NCCIT scr and NCCIT sh1GDF3 during RA-differentiation. n=6

B-C. FACS analysis of the amount of CellTrace® Violet incorporated into 14-days RA-differentiated NCCIT scr (B) and NCCIT sh1GDF3 (C) cells directly after the staining (black line) and 48h later (black line, shaded). The grey line represents unstained control. n=3

D-E. AnnexinV-Alexa405 staining of NCCIT scr and NCCIT sh1GDF3 at day 0 (D) and day 14 (E) of RA-differentiation. The black line represents NCCIT scr, the grey line – NCCIT sh1GDF3. The shaded curve represents unstained control.

F. Quantification of E. n=6

4.9.4 Expression analysis of pro-apoptotic and pro-survival markers

RA-induced apoptosis during neuronal differentiation can be prevented by transcriptional regulation of BCL2 family members' expression [139][140]. Therefore I determined the expression level of several proteins from BCL2 family, such as BCL2 (B cell lymphoma 2), BAK (BCL2 homologous antagonist killer) and BAX (BCL2 associated protein X). Among the factors tested, only BCL2 was 2-fold upregulated due to RA-treatment in NCCIT scr, but not in NCCIT sh1GDF3 cells. The expression of this pro-survival molecule remained unchanged during the course of differentiation in NCCIT sh1GDF3 cells and comparable to the level in untreated NCCIT scr cells (Fig. 4.19). Additionally the expression level of TRAIL and RARβ2 (Retinoic acid receptor β2) was determined. The expression of

both was highly upregulated due to RA-treatment, but no significant differences between GDF3 knockdown NCCIT cells and control cells were observed.

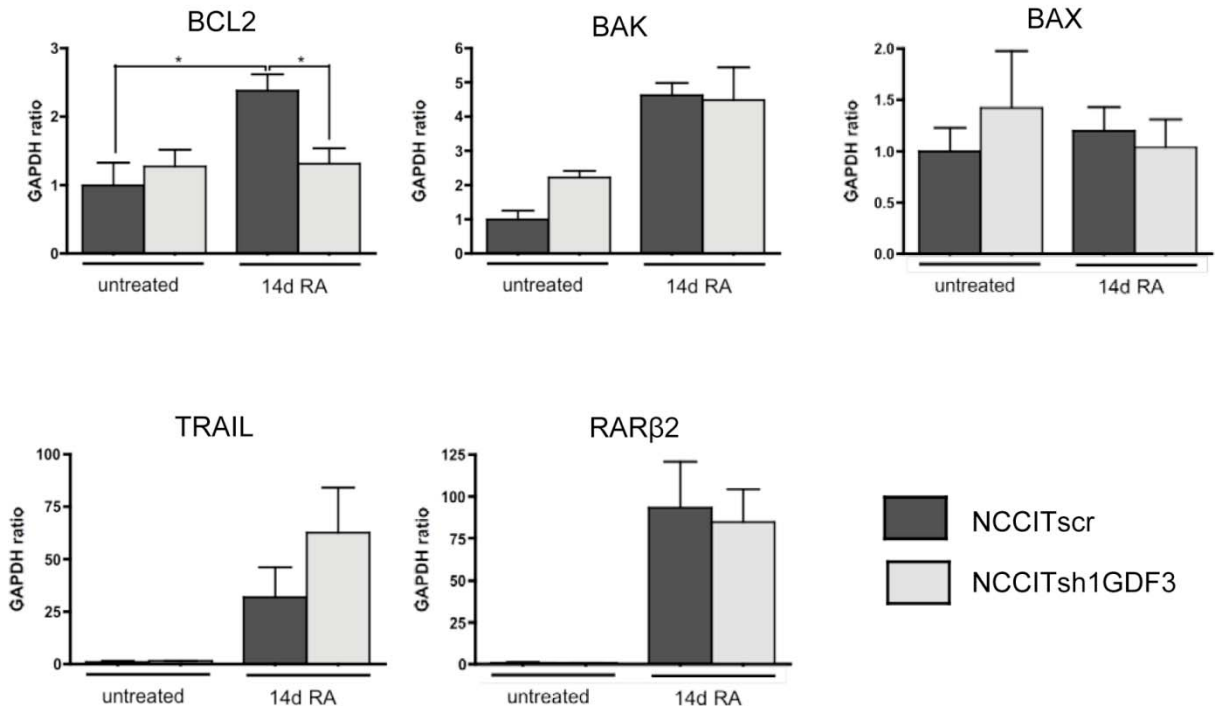

Fig. 4.19 Expression of pro-apoptotic and pro-survival genes in NCCIT sh1GDF3 and NCCIT control cells upon 14 days of RA-treatment.
The expression was determined by qPCR. The results are presented as GAPDH ratio and normalized to expression in NCCIT scr untreated. n=3

This data indicates that disruption of GDF3 pathway modulates the response of NCCIT cells to the differentiation cues *in vitro*, inducing apoptosis due to failure in BCL2 upregulation.

5 DISCUSSION

The goal of this study was to decipher the role of GDF3 in cancer stem cells (CSCs), with a focus on proliferation, modulation of gene expression profile and impact on differentiation. For this purpose, a suitable model of CSCs with active GDF3 signalling was first chosen and characterized. To comprehensively investigate the effects of GDF3 in the model, a system of graded activation of GDF3 pathway was established. It comprised of elimination of endogenous GDF3 expression by generation of GDF3-knockdown cell line, stimulation with different concentrations of the ligand and potentiation of the Smad2/3 signalling by co-stimulation with a mixture of ligands (GDF3 and Nodal). However, it was not possible to generate a GDF3-overexpressing cell line, due to instability of full-length, exogenous GDF3 precursor molecule. The impact of modulation of GDF3 signalling strength was monitored by transcriptome profiling. I could demonstrate that GDF3 robustly induces a subset of genes related to differentiation, among which are several potent tumor suppressors including HoxA9, HoxA10 and HoxB13, and influences BMP-signalling.

Furthermore, I showed that GDF3 drastically changes the fate of NCCIT cells exposed to differentiation cues. In the absence of GDF3, NCCIT cells treated with retinoic acid (RA) - the only clinically approved cyto-differentiating, anti-cancer agent - undergo apoptosis, while control cells escape the cell death by upregulation of pro-survival factor BCL2. Blocking of GDF3 combined with RA-treatment in solid cancers is, therefore, a compelling direction for further investigations, which can lead to re-design of cancer differentiation therapies.

5.1 NCCIT cells as a suitable CSC model to investigate the role of GDF3

Although the concept of the existence of small compartment of cancer cells with stem-like properties that accounts for self-renewal, phenotypic heterogeneity of tumors and disease recurrence emerged more than 40 years ago, neither an universal marker to isolate these cells, nor a standardized procedure to cultivate them *in vitro* without phenotypic changes has yet been described. The lack of a suitable model has been be the major drawback to the cancer stem cell research. Extensive profiling studies of a plethora of cancer cell populations have revealed a strong correlation between CSC phenotype, expression of pluripotency-associated markers and malignancy. The ES-like signature and the presence of factors governing stemness were therefore declared as definitive characteristics of CSCs. Based on these facts, I considered using an embryonic carcinoma cell line NCCIT as a model of CSCs. This cell line was isolated by Teshima *et al.*, and described as hyperdiploid (chromosome range from 54 to 64) with prominent chromosomal aberrations, able to differentiate into derivatives of 3 lineages [141] and highly tumorigenic *in vivo* [142]. Hence, NCCIT cells fulfil all the criteria of CSC-

like phenotype, defined by Cruz *et al.* [21]: (1) extensive self-renewal ability, (2) cancer-initiating ability on orthotopic implantation, (3) karyotypic or genetic alterations, (4) aberrant differentiation properties, (5) capacity to generate non-tumorigenic end cells, and (6) multilineage differentiation capacity.

NCCIT cells do not only express a set of pluripotency markers, but also indispensable components of the GDF3 pathway, including GDF3 itself and all its known receptors, the obligatory co-receptor Cripto and the intracellular signalling mediators Smads (Fig. 4.1). When challenged with GDF3, a robust phosphorylation of Smad2 could be detected in accordance with previous observations of GDF3 signalling in the Nodal-like pathway [117][118]. To further confirm this finding, a translocation of Smad2 into the nucleus as well as induction of known Smad2/3 target genes in ESC, such as Nodal and Smad7 [143] was detected (Fig. 4.2).

Since two possible modes of action have been reported for GDF3, I also tested the ability of GDF3 to antagonize BMP signalling. Employing BRE luciferase assay, the NCCIT cells were stimulated with BMP2 and rising molar excess of GDF3. Contrary to results published by Levine [119][144], I did not detect any inhibition of BMP2 signalling due to GDF3 presence in the culture medium in my experimental setup. The discrepancy between my results and the inhibition of Smad1/5/8 signalling due to GDF3 overexpression observed by others [144] could be explained by usage of an entirely different experimental setup. Levine *et al.* built up an artificial system injecting mouse GDF3 and BMP4 mRNA into frog embryos along with luciferase reporter constructs. However, since GDF3 bioavailability is regulated by the proteolytic processing and very likely receptor-mediated endocytosis (see also Fig. 4.4 and 4.6 and Chap. 5.2.1 and 5.4), the cellular microenvironment created by *Xenopus* embryo and human embryonal carcinoma cells might be strikingly different and lead to activation of different signalling pathways. Additionally, the luciferase assay performed in *Xenopus* acquires very fast effects, since the read out takes place as early as after approx. 8 hours, while in my experimental setup, the cells were directly stimulated (instead of mRNA injection) for at least 24h. On the other hand, the assessment of Smad2/3 phosphorylation due to GDF3 stimulation was not undertaken by Levine *et al.*, so that direct comparison does not seem to be plausible.

5.2 Genetic manipulation of GDF3 expression in NCCIT cells

5.2.1 Prodomain-mediated instability of exogenous GDF3

The bioactivity of TGFβ family members is regulated i.e. at the level of proteolytic activation. The ligands are synthesized as inactive precursors that are cleaved after the multibasic motif RSKR to yield the active, C-terminal, mature protein dimer [145]. Specific members of the proprotein

convertase (PC) family of endoproteases perform the proteolytic processing. Therefore, the inhibitory effects of a prodomain, efficiency of the cleavage and expression of PCs have to be considered while designing an overexpression system of ligands from TGFβ family. With the intention of investigating the effects of exogenous GDF3 on NCCIT cells, I designed a set of vectors to monitor the production, secretion and processing of GDF3. Expecting little biological activity of GDF3, reported already by Chen *et al.* [118] and Andersson *et al.* [117], who hypothesized that the reason is the poor processing by PCs, I tested the activity of tagged GDF3-GDF3 and chimeric BMP2-GDF3 constructs. In agreement with reports by others, GDF3-GDF3 was not able to induce the luciferase activity in a CAGA-Luc assay, while expression within the chimeric precursor along with BMP2-prodomain restored the biological activity of GDF3 (Fig. 4.4). However, tracking of the mature GDF3 yielded from different constructs in cell lysates and supernatants of transfected cells revealed that, unlike in previous observations, lack of signalling capacity by GDF3-GDF3 construct was due to degradation of the ligand. Employing double tagged constructs to track the fate of both prodomain and mature peptide, I could show by detecting large amount of GDF3-prodomain in the culture supernatant (Fig. 4.6) that chimeric precursors with GDF3-prodomain are efficiently processed, independent of the identity of the C-terminal mature peptide and despite the presence of a suboptimal sequence of the recognition site for protein convertase (RRKR). The absence of mature peptide hinted at either prodomain-mediated degradation or intrinsic instability of the processed, mature GDF3. Since rhGDF3, commercially available mature GDF3, was able to robustly induce the Smad2/3 signalling (Fig. 4.2 and 4.7), the GDF3-prodomain seems to account for the earlier described phenomenon. Similar effects have been reported for Nodal [106]. Furthermore it has been shown that Nodal is stabilized by its prodomain prior to cleavage and that mature Nodal is quickly endocytosed by the cells and degraded intracellularly [146], which happens in a receptor-dependent manner [147]. Studies using chimeric precursors with heterologous prodomains have led to the view that the activity and signalling range of the TGFβ ligands is proportional to the rate of proteolytic maturation [146]. Since the mature GDF3 released from precursor molecules appears to be quickly cleared from the extracellular space, its signalling range is likely to be very limited. This raises the possibility that *in vivo* GDF3 is transported to its destination in a more stable, unprocessed form and is subsequently converted by PC produced by recipient cell to a more labile, mature form to act in a very limited time span and spatial range. However, the presence of other TGFβ ligands might impact the life-span of GDF3 by heterodimerization, thereby changing its properties. Here, a heterodimerization with Nodal or GDF1 would be worth testing. Nodal can cooperatively potentiate GDF3 signalling (Fig. 4.7) and GDF1 has been reported previously to (1) prolong the signalling range of Nodal [130], (2) be closely related to GDF3 and (3) act cooperatively with GDF3 during mouse early embryonic development [117][122].

5.2.2 GDF3 knockdown in NCCIT cells

To replenish the system comprising NCCIT cells with manipulated GDF3 signalling strength, I generated a GDF3 knockdown in NCCIT cells, using lentivirus, containing both shRNA cassette targeting GDF3 and GFP, to monitor the transduction efficiency. The efficiency of the GDF3 knockdown was tested by qPCR, but not on the protein level, since no reliable antibody to detect human GDF3 is commercially available. Therefore, to ensure alteration of the secretion profile of NCCIT sh1GDF3 due to GDF3 knockdown in comparison to control cells - NCCIT scr, a functional assay was performed. NCCIT cells, serving as source of Cripto-dependent, CAGA-Luc activating ligands, were co-cultured with Cripto-expressing recipient cells, transfected with CAGA luciferase reporter vector. The direct co-culture was preferred to spatially separated one, because of the short range of GDF3 signalling (Chap. 4.2.2 and 5.2.2). The luciferase expression was activated in both co-cultures of Cripto-expressing cells with NCCIT cells, however, significantly less in the case of co-culture with NCCIT sh1GDF3 cells. The remaining luciferase activity can be explained by unaltered level of Nodal, a TGFβ ligand signalling in a Cripto-dependent manner, also expressed by NCCIT cells (Fig. 4.1).

5.3 Impact of GDF3 on proliferation

Unlike in both reports published by Li Q. *et al.* [128][124], where the reduction of proliferation rate of breast cancer cells MCF7 and neuronal progenitor cells PC12 after GDF3 treatment has been observed, GDF3 did not influence proliferation of cancer stem cells, NCCIT, in my experimental setup. This discrepancy can be explained as due to the usage of different cell types. The members of TGFβ family are known to display differential effects on various cell types, which can be additionally modulated by presence of other factors and/or concentration of the ligand [148][149]. Furthermore, the ligands of TGFβ family have been reported to differently impact cells already primed for differentiation (as in the studies of Li Q. *et al.*) compared to uncommited stem-like cells (such as those in my experimental setup) [150][151].

5.4 Transcriptome analysis of GDF3 effects in NCCIT cells

In this study, a comprehensive analysis of the transcriptional effects of GDF3 in NCCIT cells was performed. For this purpose I conducted a series of microarray experiments, comparing the effects of (1) elevated concentrations of GDF3 and/or Nodal, the GDF3 competitor, and (2) disruption of endogenous GDF3 signalling by lentiviral knockdown.

The design of a GDF3-overexpression system proved to be ineffective due to the spontaneous clearance of mature GDF3, when expressed along with its endogenous GDF3 prodomain. On the other hand, the usage of BMP2-GDF3 construct, which yielded a large amount of stable, mature

GDF3, could trigger unwanted side effects due to the release of BMP2-prodomain that itself might be responsible for signalling artefacts (personal communication with Prof. P.Knaus).

The profound effect of GDF3 knockdown on NCCIT cells (Fig. 4.1 and Chap. 4.7) suggests that endogenous GDF3 acts in an autocrine way and/or paracrine manner on the adjacent cells. It seems likely that GDF3 is processed by (possibly membrane-bound) PC and then quickly captured by the assembled receptor complex in its immediate vicinity. If no receptor complexes are adjacent to the GDF3 processing site, the ligand is cleared from the extracellular space or supernatant and cannot be detected by standard laboratory methods (Fig. 4.6). Therefore, the co-localisation of the processing site and the receptor complex appears to be crucial for the activation of a signalling event. In this scenario, the exogenously overexpressed GDF3 will not be able to trigger stronger signalling than endogenous GDF3, because the number of co-localised PCs and receptor complexes become the limiting step in the signalling process. However, providing stable rhGDF3 free of its degradation-mediating prodomain can potentiate the signalling (Fig. 4.7) by involving all receptor complexes in the signalling events, not only those in the proximity to PCs. Hence, a stimulation with rhGDF3 was chosen to enhance GDF3 signalling in NCCIT cells.

Due to technical limitations, GDF3-stimulation vs. GDF3-knockdown cannot be considered as complete counterparts in this experimental design. The stimulation was performed for 3h, aiming to investigate short time primary effects, while avoiding the effects of feedback loops and therefore delivering an insight into a dynamically changing system. The GDF3 knockdown was performed via lentiviral delivery of an shRNA cassette, so that a stable GDF3-knockdown and control cell line were generated by expansion of transduced cells over several passages. Thus, it is not surprising, that the transcripts regulated by GDF3 stimulation and GDF3 knockdown have a common intersection but are not congruent. However, investigations of long-term effects of GDF3 stimulation would be an interesting aspect for follow-up studies.

A common approach to address the functional interpretation of the gene subset regulated on the microarray is overrepresentation analysis, which uses the hypergeometric test (or its variants) to evaluate whether a particular functionally defined group of genes is represented more than expected by chance within a gene list [152].

Overrepresentation analysis revealed that GDF3 is strongly involved in cell signalling and developmental processes (Tab. 4.3). Especially in the latter group, genes related to ectoderm development and neurogenesis were significantly overrepresented. Some of them, such as Lefty2, Grem2 and TBX3 (Fig 4.11A-B, G) could also be validated as GDF3 targets. My results are in

corroboration with those of Chen *et al.* [118] and Levine *et al.* [119], who obtained their data in ESC and showed that GDF3 is indispensable for normal development *in vivo* and *in vitro*[120].

We learned from Nodal and GDF3 knockout mouse models [118][122][153][154] that these ligands cannot compensate for each other during gastrulation, although they have been shown to utilize the same receptor set and trigger the same signalling pathway. However, during early embryonic development not only ligand identity, but also its spatio-temporal expression pattern is of great importance. The enhanced half-life of Nodal [148][155] and its prolonged expression in comparison to GDF3 [154] could be the reason for lethality of Nodal$^{-/-}$ mice and only partial lethality of GDF3$^{-/-}$ mice. This study shows for the first time on the molecular level, that although Nodal and GDF3 trigger Smad signalling with similar strength (Fig. 4.7), they activate overlapping, but not identical gene sets. In this experimental setup, due to Nodal stimulation enrichment of genes associated with mesoderm development could be detected. This activity cannot be assigned to GDF3, which seems to predominantly induce ectoderm development. These results are consistent with previous reports about findings in zebrafish and mice confirming that Nodal constitutes an important part of the mesoderm-inducing signal [153]. Additionally, Chen *et al.* have demonstrated, that even high doses of GDF3 mRNA injected into animal caps, unlike Nodal, cannot induce expression of mesoderm markers [118]. I hypothesize, that the differences may arise from activation of an alternative signalling cascade that very likely intersects with the Smad2/3 pathway and modulates its action as a co-transcription factor. I demonstrated this indirectly, by detecting the phosphorylation of the linker region of Smad2 due to GDF3 stimulation (Fig. 4.3), which is the common indicator of Erk1/2 and/or JNK/p38 pathways activation [156]. The function of GDF3 and Nodal should therefore be analysed separately and the ligands are not interchangeable.

The role of GDF3 in developmental processes was confirmed by validation of GDF3 targets emerging from the performed microarray experiments. I considered homeobox (Hox) genes as appealing targets for further evaluation. During development, the Hox genes are involved in anterior-posterior body patterning, and in formation of limbs and genitalia. However, they do not regulate only embryonic development and tissue patterning. Their tightly regulated expression is also important in adult tissues and its perturbation frequently occurs in tumors [157–159]. Therefore, I focused primarily on HoxA9, HoxA10 and HoxB13.

HoxA9 directly regulates BRCA1 expression and restricts breast tumor aggression. Elevated HoxA9 expression can therefore be correlated with an optimistic prognosis for the patient [160]. GDF3 has been already reported to be expressed in breast cancer [125], although the expression level seem to be reduced in comparison to the surrounding, healthy tissue [124]. It would be interesting to

investigate, whether the restoration of GDF3 level in breast cancer would increase HoxA9 expression and thereby reduce malignancy of the disease and improve the clinical outcome for the patient. Interestingly, the expression of HoxA9 in unstimulated, wildtype NCCIT cells was barely detectable, which led me conclude, that endogenous GDF3 expression may not be high enough to robustly induce HoxA9 expression and that exogenous introduction of the ligand is necessary.

Although HoxA9 expression correlates with decreased malignancy of breast cancer, its expression has also been reported to accelerate tumor progression in epithelial ovarian cancer (EOC). The study of Ko *et al.* [161] has demonstrated that HoxA9 does not influence the proliferation of EOC cells directly. HoxA9-induced TGFβ2 expression in EOC cells specifically educates normal fibroblasts to acquire cancer-associated fibroblast features, such as production of CXCL12, IL-6 and VEGF-A and actively shapes the cancer microenvironment to support cancer progression. My study, however, was predominantly focussed on the short-time effect of GDF3 and the experimental setup comprised only of one cell type, the embryonic carcinoma cells NCCIT, the model cell line. Therefore, the secondary effects of GDF3 on the microenvironment cannot be evaluated in this framework.

Other highly interesting GDF3 targets were also reported to act as potent tumor suppressors. HoxA10 regulates p53 expression in breast cancer, modulates proliferation and invasiveness of breast cancer cells [162] and mediates differentiation in myeloid leukemic cells [163]. HoxB13 is known to be downregulated by hypermethylation of the promoter region in not only breast, but also colorectal [164], renal [165], prostate [166] cancer and melanoma [167]. Its re-expression diminishes tumor formation *in vivo* and *in vitro*.

Furthermore, the GDF3 stimulation experiment as well as GDF3 knockdown revealed the involvement of GDF3 in the BMP-pathway. GDF3 treatment caused upregulation of BMPR2 (Fig. 4.11C), while GDF3 knockdown diminished the expression of several members of BMP-family, including BMP-2, -4 and -7 (Fig. 4.12). This GDF3-BMP link might be considered while designing anti-cancer treatment, since active BMP signalling in tumors has been reported to be beneficial for the disease outcome [168]. Additionally, BMPs has been reported to be involved in differentiation processes, however, its impact depends on the cell type. During embryonic development, ectoderm and mesoderm are patterned along the dorso-ventral axis, governed by the morphogenetic effect of BMPs, especially BMP4 [60]. At the ectodermal level, BMP-4 behaves like a strong epidermal inducer in regions with low antagonist concentrations [61]. In the experimental model of ESC differentiation, BMP4 acts as a inhibitor of neurogenesis [169][170]. Since the embryonal carcinoma cells that were used in this study share several common characteristics with embryonic stem cells, I conclude, that decreased expression level of endogenous BMPs, among them BMP4, led to accelerated RA-

mediated neuronal differentiation (Fig. 4.17, upper panel) of NCCIT sh1GDF3 when compared to NCCIT scr.

Inhibiting angiogenesis has become an effective approach for treating cancer. Despite a variety of factors being involved in the process of vessel growth, only therapies targeting VEGF pathway have been approved to date [171]. However, a growing number of reports point out other promising targets, like Tie2. Deletion of Tie2 receptor or its ligands angiopoietin-1 and -2 (Ang1, Ang2) results in defects in the later stages of vessel remodeling, while activation of Tie2-Ang1/2 pathways leads to an increase in vessel diameter [171]. A study employing teratoma-forming ESCs to model tumor angiogenesis *in vivo* has demonstrated that systemic application of reagent that block the Tie2-Ang1/2 interaction can dramatically reduce tumor vessel size and therefore restrict tumor perfusion [172]. Furthermore, Liu D *et al.* have observed that Tie2 expression in glioma and brain CSCs modulates their interaction with endothelial cells and promotes malignant progression, by enhancing the adhesion of glioma cells to endothelial cells and the invasive capacity *in vitro* and *in vivo* [173]. Here, the analysis of the NCCIT transcriptome revealed the regulation of angiogenesis upon modulation of the GDF3 pathway (Appendix). Futhermore, I detected a significant upregulation of Tie2 upon GDF3 knockdown (Fig. 4.12) and Tie2 downregulation due to GDF3 stimulation of NCCIT cells, which indicates involvement of GDF3 in the negative regulation of the angiogenesis process.

However, it should be stressed that in this study mostly short-term effects of GDF3 were investigated and the primary and secondary effects of GDF3 were limited to NCCIT cells, so as to get more insight in the biology of CSCs. Putative secondary effects of the induction of aforementioned, validated transcription factors as well as GDF3-mediated regulation of expression of secreted molecules, expand the indirect GDF3 range of action from CSCs to cancer microenvironment, consisting of differentiated cancer cells, cancer associated fibroblasts and cells of the immune system, such as tumor associated macrophages, dendritic cells and neutrophiles. These effects need to be tested *in vivo*.

5.5 HoxA9 promoter analysis

Since HoxA9 expression was dramatically upregulated by GDF3 treatment, I investigated GDF3-HoxA9 relation in more detail. To confirm whether HoxA9 is a direct target of GDF3, I cloned several DNA fragments from the proximal HoxA9 promoter, containing SBE-elements according to *in silico* analysis (Fig. 4.14B). Unexpectedly, I found only weak, though significant activation of only promoter B, but not C (Fig. 4.14C). The reason for this phenomenon could be the large size of promoter C, which very likely accounted for (1) low transfection rate and (2) improper folding of the plasmid inside the cell, so that potential enhancer regions were unavailable for binding of relevant transcription factors.

However, little is known about the transcriptional control of proteins from the Hox-family. Proper transcriptional silencing is indispensible to Hox function since premature expression can lead to developmental defects or disease. Several studies have shown that long-range DNA contacts are important to regulate transcription. For example, enhancers or insulators (silencers) can stimulate or repress the expression of genes by physically interacting with them [174]. In a recent report by Ferraiuolo et al. a 3D organization of the human HoxA cluster has been described and a distinct pattern of chromatin loops has been demonstrated (Fig. 5.2). The loop-like chromosomal organization is believed to prevent improper Hox activation by irrelevant cellular pathways and to depend on the transcriptional activity [175]. It hints at the existence of distant regulatory elements within the Hox-cluster.

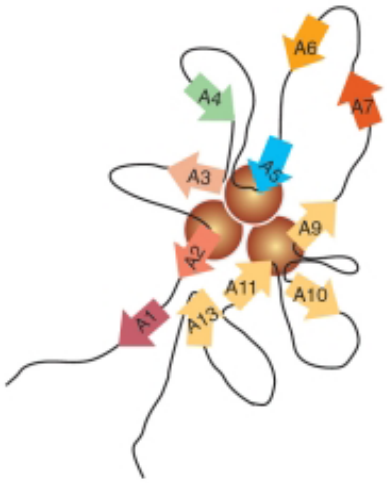

Fig. 5.2 2D schematic representation of the silent human cluster *in vivo* (from [175])
It represents an illustration of DNA contacts. Brown circles highlight an area encompassing strongest looping contacts in the cluster.

Moreover, Montavon *et al.* investigated distal regulatory sites of the HoxD cluster and found them dispersed throughout the nearby gene desert [176]. This scenario seems likely for transcriptional regulation of the HoxA cluster as well, because of the common origin of Hox clusters [177], the presence of more than 200kb of gene desert upstream and downstream of the aforementioned cluster and the very tight placement of HoxA-genes on the chromosome 7. In the scope of these assumptions the SBE-cluster in the promoter B still may play a role either as a switch or a fine-tuner of HoxA9 expression, but is not the only region regulating its expression.

5.6 RA-induced apoptosis upon GDF3-knockdown in NCCIT cells

Having confirmed the developmental role of GDF3 in the model of CSC, I treated NCCIT cells with RA *in vitro* to investigate, whether GDF3 knockdown would change the differentiation pattern. Despite a

number of genes associated with neurogenesis being regulated on the microarray (Tab. 4), I did not observe any phenotypic differences between GDF3 knockdown cells and the control (Fig. 4.15 and 4.16). However, molecular analysis of these two cell sets by qPCR revealed an altered expression pattern during the RA treatment. The expression level of both differentiation and pluripotency markers in the early stage of the process hinted at accelerated neurogenesis in the absence of GDF3 (Fig. 4.17). This data is in accord with the study of Levine *et al.* [119], which demonstrated that overexpression of GDF3 can at least partially maintain the expression of pluripotency markers in hESC challenged with BMP4. The apparent contradiction of my results to the report about the neuro-inductive potential of GDF3 in neuronal progenitor cells [128] may be due to usage of a different cellular system. A possible explanation is that the effect of GDF3 on cells already primed for differentiation can be strikingly different compared to uncommitted stem-like cells – a common phenomenon for the members of the TGFβ family.

RA is the only clinically available cyto-differentiating agent, employed in several cancer therapies, especially in treatment of acute promyelotic leukemia, but also of solid cancers, such as squamous cell carcinoma [81], neuroblastoma [82] and hepatocellular carcinoma [178] in humans and breast carcinoma [179] in mice. The concept for getting the malignant potential under control is forcing the tumor cells into terminally differentiated status. However, the success of RA application in solid tumor was limited, because RA induces a variety of cellular programs depending on cell type, ranging from simple growth inhibition and differentiation to apoptosis.

This is the first report describing the impact of GDF3 on the outcome of RA-treatment of NCCIT cells *in vitro*. I demonstrated that GDF3 protects the CSC from apoptosis mediated by RA, an agent also applied in the clinic for differentiation therapy of cancer (Fig. 6D-F). The GDF3 knockdown NCCIT cells underwent differentiation just like their GDF3 expressing counterparts. However, unlike NCCIT scr, they also initiated cell death, as detected by Annexin V staining.

Several processes may account for the pro-apoptotic effects mediated by RA. RA signals via set of RARs, from which RARβ is a highly interesting target of anti-cancer therapies. Restoration of RARβ expression in several cancer types leads to proliferation stop and apoptosis, although little is known about the molecular mechanism of its action, and target genes of RARβ remain to be discovered [87]. In the NCCIT cells, RARβ2 was highly and comparably induced in NCCIT sh1GDF3 and scr cells due to RA-treatment (Fig. 4.19).

The main cause of RA-mediated apoptosis is the induction of TRAIL expression. This molecule acts selectively on cancer cells triggering an apoptotic cascade via specific 'death receptors' [180]. In the scope of this work, I investigated the expression level of TRAIL in NCCIT sh1GDF3 cells and their

GDF3-expressing counterparts. The qPCR results hint at an increased amount of TRAIL transcript in GDF3-knockdown NCCIT cells, but the values were not significantly different (Fig. 4.19). However, TRAIL can be expressed as a membrane bound molecule as well as a secreted factor with relatively short half-life [96]. Thus, to estimate the concentration of bioactive TRAIL, the measurement on the protein level would give a better insight.

The reason for increased apoptosis maybe caused by the modulation of the balance between different groups of molecules from BCL2 family. BCL2 family members can be grouped into anti-apoptotic survival factors such as BCL2 or BCL-xL, which block caspase activation, and pro-apoptotic killer proteins such as BAX and BAK, which facilitate apoptosis via caspase-dependent and -independent mechanisms [181]. One of the unique features of BCL2 family proteins is heterodimerization between anti-apoptotic and pro-apoptotic proteins, which is considered to inhibit the biological activity of their partners [182][183]. In fact, the relative levels of these proteins in a cell determine whether a cell will live or die [184]. The level of crucial molecules from BCL2-family was assessed before differentiation and after 14 days of RA-treatment. The pro-apoptotic factors BAX and BAK followed the same expression kinetic, independent of GDF3-expression status in NCCIT cells. On the contrary, the level of BCL2 was significantly upregulated in the control cells, which escaped the apoptosis as a consequence, while NCCIT cells with GDF3 knockdown failed to do so (Fig. 4.19). These results indicate that the pro-survival effect of GDF3 is BCL2-dependent. However, it seems likely that this is an indirect, secondary effect, possibly due to changes in the epigenetic landscape of GDF3 knockdown cells, since GDF3 and Cripto expression in the control cells was already downregulated in the early phase of RA-differentiation (Fig. 4.17). For future studies it might be of relevance to investigate the impact of GDF3 overexpression on RA-induced differentiation.

However, number of other mechanisms or pathways maybe involved in RA-mediated apoptosis, such as p53, NFκB, phosphatidylinositol-3-kinase or MAPK pathways.

6 Conclusions

The main goal of this study was to define the role of GDF3 in the biology of CSCs. For this purpose, an embryonal carcinoma cell line - NCCIT, which (1) closely resembles embryonic stem cells and (2) displays major features defining CSCs was chosen as a model of CSCs. In scope of this work I extensively characterized the GDF3 signalling cascade and established cellular systems to investigate the effects of diminished and potentiated GDF3 signalling. To decipher the role of GDF3 a comprehensive transcriptome analysis by microarray technology was performed.

Figure 5.1 depicts the graphical summary of transcriptional changes caused by GDF3 in the model of CSCs. Both GDF3 stimulation and knockdown modulates the transcriptional profile of NCCIT cells. GDF3 is predominantly involved in differentiaton and developmental processes. Due to shared features between ESC and EC, genes regulated by GDF3 are associated mostly with specification of the germ lineages, mainly ectoderm, indicating the modulation of multidifferentiation potential of target cells. Among regulated genes, there are several potent transcription factors, such as proteins from Hox-families, which has been described before to act as tumor suppressors. Induction of HoxA9, HoxA10 and HoxB13 has been consistently reported in literature to be beneficial in treating patients with breast cancer. Therefore, the role of GDF3 should be further investigated in breast cancer stem cells, especially in animal models *in vivo*, to elucidate putative secondary effects of GDF3 on the cancer microenvironment.

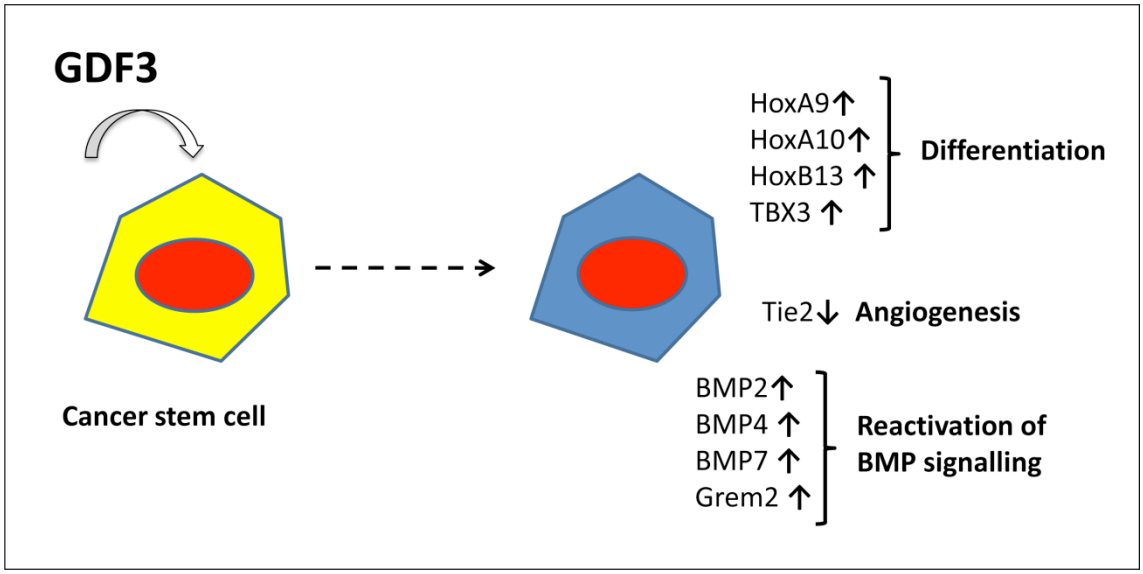

Fig. 5.1 Scheme presenting alteration of transcriptional profile in NCCIT cells, as a CSC model, due to action of GDF3.

Additionally, the overrepresentation analysis of genes regulated on the microarrays, as well as qPCR, has uncovered the previously unknown role of GDF3 in angiogenesis regulation. Tie2 is strongly

upregulated in the absence of GDF3, indicating involvement of GDF3 in negative angiogenesis regulation. I also confirmed by qPCR transcriptional changes of several molecules from the TGFβ family, among them extracellular inhibitor Gremlin2 as well as ligands triggering Smad1/5/8 pathway (BMP2, BMP4, BMP7) and a BMP-receptor (BMPR2). The expression of these molecules seems to be sustained by the presence of GDF3 and drops upon GDF3 knockdown.

In summary, GDF3-mediated alteration of expression levels of molecules depicted in Fig. 5.1, which are involved in differentiation, angiogenesis and BMP-signalling, suggests that targeting GDF3 signalling may render CSCs less malignant.

On the basis of the findings about GDF3 acting on development and differentiation, the capacity of NCCIT cells to differentiate *in vitro* upon stimulation with RA, which has been successfully employed in treatment of several cancer types, was exploited, to investigate the impact of GDF3 on the differentiation process. I made the unexpected observation that under prolonged exposure to RA GDF3-knockdown NCCIT cells underwent apoptosis to much greater extent than their GDF3-expressing counterparts (Fig. 4.18D-F). This data lead me to speculate, that GDF3 protect the CSC cells from RA-induced apoptosis. The graphical summary of the observed phenomenon is depicted in Fig. 5.3.

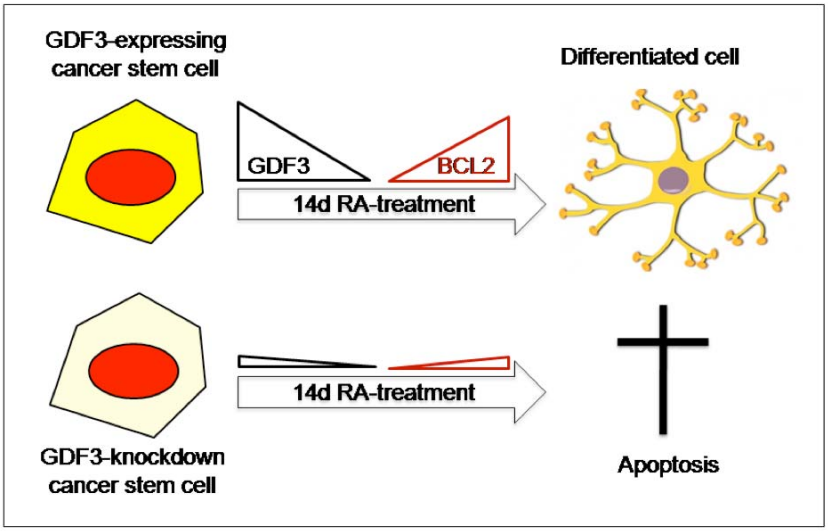

Fig. 5.3 Effects of RA-mediated neuronal differentiation on CSCs, depending on their GDF3-expression status. The black triangle symbolise the GDF3 expression level during the RA- treatment, and the red ones - fold change of BCL2 expression.

The results of this study indicate that the pro-survival effect of GDF3 is BCL2-dependent. Blocking of GDF3 combined with RA-treatment of solid cancers is a compelling direction for further investigations, which can lead to re-design of cancer differentiation therapies and may provide a mechanism to overcome the RA-non-responsiveness caused by BCL2 overexpression in some cancer types.

7 PERSPECTIVES

In my study, I have confirmed GDF3 as an important player in cancer biology. Using NCCIT cells as a system with CSC-like properties I could demonstrate that GDF3 robustly induces a panel of genes related to differentiation and signal transduction. Additionally, my work hints at a previously not reported mechanism regulating GDF3 bioavailability that depends on distinct GDF3-prodomain features. The molecular mode of action was not further characterized in the scope of this study. However, understanding of this phenomenon may not only contribute to design of new anti-cancer therapies (which could target enzymes processing GDF3), but also will also broaden our knowledge about the regulation of one of the most thoroughly investigated signaling cascades - the TGFβ cascade - which still seems to contain new dimensions to be discovered.

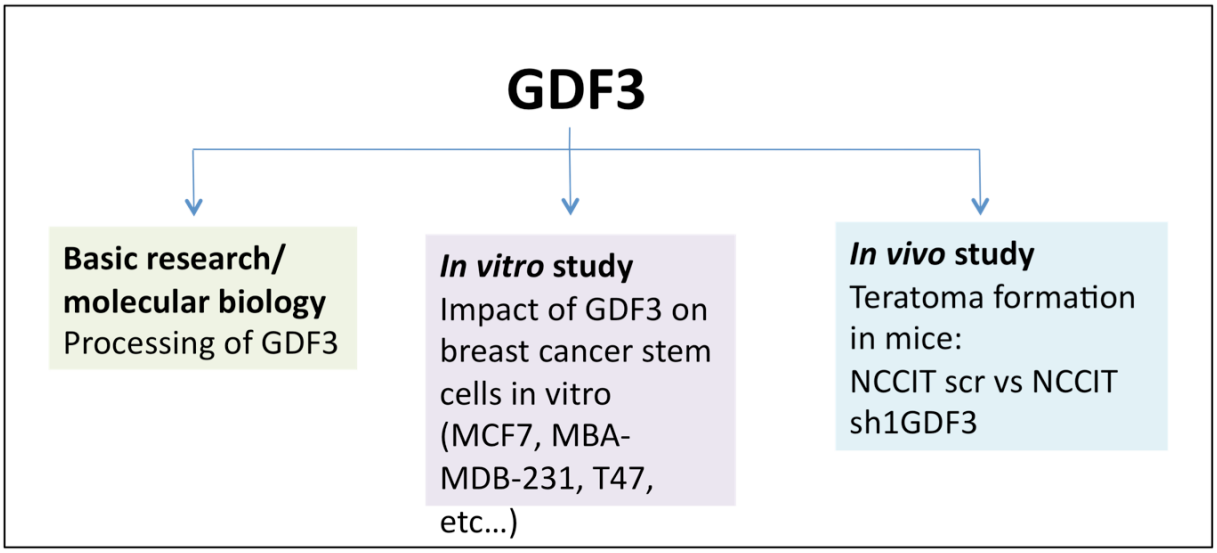

Fig.7.1 Scheme presenting putative directions of GDF3 follow-up studies.

Since GDF3 has been reported to be (re-)expressed in several cancer types, findings described in this work should be validated in other cellular systems, particularly in breast cancer. With many breast cancer cell lines available and several protocols describing enrichment of putative breast cancer stem cells *in vitro*, the investigation of GDF3 impact in this specific cancer type would be an attractive follow-up study.

My promising finding of the co-operative role of GDF3 and retinoic acid in differentiation therapy *in vitro* needs to be validated *in vivo*. With an *in vivo* teratoma formation assay in mice using NCCIT scr and NCCIT sh1GDF3 cells several urgent questions could be answered at once:

(1) How does GDF3 influence tumorigenicity of cancer stem cells *in vivo*? Does GDF3 knockdown render the cells more prone to differentiation, when exposed to the *in vivo* microenvironment?

(2) Do the GDF3-knockdown teratomas respond better to RA treatment?

(3) How does GDF3 or lack of it impacts cancer microenvironment?

The last aspect in particular, which could not be addressed in the scope of this study, is very intriguing. GDF3 signaling relies on the ubiquitously expressed Activin-type 1 and 2 receptors and the obligatory co-receptor Cripto characterized by a very narrow expression pattern. My preliminary data indicate the presence of Cripto on monocytes and macrophages, which leads to the assumption that this compartment of the immune system maybe GDF3-sensitive and should be incorporated in the investigations of GDF3 in cancer biology.

8 LIST OF REFERENCES

[1] S. I. Hajdu, “A note from history: landmarks in history of cancer, part 1.,” *Cancer*, vol. 117, no. 5, pp. 1097–102, Mar. 2011.

[2] A. Jemal, F. Bray, M. M. Center, J. Ferlay, E. Ward, and D. Forman, “Global cancer statistics.,” *CA: a cancer journal for clinicians*, vol. 61, no. 2, pp. 69–90, 2011.

[3] W. H. Organization, “No Title.”

[4] L. L. Campbell and K. Polyak, “Breast tumor heterogeneity: cancer stem cells or clonal evolution?,” *Cell cycle (Georgetown, Tex.)*, vol. 6, no. 19, pp. 2332–8, Oct. 2007.

[5] A. Marusyk, V. Almendro, and K. Polyak, “Intra-tumour heterogeneity: a looking glass for cancer?,” *Nature reviews. Cancer*, vol. 12, no. 5, pp. 323–34, May 2012.

[6] P. C. Nowell, “The clonal evolution of tumor cell populations.,” *Science (New York, N.Y.)*, vol. 194, no. 4260, pp. 23–8, Oct. 1976.

[7] S. B. Baylin and P. A. Jones, “A decade of exploring the cancer epigenome - biological and translational implications.,” *Nature reviews. Cancer*, vol. 11, no. 10, pp. 726–34, Oct. 2011.

[8] S. P. Shah, A. Roth, R. Goya, A. Oloumi, G. Ha, Y. Zhao, G. Turashvili, J. Ding, K. Tse, G. Haffari, A. Bashashati, L. M. Prentice, J. Khattra, A. Burleigh, D. Yap, V. Bernard, A. McPherson, K. Shumansky, A. Crisan, R. Giuliany, A. Heravi-Moussavi, J. Rosner, D. Lai, I. Birol, R. Varhol, A. Tam, N. Dhalla, T. Zeng, K. Ma, S. K. Chan, M. Griffith, A. Moradian, S.-W. G. Cheng, G. B. Morin, P. Watson, K. Gelmon, S. Chia, S.-F. Chin, C. Curtis, O. M. Rueda, P. D. Pharoah, S. Damaraju, J. Mackey, K. Hoon, T. Harkins, V. Tadigotla, M. Sigaroudinia, P. Gascard, T. Tlsty, J. F. Costello, I. M. Meyer, C. J. Eaves, W. W. Wasserman, S. Jones, D. Huntsman, M. Hirst, C. Caldas, M. A. Marra, and S. Aparicio, “The clonal and mutational evolution spectrum of primary triple-negative breast cancers.,” *Nature*, vol. 486, no. 7403, pp. 395–9, Jun. 2012.

[9] K. Polyak, I. Haviv, and I. G. Campbell, “Co-evolution of tumor cells and their microenvironment.,” *Trends in genetics : TIG*, vol. 25, no. 1, pp. 30–8, Jan. 2009.

[10] F. Li, B. Tiede, J. Massagué, and Y. Kang, “Beyond tumorigenesis: cancer stem cells in metastasis.,” *Cell research*, vol. 17, no. 1, pp. 3–14, Jan. 2007.

[11] B. Mintz and K. Illmensee, “Normal genetically mosaic mice produced from malignant teratocarcinoma cells.,” *Proceedings of the National Academy of Sciences of the United States of America*, vol. 72, no. 9, pp. 3585–9, Sep. 1975.

[12] J. a Magee, E. Piskounova, and S. J. Morrison, “Cancer stem cells: impact, heterogeneity, and uncertainty.,” *Cancer cell*, vol. 21, no. 3, pp. 283–96, Mar. 2012.

[13] J. E. Visvader and G. J. Lindeman, “Cancer stem cells: current status and evolving complexities.,” *Cell stem cell*, vol. 10, no. 6, pp. 717–28, Jun. 2012.

[14] M. Al-Hajj, M. S. Wicha, A. Benito-Hernandez, S. J. Morrison, and M. F. Clarke, “Prospective identification of tumorigenic breast cancer cells.,” *Proceedings of the National Academy of Sciences of the United States of America*, vol. 100, no. 7, pp. 3983–8, Apr. 2003.

[15] P. Dalerba, S. J. Dylla, I.-K. Park, R. Liu, X. Wang, R. W. Cho, T. Hoey, A. Gurney, E. H. Huang, D. M. Simeone, A. A. Shelton, G. Parmiani, C. Castelli, and M. F. Clarke, “Phenotypic characterization of human colorectal cancer stem cells.,” *Proceedings of the National Academy of Sciences of the United States of America*, vol. 104, no. 24, pp. 10158–63, Jun. 2007.

[16] C. A. O’Brien, A. Pollett, S. Gallinger, and J. E. Dick, “A human colon cancer cell capable of initiating tumour growth in immunodeficient mice.,” *Nature*, vol. 445, no. 7123, pp. 106–10, Jan. 2007.

[17] C. Li, D. G. Heidt, P. Dalerba, C. F. Burant, L. Zhang, V. Adsay, M. Wicha, M. F. Clarke, and D. M. Simeone, “Identification of pancreatic cancer stem cells.,” *Cancer research*, vol. 67, no. 3, pp. 1030–7, Feb. 2007.

[18] A. B. Alvero, H.-H. Fu, J. Holmberg, I. Visintin, L. Mor, C. C. Marquina, J. Oidtman, D.-A. Silasi, and G. Mor, “Stem-like ovarian cancer cells can serve as tumor vascular progenitors.,” *Stem cells (Dayton, Ohio)*, vol. 27, no. 10, pp. 2405–13, Oct. 2009.

[19] M. D. Curley, V. A. Therrien, C. L. Cummings, P. A. Sergent, C. R. Koulouris, A. M. Friel, D. J. Roberts, M. V Seiden, D. T. Scadden, B. R. Rueda, and R. Foster, “CD133 expression defines a tumor initiating cell population in primary human ovarian cancer.,” *Stem cells (Dayton, Ohio)*, vol. 27, no. 12, pp. 2875–83, Dec. 2009.

[20] J. M. Stewart, P. A. Shaw, C. Gedye, M. Q. Bernardini, B. G. Neel, and L. E. Ailles, “Phenotypic heterogeneity and instability of human ovarian tumor-initiating cells.,” *Proceedings of the National Academy of Sciences of the United States of America*, vol. 108, no. 16, pp. 6468–73, Apr. 2011.

[21] M. H. Cruz, a Sidén, G. M. Calaf, Z. M. Delwar, and J. S. Yakisich, “The stemness phenotype model.,” *ISRN oncology*, vol. 2012, p. 392647, Jan. 2012.

[22] A. D. Boiko, O. V Razorenova, M. van de Rijn, S. M. Swetter, D. L. Johnson, D. P. Ly, P. D. Butler, G. P. Yang, B. Joshua, M. J. Kaplan, M. T. Longaker, and I. L. Weissman, “Human melanoma-initiating cells express neural crest nerve growth factor receptor CD271.,” *Nature*, vol. 466, no. 7302, pp. 133–7, Jul. 2010.

[23] S. Sell, “Stem cell origin of cancer and differentiation therapy.,” *Critical reviews in oncology/hematology*, vol. 51, no. 1, pp. 1–28, Jul. 2004.

[24] K. Eppert, K. Takenaka, E. R. Lechman, L. Waldron, B. Nilsson, P. van Galen, K. H. Metzeler, A. Poeppl, V. Ling, J. Beyene, A. J. Canty, J. S. Danska, S. K. Bohlander, C. Buske, M. D. Minden, T. R. Golub, I. Jurisica, B. L. Ebert, and J. E. Dick, “Stem cell gene expression programs influence clinical outcome in human leukemia.,” *Nature medicine*, vol. 17, no. 9, pp. 1086–93, Sep. 2011.

[25] A. J. Gentles, A. a Alizadeh, S.-I. Lee, J. H. Myklebust, C. M. Shachaf, B. Shahbaba, R. Levy, D. Koller, and S. K. Plevritis, “A pluripotency signature predicts histologic transformation and

influences survival in follicular lymphoma patients.," *Blood*, vol. 114, no. 15, pp. 3158–66, Oct. 2009.

[26] N. P. Palmer, P. R. Schmid, B. Berger, and I. S. Kohane, "A gene expression profile of stem cell pluripotentiality and differentiation is conserved across diverse solid and hematopoietic cancers.," *Genome biology*, vol. 13, no. 8, p. R71, Aug. 2012.

[27] I. Shats, M. L. Gatza, J. T. Chang, S. Mori, J. Wang, J. Rich, and J. R. Nevins, "Using a stem cell-based signature to guide therapeutic selection in cancer.," *Cancer research*, vol. 71, no. 5, pp. 1772–80, Mar. 2011.

[28] Y. Wu, Q. Li, X. Zhou, J. Yu, Y. Mu, S. Munker, C. Xu, Z. Shen, R. Müllenbach, Y. Liu, L. Li, N. Gretz, D. Zieker, J. Li, K. Matsuzaki, Y. Li, S. Dooley, and H. Weng, "Decreased levels of active SMAD2 correlate with poor prognosis in gastric cancer.," *PloS one*, vol. 7, no. 4, p. e35684, Jan. 2012.

[29] Y.-H. Liu, Y. Li, X.-H. Liu, H.-M. Sui, Y.-X. Liu, Z.-Q. Xiao, P. Zheng, L. Chen, S. Yao, C. Xing, J. Zhou, and J.-M. Li, "A signature for induced pluripotent stem cell-associated genes in colorectal cancer.," *Medical oncology (Northwood, London, England)*, vol. 30, no. 1, p. 426, Mar. 2013.

[30] D. L. Trump, "Retinoids in bladder, testis and prostate cancer: epidemiologic, pre-clinical and clinical observations.," *Leukemia*, vol. 8 Suppl 3, pp. S50–4, Jan. 1994.

[31] K. Takahashi and S. Yamanaka, "Induction of pluripotent stem cells from mouse embryonic and adult fibroblast cultures by defined factors.," *Cell*, vol. 126, no. 4, pp. 663–76, Aug. 2006.

[32] V. Clement, P. Sanchez, N. de Tribolet, I. Radovanovic, and A. Ruiz i Altaba, "HEDGEHOG-GLI1 signaling regulates human glioma growth, cancer stem cell self-renewal, and tumorigenicity.," *Current biology : CB*, vol. 17, no. 2, pp. 165–72, Jan. 2007.

[33] I. Ben-Porath, M. W. Thomson, V. J. Carey, R. Ge, G. W. Bell, A. Regev, and R. A. Weinberg, "An embryonic stem cell-like gene expression signature in poorly differentiated aggressive human tumors.," *Nature genetics*, vol. 40, no. 5, pp. 499–507, May 2008.

[34] S. Santagata, J. L. Hornick, and K. L. Ligon, "Comparative analysis of germ cell transcription factors in CNS germinoma reveals diagnostic utility of NANOG.," *The American journal of surgical pathology*, vol. 30, no. 12, pp. 1613–8, Dec. 2006.

[35] S. Santagata, K. L. Ligon, and J. L. Hornick, "Embryonic stem cell transcription factor signatures in the diagnosis of primary and metastatic germ cell tumors.," *The American journal of surgical pathology*, vol. 31, no. 6, pp. 836–45, Jun. 2007.

[36] C. Y. Darini, D. F. Pisani, P. Hofman, F. Pedeutour, I. Sudaka, C. Chomienne, C. Dani, and A. Ladoux, "Self-renewal gene tracking to identify tumour-initiating cells associated with metastatic potential.," *Oncogene*, vol. 31, no. 19, pp. 2438–49, May 2012.

[37] A. Borrull, S. Ghislin, F. Deshayes, J. Lauriol, C. Alcaide-Loridan, and S. Middendorp, "Nanog and Oct4 overexpression increases motility and transmigration of melanoma cells.," *Journal of cancer research and clinical oncology*, vol. 138, no. 7, pp. 1145–54, Jul. 2012.

[38] Y. Jia, H. Liu, Q. Zhuang, S. Xu, Z. Yang, J. Li, J. Lou, and W. Zhang, “Tumorigenicity of cancer stem-like cells derived from hepatocarcinoma is regulated by microRNA-145.,” *Oncology reports*, vol. 27, no. 6, pp. 1865–72, Jun. 2012.

[39] C.-J. Chang, Y. Chien, K.-H. Lu, S.-C. Chang, Y.-C. Chou, C.-S. Huang, C.-H. Chang, K.-H. Chen, Y.-L. Chang, L.-M. Tseng, W.-S. Song, J.-J. Wang, J.-K. Lin, P.-I. Huang, and Y.-T. Lan, “Oct4-related cytokine effects regulate tumorigenic properties of colorectal cancer cells.,” *Biochemical and biophysical research communications*, vol. 415, no. 2, pp. 245–51, Nov. 2011.

[40] J. Liu, L. Ma, J. Xu, C. Liu, J. Zhang, J. Liu, R. Chen, and Y. Zhou, “Spheroid body-forming cells in the human gastric cancer cell line MKN-45 possess cancer stem cell properties.,” *International journal of oncology*, vol. 42, no. 2, pp. 453–9, Feb. 2013.

[41] I. Marzi, M. G. Cipolleschi, M. D’Amico, T. Stivarou, E. Rovida, M. C. Vinci, S. Pandolfi, P. Dello Sbarba, B. Stecca, and M. Olivotto, “The involvement of a Nanog, Klf4 and c-Myc transcriptional circuitry in the intertwining between neoplastic progression and reprogramming.,” *Cell cycle (Georgetown, Tex.)*, vol. 12, no. 2, pp. 353–64, Jan. 2013.

[42] L. Yang, X. Zhang, M. Zhang, J. Zhang, Y. Sheng, X. Sun, Q. Chen, and L.-X. Wang, “Increased Nanog expression promotes tumor development and Cisplatin resistance in human esophageal cancer cells.,” *Cellular physiology and biochemistry : international journal of experimental cellular physiology, biochemistry, and pharmacology*, vol. 30, no. 4, pp. 943–52, Jan. 2012.

[43] W.-D. Liu, T. Zhang, C.-L. Wang, H.-M. Meng, Y.-W. Song, Z. Zhao, Z.-M. Li, J.-K. Liu, S.-H. Pan, and W.-B. Wang, “Sphere-forming tumor cells possess stem-like properties in human fibrosarcoma primary tumors and cell lines.,” *Oncology letters*, vol. 4, no. 6, pp. 1315–1320, Dec. 2012.

[44] L. N. Abdullah and E. K.-H. Chow, “Mechanisms of chemoresistance in cancer stem cells.,” *Clinical and translational medicine*, vol. 2, no. 1, p. 3, Jan. 2013.

[45] T. M. Phillips, W. H. McBride, and F. Pajonk, “The response of CD24(-/low)/CD44+ breast cancer-initiating cells to radiation.,” *Journal of the National Cancer Institute*, vol. 98, no. 24, pp. 1777–85, Dec. 2006.

[46] F. Karimi-Busheri, A. Rasouli-Nia, J. R. Mackey, and M. Weinfeld, “Senescence evasion by MCF-7 human breast tumor-initiating cells.,” *Breast cancer research : BCR*, vol. 12, no. 3, p. R31, Jan. 2010.

[47] B. Beck, G. Driessens, S. Goossens, K. K. Youssef, A. Kuchnio, A. Caauwe, P. A. Sotiropoulou, S. Loges, G. Lapouge, A. Candi, G. Mascre, B. Drogat, S. Dekoninck, J. J. Haigh, P. Carmeliet, and C. Blanpain, “A vascular niche and a VEGF-Nrp1 loop regulate the initiation and stemness of skin tumours.,” *Nature*, vol. 478, no. 7369, pp. 399–403, Oct. 2011.

[48] L. Vermeulen, F. De Sousa E Melo, M. van der Heijden, K. Cameron, J. H. de Jong, T. Borovski, J. B. Tuynman, M. Todaro, C. Merz, H. Rodermond, M. R. Sprick, K. Kemper, D. J. Richel, G. Stassi, and J. P. Medema, “Wnt activity defines colon cancer stem cells and is regulated by the microenvironment.,” *Nature cell biology*, vol. 12, no. 5, pp. 468–76, May 2010.

[49] S. Astigiano, P. Damonte, S. Fossati, L. Boni, and O. Barbieri, “Fate of embryonal carcinoma cells injected into postimplantation mouse embryos.,” *Differentiation; research in biological diversity*, vol. 73, no. 9–10, pp. 484–90, Dec. 2005.

[50] P. W. Andrews, M. M. Matin, A. R. Bahrami, I. Damjanov, P. Gokhale, and J. S. Draper, “Embryonic stem (ES) cells and embryonal carcinoma (EC) cells: opposite sides of the same coin.,” *Biochemical Society transactions*, vol. 33, no. Pt 6, pp. 1526–30, Dec. 2005.

[51] T. Sharif, C. Auger, C. Bronner, M. Alhosin, T. Klein, N. Etienne-Selloum, V. B. Schini-Kerth, and G. Fuhrmann, “Selective proapoptotic activity of polyphenols from red wine on teratocarcinoma cell, a model of cancer stem-like cell.,” *Investigational new drugs*, vol. 29, no. 2, pp. 239–47, Apr. 2011.

[52] J. S. You, J. K. Kang, D.-W. Seo, J. H. Park, J. W. Park, J. C. Lee, Y. J. Jeon, E. J. Cho, and J.-W. Han, “Depletion of embryonic stem cell signature by histone deacetylase inhibitor in NCCIT cells: involvement of Nanog suppression.,” *Cancer research*, vol. 69, no. 14, pp. 5716–25, Jul. 2009.

[53] C. C. B. B. Heffron, M. F. Gallagher, S. Guenther, J. Sherlock, R. Henfrey, C. Martin, O. Sheils, and J. J. O’Leary, “Global mRNA analysis to determine a transcriptome profile of cancer stemness in a mouse model.,” *Anticancer research*, vol. 27, no. 3A, pp. 1319–24, 2007.

[54] S. Sell and G. B. Pierce, “Maturation arrest of stem cell differentiation is a common pathway for the cellular origin of teratocarcinomas and epithelial cancers.,” *Laboratory investigation; a journal of technical methods and pathology*, vol. 70, no. 1, pp. 6–22, Jan. 1994.

[55] M. J. Spinella, J. S. Kerley, K. A. White, and J. C. Curtin, “Retinoid target gene activation during induced tumor cell differentiation: human embryonal carcinoma as a model.,” *The Journal of nutrition*, vol. 133, no. 1, p. 273S–276S, Jan. 2003.

[56] S. Sell, “On the stem cell origin of cancer.,” *The American journal of pathology*, vol. 176, no. 6, pp. 2584–494, Jun. 2010.

[57] T. Asklund, S. Kvarnbrink, C. Holmlund, C. Wibom, T. Bergenheim, R. Henriksson, and H. Hedman, “Synergistic killing of glioblastoma stem-like cells by bortezomib and HDAC inhibitors.,” *Anticancer research*, vol. 32, no. 7, pp. 2407–13, Jul. 2012.

[58] A.-M. Marino, A. Sofiadis, N. Baryawno, J. I. Johnsen, C. Larsson, V. Vukojević, and T. J. Ekström, “Enhanced effects by 4-phenylbutyrate in combination with RTK inhibitors on proliferation in brain tumor cell models.,” *Biochemical and biophysical research communications*, vol. 411, no. 1, pp. 208–12, Jul. 2011.

[59] S. D. Gore, L.-J. Weng, W. D. Figg, S. Zhai, R. C. Donehower, G. Dover, M. R. Grever, C. Griffin, L. B. Grochow, A. Hawkins, K. Burks, Y. Zabelena, and C. B. Miller, “Impact of prolonged infusions of the putative differentiating agent sodium phenylbutyrate on myelodysplastic syndromes and acute myeloid leukemia.,” *Clinical cancer research : an official journal of the American Association for Cancer Research*, vol. 8, no. 4, pp. 963–70, Apr. 2002.

[60] B. L. Hogan, “Bone morphogenetic proteins: multifunctional regulators of vertebrate development.,” *Genes & development*, vol. 10, no. 13, pp. 1580–94, Jul. 1996.

[61] A. Hemmati-Brivanlou and D. Melton, “Vertebrate neural induction.,” *Annual review of neuroscience*, vol. 20, pp. 43–60, Jan. 1997.

[62] Y. Lombardo, A. Scopelliti, P. Cammareri, M. Todaro, F. Iovino, L. Ricci-Vitiani, G. Gulotta, F. Dieli, R. de Maria, and G. Stassi, “Bone morphogenetic protein 4 induces differentiation of colorectal cancer stem cells and increases their response to chemotherapy in mice.,” *Gastroenterology*, vol. 140, no. 1, pp. 297–309, Jan. 2011.

[63] Z. Zhou, L. Sun, Y. Wang, Z. Wu, J. Geng, W. Miu, Y. Pu, Y. You, Z. Yang, and N. Liu, “Bone morphogenetic protein 4 inhibits cell proliferation and induces apoptosis in glioma stem cells.,” *Cancer biotherapy & radiopharmaceuticals*, vol. 26, no. 1, pp. 77–83, Feb. 2011.

[64] T. Ishibe, T. Nakayama, T. Aoyama, T. Nakamura, and J. Toguchida, “Neuronal differentiation of synovial sarcoma and its therapeutic application.,” *Clinical orthopaedics and related research*, vol. 466, no. 9, pp. 2147–55, Sep. 2008.

[65] J. M. Ketolainen, E.-L. Alarmo, V. J. Tuominen, and A. Kallioniemi, “Parallel inhibition of cell growth and induction of cell migration and invasion in breast cancer cells by bone morphogenetic protein 4.,” *Breast cancer research and treatment*, vol. 124, no. 2, pp. 377–86, Nov. 2010.

[66] Y.-C. Lee, C.-J. Cheng, M. A. Bilen, J.-F. Lu, R. L. Satcher, L.-Y. Yu-Lee, G. E. Gallick, S. N. Maity, and S.-H. Lin, “BMP4 promotes prostate tumor growth in bone through osteogenesis.,” *Cancer research*, vol. 71, no. 15, pp. 5194–203, Aug. 2011.

[67] N. Bushue and Y.-J. Y. Wan, “Retinoid pathway and cancer therapeutics.,” *Advanced drug delivery reviews*, vol. 62, no. 13, pp. 1285–98, Oct. 2010.

[68] H. de Thé, C. Chomienne, M. Lanotte, L. Degos, and A. Dejean, “The t(15;17) translocation of acute promyelocytic leukaemia fuses the retinoic acid receptor alpha gene to a novel transcribed locus.,” *Nature*, vol. 347, no. 6293, pp. 558–61, Oct. 1990.

[69] H. de Thé, C. Lavau, A. Marchio, C. Chomienne, L. Degos, and A. Dejean, “The PML-RAR alpha fusion mRNA generated by the t(15;17) translocation in acute promyelocytic leukemia encodes a functionally altered RAR.,” *Cell*, vol. 66, no. 4, pp. 675–84, Aug. 1991.

[70] T. Casini and P. G. Pelicci, “A function of p21 during promyelocytic leukemia cell differentiation independent of CDK inhibition and cell cycle arrest.,” *Oncogene*, vol. 18, no. 21, pp. 3235–43, May 1999.

[71] a M. Jiménez-Lara, N. Clarke, L. Altucci, and H. Gronemeyer, “Retinoic-acid-induced apoptosis in leukemia cells.,” *Trends in molecular medicine*, vol. 10, no. 10, pp. 508–15, Oct. 2004.

[72] M. H. Bukhari, S. S. Qureshi, S. Niazi, M. Asef, M. Naheed, S. A. Khan, N. A. Chaudhry, M. Tayyab, and M. Hasan, “Chemotherapeutic/chemopreventive role of retinoids in chemically induced skin carcinogenesis in albino mice.,” *International journal of dermatology*, vol. 46, no. 11, pp. 1160–5, Nov. 2007.

[73] C. Pisano, L. Vesci, R. Foderà, F. F. Ferrara, C. Rossi, M. De Cesare, V. Zuco, G. Pratesi, R. Supino, and F. Zunino, “Antitumor activity of the combination of synthetic retinoid ST1926 and cisplatin in ovarian carcinoma models.,” *Annals of oncology : official journal of the European Society for Medical Oncology / ESMO*, vol. 18, no. 9, pp. 1500–5, Sep. 2007.

[74] R. K. Shah, T. A. Valdez, Z. Wang, and S. M. Shapshay, “Pulsed-dye laser and retinoic acid delay progression of oral squamous cell carcinoma: a murine model.,” *The Laryngoscope*, vol. 111, no. 7, pp. 1203–8, Jul. 2001.

[75] Y. Li, Y. Zhang, J. Hill, H.-T. Kim, Q. Shen, R. P. Bissonnette, W. W. Lamph, and P. H. Brown, “The rexinoid, bexarotene, prevents the development of premalignant lesions in MMTV-erbB2 mice.,” *British journal of cancer*, vol. 98, no. 8, pp. 1380–8, Apr. 2008.

[76] B. Liu, K.-W. Lee, H. Li, L. Ma, G. L. Lin, R. A. S. Chandraratna, and P. Cohen, “Combination therapy of insulin-like growth factor binding protein-3 and retinoid X receptor ligands synergize on prostate cancer cell apoptosis in vitro and in vivo.,” *Clinical cancer research : an official journal of the American Association for Cancer Research*, vol. 11, no. 13, pp. 4851–6, Jul. 2005.

[77] F. Recchia, G. Sica, G. Candeloro, S. Necozione, R. Bisegna, M. Bratta, and S. Rea, “Beta-interferon, retinoids and tamoxifen in metastatic breast cancer: long-term follow-up of a phase II study.,” *Oncology reports*, vol. 21, no. 4, pp. 1011–6, Apr. 2009.

[78] M. J. Edelman, R. Smith, P. Hausner, L. A. Doyle, K. Kalra, J. Kendall, M. Bedor, and S. Bisaccia, “Phase II trial of the novel retinoid, bexarotene, and gemcitabine plus carboplatin in advanced non-small-cell lung cancer.,” *Journal of clinical oncology : official journal of the American Society of Clinical Oncology*, vol. 23, no. 24, pp. 5774–8, Aug. 2005.

[79] N. Colombo, F. Formelli, M. G. Cantù, G. Parma, M. Gasco, A. Argusti, A. Santinelli, R. Montironi, E. Cavadini, L. Baglietto, A. Guerrieri-Gonzaga, G. Viale, and A. Decensi, “A phase I-II preoperative biomarker trial of fenretinide in ascitic ovarian cancer.,” *Cancer epidemiology, biomarkers & prevention : a publication of the American Association for Cancer Research, cosponsored by the American Society of Preventive Oncology*, vol. 15, no. 10, pp. 1914–9, Oct. 2006.

[80] R. Connolly, N. K. Nguyen, and S. Sukumar, “Molecular Pathways: Current Role and Future Directions of the Retinoic Acid Pathway In Cancer Prevention and Treatment.,” *Clinical cancer research : an official journal of the American Association for Cancer Research*, Jan. 2013.

[81] W. K. Hong, S. M. Lippman, L. M. Itri, D. D. Karp, J. S. Lee, R. M. Byers, S. P. Schantz, A. M. Kramer, R. Lotan, and L. J. Peters, “Prevention of second primary tumors with isotretinoin in squamous-cell carcinoma of the head and neck.,” *The New England journal of medicine*, vol. 323, no. 12, pp. 795–801, Sep. 1990.

[82] C. P. Reynolds, K. K. Matthay, J. G. Villablanca, and B. J. Maurer, “Retinoid therapy of high-risk neuroblastoma.,” *Cancer letters*, vol. 197, no. 1–2, pp. 185–92, Jul. 2003.

[83] K. Dalhoff, J. Dancey, L. Astrup, T. Skovsgaard, K. J. Hamberg, F. J. Lofts, O. Rosmorduc, S. Erlinger, J. Bach Hansen, W. P. Steward, T. Skov, F. Burcharth, and T. R. J. Evans, “A phase II study of the vitamin D analogue Seocalcitol in patients with inoperable hepatocellular carcinoma.,” *British journal of cancer*, vol. 89, no. 2, pp. 252–7, Jul. 2003.

[84] X. K. Zhang, Y. Liu, and M. O. Lee, “Retinoid receptors in human lung cancer and breast cancer.,” *Mutation research*, vol. 350, no. 1, pp. 267–77, Feb. 1996.

[85] N. Bushue and Y.-J. Y. Wan, “Retinoid pathway and cancer therapeutics.,” *Advanced drug delivery reviews*, vol. 62, no. 13, pp. 1285–98, Oct. 2010.

[86] R. S. Larson and M. S. Tallman, “Retinoic acid syndrome: manifestations, pathogenesis, and treatment.,” *Best practice & research. Clinical haematology*, vol. 16, no. 3, pp. 453–61, Sep. 2003.

[87] V. Duong and C. Rochette-Egly, “The molecular physiology of nuclear retinoic acid receptors. From health to disease.,” *Biochimica et biophysica acta*, vol. 1812, no. 8, pp. 1023–31, Aug. 2011.

[88] N. Clarke, P. Germain, L. Altucci, and H. Gronemeyer, “Retinoids: potential in cancer prevention and therapy.,” *Expert reviews in molecular medicine*, vol. 6, no. 25, pp. 1–23, Nov. 2004.

[89] Z. Al Tanoury, A. Piskunov, and C. Rochette-Egly, “Vitamin A and retinoid signaling: genomic and non-genomic effects.,” *Journal of lipid research*, Feb. 2013.

[90] E. F. Farias, K. Petrie, B. Leibovitch, J. Murtagh, M. B. Chornet, T. Schenk, A. Zelent, and S. Waxman, “Interference with Sin3 function induces epigenetic reprogramming and differentiation in breast cancer cells.,” *Proceedings of the National Academy of Sciences of the United States of America*, vol. 107, no. 26, pp. 11811–6, Jun. 2010.

[91] A. Cras, D. Darsin-Bettinger, N. Balitrand, B. Cassinat, A. Soulié, M.-E. Toubert, L. Delva, and C. Chomienne, “Epigenetic patterns of the retinoic acid receptor beta2 promoter in retinoic acid-resistant thyroid cancer cells.,” *Oncogene*, vol. 26, no. 27, pp. 4018–24, Jun. 2007.

[92] Z. Wang, M. Boudjelal, S. Kang, J. J. Voorhees, and G. J. Fisher, “Ultraviolet irradiation of human skin causes functional vitamin A deficiency, preventable by all-trans retinoic acid pre-treatment.,” *Nature medicine*, vol. 5, no. 4, pp. 418–22, Apr. 1999.

[93] A. Almasan and A. Ashkenazi, “Apo2L/TRAIL: apoptosis signaling, biology, and potential for cancer therapy.,” *Cytokine & growth factor reviews*, vol. 14, no. 3–4, pp. 337–48.

[94] R. Yerbes, C. Palacios, and A. López-Rivas, “The therapeutic potential of TRAIL receptor signalling in cancer cells.,” *Clinical & translational oncology : official publication of the Federation of Spanish Oncology Societies and of the National Cancer Institute of Mexico*, vol. 13, no. 12, pp. 839–47, Dec. 2011.

[95] S. Shankar and R. K. Srivastava, “Enhancement of therapeutic potential of TRAIL by cancer chemotherapy and irradiation: mechanisms and clinical implications.,” *Drug resistance updates : reviews and commentaries in antimicrobial and anticancer chemotherapy*, vol. 7, no. 2, pp. 139–56, Apr. 2004.

[96] F. a E. Kruyt, “TRAIL and cancer therapy.,” *Cancer letters*, vol. 263, no. 1, pp. 14–25, May 2008.

[97] R. Nitsch, I. Bechmann, R. A. Deisz, D. Haas, T. N. Lehmann, U. Wendling, and F. Zipp, “Human brain-cell death induced by tumour-necrosis-factor-related apoptosis-inducing ligand (TRAIL),” *Lancet*, vol. 356, no. 9232, pp. 827–8, Sep. 2000.

[98] C. Carlo-Stella, C. Lavazza, A. Locatelli, L. Viganò, A. M. Gianni, and L. Gianni, “Targeting TRAIL agonistic receptors for cancer therapy.,” *Clinical cancer research : an official journal of the American Association for Cancer Research*, vol. 13, no. 8, pp. 2313–7, Apr. 2007.

[99] S. Fulda, E. Meyer, and K.-M. Debatin, “Inhibition of TRAIL-induced apoptosis by Bcl-2 overexpression.,” *Oncogene*, vol. 21, no. 15, pp. 2283–94, Apr. 2002.

[100] E. S. Lander, L. M. Linton, B. Birren, C. Nusbaum, M. C. Zody, J. Baldwin, K. Devon, K. Dewar, M. Doyle, W. FitzHugh, R. Funke, D. Gage, K. Harris, A. Heaford, J. Howland, L. Kann, J. Lehoczky, R. LeVine, P. McEwan, K. McKernan, J. Meldrim, J. P. Mesirov, C. Miranda, W. Morris, J. Naylor, C. Raymond, M. Rosetti, R. Santos, A. Sheridan, C. Sougnez, N. Stange-Thomann, N. Stojanovic, A. Subramanian, D. Wyman, J. Rogers, J. Sulston, R. Ainscough, S. Beck, D. Bentley, J. Burton, C. Clee, N. Carter, A. Coulson, R. Deadman, P. Deloukas, A. Dunham, I. Dunham, R. Durbin, L. French, D. Grafham, S. Gregory, T. Hubbard, S. Humphray, A. Hunt, M. Jones, C. Lloyd, A. McMurray, L. Matthews, S. Mercer, S. Milne, J. C. Mullikin, A. Mungall, R. Plumb, M. Ross, R. Shownkeen, S. Sims, R. H. Waterston, R. K. Wilson, L. W. Hillier, J. D. McPherson, M. A. Marra, E. R. Mardis, L. A. Fulton, A. T. Chinwalla, K. H. Pepin, W. R. Gish, S. L. Chissoe, M. C. Wendl, K. D. Delehaunty, T. L. Miner, A. Delehaunty, J. B. Kramer, L. L. Cook, R. S. Fulton, D. L. Johnson, P. J. Minx, S. W. Clifton, T. Hawkins, E. Branscomb, P. Predki, P. Richardson, S. Wenning, T. Slezak, N. Doggett, J. F. Cheng, A. Olsen, S. Lucas, C. Elkin, E. Uberbacher, M. Frazier, R. A. Gibbs, D. M. Muzny, S. E. Scherer, J. B. Bouck, E. J. Sodergren, K. C. Worley, C. M. Rives, J. H. Gorrell, M. L. Metzker, S. L. Naylor, R. S. Kucherlapati, D. L. Nelson, G. M. Weinstock, Y. Sakaki, A. Fujiyama, M. Hattori, T. Yada, A. Toyoda, T. Itoh, C. Kawagoe, H. Watanabe, Y. Totoki, T. Taylor, J. Weissenbach, R. Heilig, W. Saurin, F. Artiguenave, P. Brottier, T. Bruls, E. Pelletier, C. Robert, P. Wincker, D. R. Smith, L. Doucette-Stamm, M. Rubenfield, K. Weinstock, H. M. Lee, J. Dubois, A. Rosenthal, M. Platzer, G. Nyakatura, S. Taudien, A. Rump, H. Yang, J. Yu, J. Wang, G. Huang, J. Gu, L. Hood, L. Rowen, A. Madan, S. Qin, R. W. Davis, N. A. Federspiel, A. P. Abola, M. J. Proctor, R. M. Myers, J. Schmutz, M. Dickson, J. Grimwood, D. R. Cox, M. V Olson, R. Kaul, N. Shimizu, K. Kawasaki, S. Minoshima, G. A. Evans, M. Athanasiou, R. Schultz, B. A. Roe, F. Chen, H. Pan, J. Ramser, H. Lehrach, R. Reinhardt, W. R. McCombie, M. de la Bastide, N. Dedhia, H. Blöcker, K. Hornischer, G. Nordsiek, R. Agarwala, L. Aravind, J. A. Bailey, A. Bateman, S. Batzoglou, E. Birney, P. Bork, D. G. Brown, C. B. Burge, L. Cerutti, H. C. Chen, D. Church, M. Clamp, R. R. Copley, T. Doerks, S. R. Eddy, E. E. Eichler, T. S. Furey, J. Galagan, J. G. Gilbert, C. Harmon, Y. Hayashizaki, D. Haussler, H. Hermjakob, K. Hokamp, W. Jang, L. S. Johnson, T. A. Jones, S. Kasif, A. Kaspryzk, S. Kennedy, W. J. Kent, P. Kitts, E. V Koonin, I. Korf, D. Kulp, D. Lancet, T. M. Lowe, A. McLysaght, T. Mikkelsen, J. V Moran, N. Mulder, V. J. Pollara, C. P. Ponting, G. Schuler, J. Schultz, G. Slater, A. F. Smit, E. Stupka, J. Szustakowski, D. Thierry-Mieg, J. Thierry-Mieg, L. Wagner, J. Wallis, R. Wheeler, A. Williams, Y. I. Wolf, K. H. Wolfe, S. P. Yang, R. F. Yeh, F. Collins, M. S. Guyer, J. Peterson, A. Felsenfeld, K. A. Wetterstrand, A. Patrinos, M. J. Morgan, P. de Jong, J. J. Catanese, K. Osoegawa, H. Shizuya, S. Choi, Y. J. Chen, and J. Szustakowki, “Initial sequencing and analysis of the human genome.,” *Nature*, vol. 409, no. 6822, pp. 860–921, Feb. 2001.

[101] Y. Shi and J. Massagué, “Mechanisms of TGF-beta signaling from cell membrane to the nucleus.,” *Cell*, vol. 113, no. 6, pp. 685–700, Jun. 2003.

[102] C. M. Dubois, M. H. Laprise, F. Blanchette, L. E. Gentry, and R. Leduc, “Processing of transforming growth factor beta 1 precursor by human furin convertase.,” *The Journal of biological chemistry*, vol. 270, no. 18, pp. 10618–24, May 1995.

[103] N. Q. McDonald and W. A. Hendrickson, “A structural superfamily of growth factors containing a cystine knot motif.,” *Cell*, vol. 73, no. 3, pp. 421–4, May 1993.

[104] D. E. Bassi, J. Fu, R. Lopez de Cicco, and A. J. P. Klein-Szanto, “Proprotein convertases: ‘master switches’ in the regulation of tumor growth and progression.,” *Molecular carcinogenesis*, vol. 44, no. 3, pp. 151–61, Nov. 2005.

[105] D. Mesnard and D. B. Constam, “Imaging proprotein convertase activities and their regulation in the implanting mouse blastocyst.,” *The Journal of cell biology*, vol. 191, no. 1, pp. 129–39, Oct. 2010.

[106] D. B. Constam and E. J. Robertson, “Regulation of bone morphogenetic protein activity by pro domains and proprotein convertases.,” *The Journal of cell biology*, vol. 144, no. 1, pp. 139–49, Jan. 1999.

[107] et al. Alberts B, Johnson A, Lewis J, *Molecular Biology of the Cell. 4th edition.* New York: Garland Science, 2002.

[108] D. Wotton and J. Massague, “NEW EMBO MEMBER ’ S REVIEW Transcriptional control by the TGF-b / Smad signaling system,” vol. 19, no. 8, pp. 1745–1754, 2000.

[109] J. Massague, “Integration of Smad and MAPK pathways: a link and a linker revisited.,” *Genes & development*, vol. 17, no. 24, pp. 2993–7, Dec. 2003.

[110] E. Gazzerro and E. Canalis, “Bone morphogenetic proteins and their antagonists.,” *Reviews in endocrine & metabolic disorders*, vol. 7, no. 1–2, pp. 51–65, Jun. 2006.

[111] P. Müller, K. W. Rogers, B. M. Jordan, J. S. Lee, D. Robson, S. Ramanathan, and A. F. Schier, “Differential diffusivity of Nodal and Lefty underlies a reaction-diffusion patterning system.,” *Science (New York, N.Y.)*, vol. 336, no. 6082, pp. 721–4, May 2012.

[112] J. Massagué, “TGFβ signalling in context.,” *Nature reviews. Molecular cell biology*, vol. 13, no. 10, pp. 616–30, Oct. 2012.

[113] P. ten Dijke and C. S. Hill, “New insights into TGF-beta-Smad signalling.,” *Trends in biochemical sciences*, vol. 29, no. 5, pp. 265–73, May 2004.

[114] A. C. McPherron and S. J. Lee, “GDF-3 and GDF-9: two new members of the transforming growth factor-beta superfamily containing a novel pattern of cysteines.,” *The Journal of biological chemistry*, vol. 268, no. 5, pp. 3444–9, Feb. 1993.

[115] C. M. Jones, D. Simon-Chazottes, J. L. Guenet, and B. L. Hogan, “Isolation of Vgr-2, a novel member of the transforming growth factor-beta-related gene family.,” *Molecular endocrinology (Baltimore, Md.)*, vol. 6, no. 11, pp. 1961–8, Nov. 1992.

[116] J. Groppe, J. Greenwald, E. Wiater, J. Rodriguez-Leon, A. N. Economides, W. Kwiatkowski, M. Affolter, W. W. Vale, J. C. Izpisua Belmonte, and S. Choe, “Structural basis of BMP signalling inhibition by the cystine knot protein Noggin.,” *Nature*, vol. 420, no. 6916, pp. 636–42, Dec. 2002.

[117] O. Andersson, M. Korach-Andre, E. Reissmann, C. F. Ibáñez, and P. Bertolino, “Growth/differentiation factor 3 signals through ALK7 and regulates accumulation of adipose tissue and diet-induced obesity.,” *Proceedings of the National Academy of Sciences of the United States of America*, vol. 105, no. 20, pp. 7252–6, May 2008.

[118] C. Chen, S. M. Ware, A. Sato, D. E. Houston-Hawkins, R. Habas, M. M. Matzuk, M. M. Shen, and C. W. Brown, “The Vg1-related protein Gdf3 acts in a Nodal signaling pathway in the pre-gastrulation mouse embryo.,” *Development (Cambridge, England)*, vol. 133, no. 2, pp. 319–29, Jan. 2006.

[119] A. J. Levine and A. H. Brivanlou, “GDF3, a BMP inhibitor, regulates cell fate in stem cells and early embryos.,” *Development (Cambridge, England)*, vol. 133, no. 2, pp. 209–16, Jan. 2006.

[120] N. Sato, I. M. Sanjuan, M. Heke, M. Uchida, F. Naef, and A. H. Brivanlou, “Molecular signature of human embryonic stem cells and its comparison with the mouse.,” *Developmental biology*, vol. 260, no. 2, pp. 404–13, Aug. 2003.

[121] O. Adewumi, B. Aflatoonian, L. Ahrlund-Richter, M. Amit, P. W. Andrews, G. Beighton, P. A. Bello, N. Benvenisty, L. S. Berry, S. Bevan, B. Blum, J. Brooking, K. G. Chen, A. B. H. Choo, G. A. Churchill, M. Corbel, I. Damjanov, J. S. Draper, P. Dvorak, K. Emanuelsson, R. A. Fleck, A. Ford, K. Gertow, M. Gertsenstein, P. J. Gokhale, R. S. Hamilton, A. Hampl, L. E. Healy, O. Hovatta, J. Hyllner, M. P. Imreh, J. Itskovitz-Eldor, J. Jackson, J. L. Johnson, M. Jones, K. Kee, B. L. King, B. B. Knowles, M. Lako, F. Lebrin, B. S. Mallon, D. Manning, Y. Mayshar, R. D. G. McKay, A. E. Michalska, M. Mikkola, M. Mileikovsky, S. L. Minger, H. D. Moore, C. L. Mummery, A. Nagy, N. Nakatsuji, C. M. O’Brien, S. K. W. Oh, C. Olsson, T. Otonkoski, K.-Y. Park, R. Passier, H. Patel, M. Patel, R. Pedersen, M. F. Pera, M. S. Piekarczyk, R. A. R. Pera, B. E. Reubinoff, A. J. Robins, J. Rossant, P. Rugg-Gunn, T. C. Schulz, H. Semb, E. S. Sherrer, H. Siemen, G. N. Stacey, M. Stojkovic, H. Suemori, J. Szatkiewicz, T. Turetsky, T. Tuuri, S. van den Brink, K. Vintersten, S. Vuoristo, D. Ward, T. A. Weaver, L. A. Young, and W. Zhang, “Characterization of human embryonic stem cell lines by the International Stem Cell Initiative.,” *Nature biotechnology*, vol. 25, no. 7, pp. 803–16, Jul. 2007.

[122] O. Andersson, P. Bertolino, and C. F. Ibáñez, “Distinct and cooperative roles of mammalian Vg1 homologs GDF1 and GDF3 during early embryonic development.,” *Developmental biology*, vol. 311, no. 2, pp. 500–11, Nov. 2007.

[123] W. Wang, Y. Yang, Y. Meng, and Y. Shi, “GDF-3 is an adipogenic cytokine under high fat dietary condition.,” *Biochemical and biophysical research communications*, vol. 321, no. 4, pp. 1024–31, Sep. 2004.

[124] Q. Li, Y. Ling, and L. Yu, “GDF3 inhibits the growth of breast cancer cells and promotes the apoptosis induced by Taxol.,” *Journal of cancer research and clinical oncology*, vol. 138, no. 6, pp. 1073–9, Jun. 2012.

[125] U. I. Ezeh, P. J. Turek, R. a Reijo, and A. T. Clark, “Human embryonic stem cell genes OCT4, NANOG, STELLAR, and GDF3 are expressed in both seminoma and breast carcinoma.,” *Cancer*, vol. 104, no. 10, pp. 2255–65, Nov. 2005.

[126] N. Ehira, H. Oshiumi, M. Matsumoto, T. Kondo, M. Asaka, and T. Seya, “An embryo-specific expressing TGF-β family protein, growth-differentiation factor 3 (GDF3), augments progression of B16 melanoma.,” *Journal of experimental & clinical cancer research : CR*, vol. 29, no. 1, p. 135, Jan. 2010.

[127] a a Caricasole, R. H. van Schaik, L. M. Zeinstra, C. D. Wierikx, R. J. van Gurp, M. van den Pol, L. H. Looijenga, J. W. Oosterhuis, M. F. Pera, a Ward, D. de Bruijn, P. Kramer, F. H. de Jong, and a J. van den Eijnden-van Raaij, “Human growth-differentiation factor 3 (hGDF3): developmental regulation in human teratocarcinoma cell lines and expression in primary testicular germ cell tumours.,” *Oncogene*, vol. 16, no. 1, pp. 95–103, Jan. 1998.

[128] Q. Li, X. Liu, Y. Wu, J. An, S. Hexige, Y. Ling, M. Zhang, X. Yang, and L. Yu, “The conditioned medium from a stable human GDF3-expressing CHO cell line, induces the differentiation of PC12 cells.,” *Molecular and cellular biochemistry*, vol. 359, no. 1–2, pp. 115–23, Jan. 2012.

[129] D. A. Rubinson, C. P. Dillon, A. V Kwiatkowski, C. Sievers, L. Yang, J. Kopinja, D. L. Rooney, M. Zhang, M. M. Ihrig, M. T. McManus, F. B. Gertler, M. L. Scott, and L. Van Parijs, "A lentivirus-based system to functionally silence genes in primary mammalian cells, stem cells and transgenic mice by RNA interference.," *Nature genetics*, vol. 33, no. 3, pp. 401–6, Mar. 2003.

[130] M. M. Shen, "Nodal signaling: developmental roles and regulation.," *Development (Cambridge, England)*, vol. 134, no. 6, pp. 1023–34, Mar. 2007.

[131] A. M. Cheng, B. Thisse, C. Thisse, and C. V Wright, "The lefty-related factor Xatv acts as a feedback inhibitor of nodal signaling in mesoderm induction and L-R axis development in xenopus.," *Development (Cambridge, England)*, vol. 127, no. 5, pp. 1049–61, Mar. 2000.

[132] M. Guzman-Ayala, K. L. Lee, K. J. Mavrakis, P. Goggolidou, D. P. Norris, and V. Episkopou, "Graded Smad2/3 activation is converted directly into levels of target gene expression in embryonic stem cells.," *PloS one*, vol. 4, no. 1, p. e4268, Jan. 2009.

[133] K. L. Lee, S. K. Lim, Y. L. Orlov, L. Y. Yit, H. Yang, L. T. Ang, L. Poellinger, and B. Lim, "Graded Nodal/Activin signaling titrates conversion of quantitative phospho-Smad2 levels into qualitative embryonic stem cell fate decisions.," *PLoS genetics*, vol. 7, no. 6, p. e1002130, Jun. 2011.

[134] A. von Bubnoff and K. W. Cho, "Intracellular BMP signaling regulation in vertebrates: pathway or network?," *Developmental biology*, vol. 239, no. 1, pp. 1–14, Nov. 2001.

[135] X. Zhou, H. Sasaki, L. Lowe, B. L. Hogan, and M. R. Kuehn, "Nodal is a novel TGF-beta-like gene expressed in the mouse node during gastrulation.," *Nature*, vol. 361, no. 6412, pp. 543–7, Feb. 1993.

[136] D. W. Huang, B. T. Sherman, and R. A. Lempicki, "Systematic and integrative analysis of large gene lists using DAVID bioinformatics resources.," *Nature protocols*, vol. 4, no. 1, pp. 44–57, Jan. 2009.

[137] H. Hamada, C. Meno, D. Watanabe, and Y. Saijoh, "Establishment of vertebrate left-right asymmetry.," *Nature reviews. Genetics*, vol. 3, no. 2, pp. 103–13, Feb. 2002.

[138] T. Esmailpour and T. Huang, "TBX3 promotes human embryonic stem cell proliferation and neuroepithelial differentiation in a differentiation stage-dependent manner.," *Stem cells (Dayton, Ohio)*, vol. 30, no. 10, pp. 2152–63, Oct. 2012.

[139] H. Okazawa, J. Shimizu, M. Kamei, I. Imafuku, H. Hamada, and I. Kanazawa, "Bcl-2 inhibits retinoic acid-induced apoptosis during the neural differentiation of embryonal stem cells.," *The Journal of cell biology*, vol. 132, no. 5, pp. 955–68, Mar. 1996.

[140] A. Burlacu, "Regulation of apoptosis by Bcl-2 family proteins.," *Journal of cellular and molecular medicine*, vol. 7, no. 3, pp. 249–57, 2003.

[141] I. Damjanov, B. Horvat, and Z. Gibas, "Retinoic acid-induced differentiation of the developmentally pluripotent human germ cell tumor-derived cell line, NCCIT.," *Laboratory investigation; a journal of technical methods and pathology*, vol. 68, no. 2, pp. 220–32, Feb. 1993.

[142] S. Teshima, Y. Shimosato, S. Hirohashi, Y. Tome, I. Hayashi, H. Kanazawa, and T. Kakizoe, “Four new human germ cell tumor cell lines.,” *Laboratory investigation; a journal of technical methods and pathology*, vol. 59, no. 3, pp. 328–36, Sep. 1988.

[143] D. Besser, “Expression of nodal, lefty-a, and lefty-B in undifferentiated human embryonic stem cells requires activation of Smad2/3.,” *The Journal of biological chemistry*, vol. 279, no. 43, pp. 45076–84, Oct. 2004.

[144] A. J. Levine, Z. J. Levine, and A. H. Brivanlou, “GDF3 is a BMP inhibitor that can activate Nodal signaling only at very high doses.,” *Developmental biology*, vol. 325, no. 1, pp. 43–8, Jan. 2009.

[145] A. Aono, M. Hazama, K. Notoya, S. Taketomi, H. Yamasaki, R. Tsukuda, S. Sasaki, and Y. Fujisawa, “Potent ectopic bone-inducing activity of bone morphogenetic protein-4/7 heterodimer.,” *Biochemical and biophysical research communications*, vol. 210, no. 3, pp. 670–7, May 1995.

[146] J. A. Le Good, K. Joubin, A. J. Giraldez, N. Ben-Haim, S. Beck, Y. Chen, A. F. Schier, and D. B. Constam, “Nodal stability determines signaling range.,” *Current biology : CB*, vol. 15, no. 1, pp. 31–6, Jan. 2005.

[147] M.-H. Blanchet, J. A. Le Good, D. Mesnard, V. Oorschot, S. Baflast, G. Minchiotti, J. Klumperman, and D. B. Constam, “Cripto recruits Furin and PACE4 and controls Nodal trafficking during proteolytic maturation.,” *The EMBO journal*, vol. 27, no. 19, pp. 2580–91, Oct. 2008.

[148] C. Tanaka, R. Sakuma, T. Nakamura, H. Hamada, and Y. Saijoh, “Long-range action of Nodal requires interaction with GDF1.,” *Genes & development*, vol. 21, no. 24, pp. 3272–82, Dec. 2007.

[149] J. Massagué, “How cells read TGF-beta signals.,” *Nature reviews. Molecular cell biology*, vol. 1, no. 3, pp. 169–78, Dec. 2000.

[150] M. A. Khajah, S. Al Saleh, P. M. Mathew, and Y. A. Luqmani, “Differential effect of growth factors on invasion and proliferation of endocrine resistant breast cancer cells.,” *PloS one*, vol. 7, no. 7, p. e41847, Jan. 2012.

[151] K. Sagorny, M. Chapellier, B. Laperrousaz, and V. Maguer-Satta, “[BMP and cancer: the Yin and Yang of stem cells].,” *Médecine sciences : M/S*, vol. 28, no. 4, pp. 416–22, Apr. 2012.

[152] H. S. Leong and D. Kipling, “Text-based over-representation analysis of microarray gene lists with annotation bias.,” *Nucleic acids research*, vol. 37, no. 11, p. e79, Jun. 2009.

[153] F. L. Conlon, K. M. Lyons, N. Takaesu, K. S. Barth, a Kispert, B. Herrmann, and E. J. Robertson, “A primary requirement for nodal in the formation and maintenance of the primitive streak in the mouse.,” *Development (Cambridge, England)*, vol. 120, no. 7, pp. 1919–28, Jul. 1994.

[154] L. a Lowe, S. Yamada, and M. R. Kuehn, “Genetic dissection of nodal function in patterning the mouse embryo.,” *Development (Cambridge, England)*, vol. 128, no. 10, pp. 1831–43, May 2001.

[155] D. Mesnard, M. Donnison, C. Fuerer, P. L. Pfeffer, and D. B. Constam, “The microenvironment patterns the pluripotent mouse epiblast through paracrine Furin and Pace4 proteolytic activities.,” *Genes & development*, vol. 25, no. 17, pp. 1871–80, Sep. 2011.

[156] Y. E. Zhang, “Non-Smad pathways in TGF-beta signaling.,” *Cell research*, vol. 19, no. 1, pp. 128–39, Jan. 2009.

[157] D. G. Grier, A. Thompson, A. Kwasniewska, G. J. McGonigle, H. L. Halliday, and T. R. Lappin, “The pathophysiology of HOX genes and their role in cancer.,” *The Journal of pathology*, vol. 205, no. 2, pp. 154–71, Jan. 2005.

[158] S. Samuel and H. Naora, “Homeobox gene expression in cancer: insights from developmental regulation and deregulation.,” *European journal of cancer (Oxford, England : 1990)*, vol. 41, no. 16, pp. 2428–37, Nov. 2005.

[159] C. Abate-Shen, “Deregulated homeobox gene expression in cancer: cause or consequence?,” *Nature reviews. Cancer*, vol. 2, no. 10, pp. 777–85, Oct. 2002.

[160] P. M. Gilbert, J. K. Mouw, M. A. Unger, J. N. Lakins, M. K. Gbegnon, V. B. Clemmer, M. Benezra, J. D. Licht, N. J. Boudreau, K. K. C. Tsai, A. L. Welm, M. D. Feldman, B. L. Weber, and V. M. Weaver, “HOXA9 regulates BRCA1 expression to modulate human breast tumor phenotype.,” *The Journal of clinical investigation*, vol. 120, no. 5, pp. 1535–50, May 2010.

[161] S. Y. Ko, N. Barengo, A. Ladanyi, J.-S. Lee, F. Marini, E. Lengyel, and H. Naora, “HOXA9 promotes ovarian cancer growth by stimulating cancer-associated fibroblasts.,” *The Journal of clinical investigation*, vol. 122, no. 10, pp. 3603–17, Oct. 2012.

[162] M. C. Chu, F. B. Selam, and H. S. Taylor, “HOXA10 regulates p53 expression and matrigel invasion in human breast cancer cells.,” *Cancer biology & therapy*, vol. 3, no. 6, pp. 568–72, Jun. 2004.

[163] N. Y. Rots, M. Liu, E. C. Anderson, and L. P. Freedman, “A differential screen for ligand-regulated genes: identification of HoxA10 as a target of vitamin D3 induction in myeloid leukemic cells.,” *Molecular and cellular biology*, vol. 18, no. 4, pp. 1911–8, Apr. 1998.

[164] K. Ghoshal, T. Motiwala, R. Claus, P. Yan, H. Kutay, J. Datta, S. Majumder, S. Bai, A. Majumder, T. Huang, C. Plass, and S. T. Jacob, “HOXB13, a target of DNMT3B, is methylated at an upstream CpG island, and functions as a tumor suppressor in primary colorectal tumors.,” *PloS one*, vol. 5, no. 4, p. e10338, Jan. 2010.

[165] H. Okuda, M. Toyota, W. Ishida, M. Furihata, M. Tsuchiya, M. Kamada, T. Tokino, and T. Shuin, “Epigenetic inactivation of the candidate tumor suppressor gene HOXB13 in human renal cell carcinoma.,” *Oncogene*, vol. 25, no. 12, pp. 1733–42, Mar. 2006.

[166] C. Jung, R.-S. Kim, H.-J. Zhang, S.-J. Lee, and M.-H. Jeng, “HOXB13 induces growth suppression of prostate cancer cells as a repressor of hormone-activated androgen receptor signaling.,” *Cancer research*, vol. 64, no. 24, pp. 9185–92, Dec. 2004.

[167] V. Muthusamy, S. Duraisamy, C. M. Bradbury, C. Hobbs, D. P. Curley, B. Nelson, and M. Bosenberg, “Epigenetic silencing of novel tumor suppressors in malignant melanoma.,” *Cancer research*, vol. 66, no. 23, pp. 11187–93, Dec. 2006.

[168] A. Kallioniemi, “Bone morphogenetic protein 4-a fascinating regulator of cancer cell behavior.,” *Cancer genetics*, vol. 205, no. 6, pp. 267–77, Jun. 2012.

[169] H. Kawasaki, K. Mizuseki, S. Nishikawa, S. Kaneko, Y. Kuwana, S. Nakanishi, S. I. Nishikawa, and Y. Sasai, “Induction of midbrain dopaminergic neurons from ES cells by stromal cell-derived inducing activity.,” *Neuron*, vol. 28, no. 1, pp. 31–40, Oct. 2000.

[170] M. F. Finley, S. Devata, and J. E. Huettner, “BMP-4 inhibits neural differentiation of murine embryonic stem cells.,” *Journal of neurobiology*, vol. 40, no. 3, pp. 271–87, Sep. 1999.

[171] N. Ferrara and R. S. Kerbel, “Angiogenesis as a therapeutic target.,” *Nature*, vol. 438, no. 7070, pp. 967–74, Dec. 2005.

[172] Z. Li, H. Huang, P. Boland, M. G. Dominguez, P. Burfeind, K.-M. Lai, H.-C. Lin, N. W. Gale, C. Daly, W. Auerbach, D. Valenzuela, G. D. Yancopoulos, and G. Thurston, “Embryonic stem cell tumor model reveals role of vascular endothelial receptor tyrosine phosphatase in regulating Tie2 pathway in tumor angiogenesis.,” *Proceedings of the National Academy of Sciences of the United States of America*, vol. 106, no. 52, pp. 22399–404, Dec. 2009.

[173] D. Liu, V. Martin, J. Fueyo, O. Lee, J. Xu, N. Cortes-, M. M. Alonso, K. Aldape, and H. Colman, “Tie2 / TEK Modulates the Interaction of Glioma and Brain Tumor Stem Cells with Endothelial Cells and Promotes an Invasive Phenotype AbstrAct :,” vol. 1, no. 8, pp. 700–709, 2010.

[174] D. Noordermeer, M. Leleu, E. Splinter, J. Rougemont, W. De Laat, and D. Duboule, “The dynamic architecture of Hox gene clusters.,” *Science (New York, N.Y.)*, vol. 334, no. 6053, pp. 222–5, Oct. 2011.

[175] M. a Ferraiuolo, M. Rousseau, C. Miyamoto, S. Shenker, X. Q. D. Wang, M. Nadler, M. Blanchette, and J. Dostie, “The three-dimensional architecture of Hox cluster silencing.,” *Nucleic acids research*, vol. 38, no. 21, pp. 7472–84, Nov. 2010.

[176] T. Montavon, N. Soshnikova, B. Mascrez, E. Joye, L. Thevenet, E. Splinter, W. de Laat, F. Spitz, and D. Duboule, “A regulatory archipelago controls Hox genes transcription in digits.,” *Cell*, vol. 147, no. 5, pp. 1132–45, Nov. 2011.

[177] D. E. Ferrier and P. W. Holland, “Ancient origin of the Hox gene cluster.,” *Nature reviews. Genetics*, vol. 2, no. 1, pp. 33–8, Jan. 2001.

[178] K. Dalhoff, J. Dancey, L. Astrup, T. Skovsgaard, K. J. Hamberg, F. J. Lofts, O. Rosmorduc, S. Erlinger, J. Bach Hansen, W. P. Steward, T. Skov, F. Burcharth, and T. R. J. Evans, “A phase II study of the vitamin D analogue Seocalcitol in patients with inoperable hepatocellular carcinoma.,” *British journal of cancer*, vol. 89, no. 2, pp. 252–7, Jul. 2003.

[179] D. Manor, E. N. Shmidt, A. Budhu, A. Flesken-Nikitin, M. Zgola, R. Page, A. Y. Nikitin, and N. Noy, “Mammary carcinoma suppression by cellular retinoic acid binding protein-II.,” *Cancer research*, vol. 63, no. 15, pp. 4426–33, Aug. 2003.

[180] L. Altucci and H. Gronemeyer, “Retinoids and TRAIL: two cooperating actors to fight against cancer.,” *Vitamins and hormones*, vol. 67, pp. 319–45, Jan. 2004.

[181] J. C. Reed, “Double identity for proteins of the Bcl-2 family.,” *Nature*, vol. 387, no. 6635, pp. 773–6, Jun. 1997.

[182] Z. N. Oltvai, C. L. Milliman, and S. J. Korsmeyer, “Bcl-2 heterodimerizes in vivo with a conserved homolog, Bax, that accelerates programmed cell death.,” *Cell*, vol. 74, no. 4, pp. 609–19, Aug. 1993.

[183] E. Yang, J. Zha, J. Jockel, L. H. Boise, C. B. Thompson, and S. J. Korsmeyer, “Bad, a heterodimeric partner for Bcl-XL and Bcl-2, displaces Bax and promotes cell death.,” *Cell*, vol. 80, no. 2, pp. 285–91, Jan. 1995.

[184] X. M. Yin, Z. N. Oltvai, and S. J. Korsmeyer, “BH1 and BH2 domains of Bcl-2 are required for inhibition of apoptosis and heterodimerization with Bax.,” *Nature*, vol. 369, no. 6478, pp. 321–3, May 1994.

9 APPENDIX

Microarray A				
Term	**Count**	**%**	**P-Value**	**Benjamini**
BP00193:Developmental processes	176	15,5	1,40E-07	2,80E-05
BP00248:Mesoderm development	54	4,7	1,90E-04	1,90E-02
BP00040:mRNA transcription	140	12,3	5,40E-04	3,50E-02
BP00044:mRNA transcription regulation	109	9,6	1,80E-03	8,70E-02
BP00281:Oncogenesis	41	3,6	2,10E-03	7,90E-02
BP00199:Neurogenesis	52	4,6	2,20E-03	7,10E-02
BP00207:Cell cycle control	39	3,4	2,30E-03	6,20E-02
BP00246:Ectoderm development	57	5	4,30E-03	1,00E-01
BP00284:Hematopoiesis	11	1	8,50E-03	1,70E-01
BP00031:Nucleoside, nucleotide and nucleic acid metabolism	207	18,2	1,80E-02	3,00E-01
BP00119:Other intracellular signalling cascade	21	1,8	2,80E-02	4,10E-01
BP00265:Oncogene	12	1,1	3,30E-02	4,30E-01
BP00285:Cell structure and motility	78	6,8	4,00E-02	4,60E-01
BP00110:Other receptor mediated signalling pathway	20	1,8	4,00E-02	4,40E-01
BP00124:Cell adhesion	46	4	4,10E-02	4,30E-01
BP00170:Neuromuscular synaptic transmission	5	0,4	4,10E-02	4,10E-01
BP00103:Cell surface receptor mediated signal transduction	111	9,7	5,00E-02	4,50E-01
BP00064:Protein phosphorylation	48	4,2	6,00E-02	4,90E-01
BP00201:Skeletal development	13	1,1	6,40E-02	5,00E-01
BP00156:Interferon-mediated immunity	8	0,7	8,10E-02	5,70E-01
BP00223:Angiogenesis	7	0,6	9,40E-02	6,10E-01

Microarray B				
Term	**Count**	**%**	**P-Value**	**Benjamini**
BP00193:Developmental processes	106	19,3	4,20E-10	6,70E-08
BP00102:Signal transduction	137	25	5,80E-07	4,60E-05
BP00199:Neurogenesis	39	7,1	1,10E-06	5,70E-05
BP00246:Ectoderm development	41	7,5	5,60E-06	2,20E-04
BP00248:Mesoderm development	33	6	7,30E-05	2,30E-03
BP00103:Cell surface receptor mediated signal transduction	70	12,8	2,60E-04	6,90E-03
BP00223:Angiogenesis	8	1,5	7,50E-04	1,70E-02
BP00245:Segment specification	10	1,8	2,00E-03	3,90E-02
BP00201:Skeletal development	11	2	2,90E-03	5,00E-02
BP00274:Cell communication	50	9,1	3,10E-03	4,80E-02
BP00224:Cell proliferation and differentiation	43	7,8	4,60E-03	6,40E-02
BP00110:Other receptor mediated signalling pathway	14	2,6	6,80E-03	8,70E-02
BP00275:Extracellular matrix protein-mediated signalling	7	1,3	8,00E-03	9,40E-02
BP00044:mRNA transcription regulation	53	9,7	2,50E-02	2,50E-01
BP00040:mRNA transcription	66	12	2,70E-02	2,50E-01
BP00108:Receptor protein tyrosine kinase signalling pathway	12	2,2	2,80E-02	2,50E-01
BP00281:Oncogenesis	20	3,6	3,30E-02	2,70E-01
BP00207:Cell cycle control	19	3,5	3,50E-02	2,70E-01
BP00173:Muscle contraction	11	2	3,70E-02	2,70E-01
BP00143:Cation transport	21	3,8	4,50E-02	3,10E-01
BP00166:Neuronal activities	23	4,2	7,40E-02	4,40E-01
BP00240:Fertilization	4	0,7	7,60E-02	4,40E-01
BP00209:Blood circulation and gas exchange	6	1,1	8,90E-02	4,80E-01
BP00167:Synaptic transmission	13	2,4	9,00E-02	4,70E-01

Microarray C				
Term	**Count**	**%**	**P-Value**	**Benjamini**
BP00102:Signal transduction	103	26,8	4,70E-05	7,00E-03
BP00103:Cell surface receptor mediated signal transduction	56	14,5	4,20E-04	3,10E-02
BP00199:Neurogenesis	25	6,5	1,80E-03	8,60E-02
BP00178:Stress response	11	2,9	9,20E-03	2,90E-01
BP00267:Homeostasis	11	2,9	1,00E-02	2,60E-01
BP00166:Neuronal activities	22	5,7	1,10E-02	2,30E-01
BP00246:Ectoderm development	25	6,5	1,10E-02	2,10E-01
BP00274:Cell communication	38	9,9	1,20E-02	2,00E-01
BP00018:Other amino acid metabolism	4	1	2,20E-02	3,10E-01
BP00193:Developmental processes	59	15,3	2,30E-02	2,90E-01
BP00148:Immunity and defense	39	10,1	2,40E-02	2,80E-01
BP00122:Ligand-mediated signalling	16	4,2	2,80E-02	3,00E-01
BP00288:Granulocyte-mediated immunity	5	1,3	4,60E-02	4,20E-01
BP00124:Cell adhesion	20	5,2	5,40E-02	4,50E-01
BP00277:Phagocytosis	4	1	5,70E-02	4,40E-01
BP00104:G-protein mediated signalling	26	6,8	5,80E-02	4,30E-01
BP00281:Oncogenesis	15	3,9	8,00E-02	5,20E-01
BP00107:Cytokine and chemokine mediated signalling pathway	10	2,6	8,10E-02	5,00E-01
BP00224:Cell proliferation and differentiation	29	7,5	8,40E-02	5,00E-01
BP00040:mRNA transcription	49	12,7	8,90E-02	5,00E-01
BP00110:Other receptor mediated signalling pathway	9	2,3	8,90E-02	4,80E-01
BP00044:mRNA transcription regulation	39	10,1	9,10E-02	4,80E-01
BP00207:Cell cycle control	14	3,6	9,70E-02	4,80E-01
BP00004:Carbohydrate transport	4	1	9,80E-02	4,70E-01

Microarray D				
Term	**Count**	**%**	**P-Value**	**Benjamini**
BP00103:Cell surface receptor mediated signal transduction	51	13,9	8,20E-04	1,20E-01
BP00281:Oncogenesis	18	4,9	4,80E-03	3,10E-01
BP00102:Signal transduction	85	23,1	6,40E-03	2,80E-01
BP00104:G-protein mediated signaling	27	7,3	1,30E-02	4,00E-01
BP00122:Ligand-mediated signaling	16	4,3	1,40E-02	3,40E-01
BP00166:Neuronal activities	19	5,2	3,00E-02	5,40E-01
BP00274:Cell communication	33	9	3,70E-02	5,50E-01
BP00265:Oncogene	6	1,6	4,90E-02	6,20E-01
BP00193:Developmental processes	52	14,1	5,60E-02	6,20E-01
BP00110:Other receptor mediated signaling pathway	9	2,4	5,80E-02	6,00E-01
BP00001:Carbohydrate metabolism	17	4,6	8,90E-02	7,30E-01
BP00267:Homeostasis	8	2,2	9,30E-02	7,10E-01

Microarray E				
Term	**Count**	**%**	**P-Value**	**Benjamini**
BP00193:Developmental processes	329	18,2	1,40E-21	2,90E-19
BP00246:Ectoderm development	117	6,5	4,10E-10	4,40E-08
BP00199:Neurogenesis	105	5,8	4,70E-10	3,30E-08
BP00102:Signal transduction	415	23	4,40E-09	2,30E-07
BP00248:Mesoderm development	95	5,3	2,90E-08	1,20E-06
BP00281:Oncogenesis	73	4	2,50E-06	8,60E-05
BP00103:Cell surface receptor mediated signal transduction	208	11,5	1,60E-05	4,90E-04
BP00201:Skeletal development	28	1,6	6,60E-05	1,70E-03
BP00274:Cell communication	154	8,5	7,50E-05	1,80E-03
BP00108:Receptor protein tyrosine kinase signalling pathway	38	2,1	1,40E-04	2,90E-03
BP00223:Angiogenesis	16	0,9	1,40E-04	2,70E-03
BP00173:Muscle contraction	34	1,9	4,80E-04	8,30E-03
BP00275:Extracellular matrix protein-mediated signalling	16	0,9	7,80E-04	1,30E-02
BP00285:Cell structure and motility	137	7,6	1,10E-03	1,70E-02
BP00110:Other receptor mediated signalling pathway	36	2	1,30E-03	1,80E-02
BP00040:mRNA transcription	215	11,9	2,20E-03	2,80E-02
BP00166:Neuronal activities	76	4,2	3,20E-03	3,80E-02
BP00124:Cell adhesion	79	4,4	3,50E-03	4,10E-02
BP00265:Oncogene	20	1,1	3,80E-03	4,10E-02
BP00044:mRNA transcription regulation	168	9,3	4,20E-03	4,40E-02
BP00224:Cell proliferation and differentiation	122	6,8	4,50E-03	4,50E-02
BP00287:Cell motility	48	2,7	6,70E-03	6,30E-02
BP00111:Intracellular signalling cascade	106	5,9	8,90E-03	7,80E-02
BP00283:Other oncogenesis	14	0,8	9,80E-03	8,30E-02
BP00178:Stress response	29	1,6	2,10E-02	1,60E-01
BP00267:Homeostasis	29	1,6	2,50E-02	1,90E-01
BP00242:Embryogenesis	22	1,2	3,00E-02	2,10E-01
BP00250:Muscle development	22	1,2	3,20E-02	2,20E-01
BP00269:Glucose homeostasis	6	0,3	3,80E-02	2,40E-01
BP00120:Cell adhesion-mediated signalling	48	2,7	3,90E-02	2,50E-01
BP00172:Other neuronal activity	21	1,2	4,50E-02	2,70E-01
BP00251:Heart development	10	0,6	5,10E-02	2,90E-01
BP00064:Protein phosphorylation	76	4,2	5,20E-02	2,90E-01
BP00107:Cytokine and chemokine mediated signalling pathway	32	1,8	7,30E-02	3,70E-01
BP00056:Metabolism of cyclic nucleotides	9	0,5	7,30E-02	3,70E-01
BP00119:Other intracellular signalling cascade	29	1,6	7,60E-02	3,70E-01
BP00009:Other polysaccharide metabolism	19	1,1	8,20E-02	3,90E-01
BP00148:Immunity and defense	139	7,7	8,90E-02	4,00E-01
BP00112:Calcium mediated signalling	17	0,9	9,10E-02	4,00E-01
BP00020:Fatty acid metabolism	24	1,3	9,60E-02	4,10E-01

LIST OF PUBLICATIONS AND PRESENTATIONS

Publications

1. **Tykwinska K**, Rosowski M, Knaus P, Lauster R. Growth and Differentition Factor 3 induces expression of genes related to differentiation in a model of cancer stem cells and protects them from retinoic acid-induced apoptosis. Submitted at PloS One
2. Gaber T, Schellmann S, Erekul KB, Fangradt M, **Tykwinska K**, Hahne M, Maschmeyer P, Wagegg M, Stahn C, Kolar P, Dziurla R, Löhning M, Burmester GR, Buttgereit F. Macrophage Migration Inhibitory Factor Counterregulates Dexamethasone-Mediated Suppression of Hypoxia-Inducible Factor-1{alpha} Function and Differentially Influences Human CD4+ T Cell Proliferation under Hypoxia. J Immunol. 2011 Jan 15;186(2):764-74 [Pubmed]
3. Gaber T, Häupl T, Sandig G, **Tykwinska K**, Fangradt M, Tschirschmann M, Hahne M, Dziurla R, Erekul K, Lautenbach M, Kolar P, Burmester GR, Buttgereit F. Adaptation of human CD4+ T cells to pathophysiological hypoxia: a transcriptome analysis. J Rheumatol. 2009 Dec;36(12):2655-69 [Pubmed]

Presentations

1. Oral presentation: Crazy little thing called Cripto. 3rd BSRT PhD Symposium The Show of Regeneration: Easy to see, hard to forsee, Berlin 2012
2. Poster presentation: Maintenance of vitality and viability of liquid brewing yeast during long-time storage. Bockisch A., Glazyrina J., **Tykwinska K.**, Neubauer P. 8th European Congress of Chemical Engineering, Berlin 2011
3. Poster presentation: GDF3 in the stem cell biology. **Tykwinska K.**, Rosowski M., Lauster R. 1st BSRT PhD Symposium on Stem Cells: Hopes, Fears and Reality, Berlin 2010
4. Poster presentation: GDF3 in the stem cell biology. **Tykwinska K.**, Rosowski M., Lauster R. The International Abcam Stem Cell Conference, Antigua 2009
5. Poster presentation: GDF3 expression pattern and regulation of expression in lymphoid tissues. Sethmann S., **Tykwinska K.**, Rosowski M., Lauster R. 1st International BMP Workshop. Modern Trends in BMP Signaling, Berlin 2009

EIDESSTATTLICHE ERKLÄRUNG

Ich erkläre an Eides Statt, dass die vorliegende Dissertation in allen Teilen von mir selbständig angefertigt wurde und die benutzten Hilfsmittel vollständig angegeben worden sind.

Ich versichere, dass diese Dissertation noch keiner anderen Fakultät oder Universität zur Prüfung vorgelegen hat.

Veröffentlichungen von irgendwelchen Teilen der vorliegenden Dissertation sind wie folgt vorgenommen worden: Die Teile der Arbeit wurden in Form einer wissenschaftlichen Publikation bei PloS ONE eingereicht.

Tykwinska K, Rosowski M, Knaus P, Lauster R. Growth and Differentition Factor 3 induces expression of genes related to differentiation in a model of cancer stem cells and protects them from retinoic acid-induced apoptosis.

Die Bestimmungen der Promotionsordnung sind mir bekannt.

Karolina Tykwinska